TECHNICAL REPORT EL-88-15

US Army Corps of Engineers

NEW BEDFORD HARBOR SUPERFUND PROJECT, ACUSHNET RIVER ESTUARY ENGINEERING FEASIBILITY STUDY OF DREDGING AND DREDGED MATERIAL DISPOSAL ALTERNATIVES

Report 2

SEDIMENT AND CONTAMINANT HYDRAULIC TRANSPORT INVESTIGATIONS

by

Allen M. Teeter

Hydraulics Laboratory

DEPARTMENT OF THE ARMY
Waterways Experiment Station, Corps of Engineers
PO Box 631, Vicksburg, Mississippi 39181-0631

December 1988
Report 2 of a Series

Prepared for US Environmental Protection Agency
Region 1, Boston, Massachusetts 02203-2211

Monitored by Environmental Laboratory
US Army Engineer Waterways Experiment Station
PO Box 631, Vicksburg, Mississippi 39181-0631

Unclassified

SECURITY CLASSIFICATION OF THIS PAGE

REPORT DOCUMENTATION PAGE

Form Approved OMB No. 0704-0188

1a. REPORT SECURITY CLASSIFICATION Unclassified	1b. RESTRICTIVE MARKINGS
2a. SECURITY CLASSIFICATION AUTHORITY	3. DISTRIBUTION/AVAILABILITY OF REPORT Approved for public release; distribution unlimited.
2b. DECLASSIFICATION/DOWNGRADING SCHEDULE	
4. PERFORMING ORGANIZATION REPORT NUMBER(S)	5. MONITORING ORGANIZATION REPORT NUMBER(S) Technical Report EL-88-15
6a. NAME OF PERFORMING ORGANIZATION USAEWES Hydraulics Laboratory 6b. OFFICE SYMBOL (If applicable)	7a. NAME OF MONITORING ORGANIZATION USAEWES Environmental Laboratory
6c. ADDRESS (City, State, and ZIP Code) PO Box 631 Vicksburg, MS 39181-0631	7b. ADDRESS (City, State, and ZIP Code) PO Box 631 Vicksburg, MS 39181-0631
8a. NAME OF FUNDING/SPONSORING ORGANIZATION US Environmental Protection Agency, Region 1 8b. OFFICE SYMBOL (If applicable)	9. PROCUREMENT INSTRUMENT IDENTIFICATION NUMBER
8c. ADDRESS (City, State, and ZIP Code) J. F. Kennedy Federal Building Boston, MA 02203-2211	10. SOURCE OF FUNDING NUMBERS PROGRAM ELEMENT NO. / PROJECT NO. / TASK NO. / WORK UNIT ACCESSION NO.
11. TITLE (Include Security Classification) New Bedford Harbor Superfund Project, Acushnet River Estuary Engineering Feasibility Study of Dredging and Dredged Material Disposal Alternatives; Report 2, Sediment and Contaminant Hydraulic Transport Investigations	
12. PERSONAL AUTHOR(S) Teeter, Allen M.	
13a. TYPE OF REPORT Report 2 of a series 13b. TIME COVERED FROM Feb 86 TO Jul 87	14. DATE OF REPORT (Year, Month, Day) December 1988 15. PAGE COUNT 124
16. SUPPLEMENTARY NOTATION Available from National Technical Information Service, 5285 Port Royal Road, Springfield, VA 22161.	
17. COSATI CODES FIELD / GROUP / SUB-GROUP	18. SUBJECT TERMS (Continue on reverse if necessary and identify by block number) CAD cell, Deposition, Dredging, Contaminant, Disposal, Migration (Continued)

19. ABSTRACT (Continue on reverse if necessary and identify by block number)

This report documents the evaluation of hydraulic conditions and sediment migration associated with the dredging and dredged material disposal alternatives proposed for the upper Acushnet River Estuary upstream of New Bedford Harbor, Massachusetts. Dredging and onsite disposal is one remedial measure being considered by the US Environmental Protection Agency.

Assessments of sediment and contaminant migration beyond the upper New Bedford Harbor from proposed dredging and disposal alternatives were made based on field, laboratory, and various model studies. The upper estuary was found to be depositional and a reasonably efficient sediment trap. Total suspended material (TSM) concentrations were very low in the system.

(Continued)

20. DISTRIBUTION/AVAILABILITY OF ABSTRACT ☒ UNCLASSIFIED/UNLIMITED ☐ SAME AS RPT. ☐ DTIC USERS	21. ABSTRACT SECURITY CLASSIFICATION Unclassified
22a. NAME OF RESPONSIBLE INDIVIDUAL	22b. TELEPHONE (Include Area Code) / 22c. OFFICE SYMBOL

DD Form 1473, JUN 86 *Previous editions are obsolete.*

SECURITY CLASSIFICATION OF THIS PAGE
Unclassified

18. SUBJECT TERMS (Continued).

Numerical transport model	Sediment	Water tunnel
~~PCB — Aroclor~~	Settling velocity	
Resuspension	Total suspended material	

19. ABSTRACT (Continued).

Present tidal-averaged polychlorinated biphenyl (PCB)-Aroclor seaward flux from the upper estuary through the Coggeshall Bridge was about 0.035 g PCB per second, or about 1.55 kg per tidal cycle. The direction of the PCB flux was opposite that of TSM. Diffusion, exchange processes, and soluble transport were concluded to be more important to PCB flux than erosion and transport of bed sediment material. Surface transport of PCB-Aroclor by floatable film was found not to be an important transport mode.

Sampling at and around two composite sampling sites was performed to estimate resuspension rates under actual site conditions. The operation of the sampling vessel caused more resuspension than the box core dredging, indicating that control of vessel operations in the shallow waters in the upper estuary might be more important than controlling dredgehead resuspension. Overall resuspension rates, vessel plus box core dredging, were 40 to 70 g per second.

Resuspension by the dredge was apparently less than about 10 g per second. Settling velocities of bed sediments resuspended during composite sampling operations were relatively high for fine sediments.

Experimentally determined erosion thresholds indicate that confined aquatic disposal (CAD) cells should be sited in areas with relatively low current speeds, and particularly in areas where maximum shear stresses are below 0.06 N/sq m (current speeds below about 12 cm/sec) to avoid resuspension.

Near-field dredge plume and CAD cell deposition models were applied to cleanup dredging scenarios. Results from the dredge plume model indicated that an average, weighted by occurrence frequencies, of about 29 percent of the resuspended material will escape the 100-m radius of the dredging site. Results from the CAD cell model indicated that all of the fine resuspended material expelled from the slurry with the pore water will escape from the CAD cell.

A vertically averaged two-dimensional numerical transport model was also applied to the estuary. Results indicate that the flux of sediment material from the upper estuary would be 15 to 20 percent of the rate of sediment resuspension.

Sediment migration simulation results combined with assumed resuspension rates (40 g/sec) indicated that the average flux of suspended sediment during midestuary dredging would be about 11.6 g/sec at the 100-m radius and about 7.6 g/per sec through the Coggeshall Street Bridge.

PREFACE

This study was conducted as a part of the Acushnet River Estuary Engineering Feasibility Study (EFS) of Alternatives for Dredging and Dredged Material Disposal. The US Army Corps of Engineers (USACE) performed the EFS for the US Environmental Protection Agency (USEPA), Region 1, as a component of the comprehensive USEPA Feasibility Study for the New Bedford Harbor Superfund Site, New Bedford, MA. This report, Report 2 of a series, was prepared at the US Army Engineer Waterways Experiment Station (WES) in cooperation with the New England Division, USACE. Coordination and management support was provided by the Omaha District, USACE, and dredging program coordination was provided by the Dredging Division, USACE.

Project manager for the USEPA was Mr. Frank Ciavattieri. The New England Division project managers were Messrs. Mark J. Otis and Alan Randall. Omaha District project managers were Messrs. Kevin Mayberry and William Bonneau. Project managers for the WES were Messrs. Norman R. Francingues, Jr., and Daniel E. Averett.

The study was conducted and the report prepared by Mr. Allen M. Teeter, Hydraulics Laboratory (HL), WES. Mr. Walter Pankow assisted in the preparation of the report. Mr. Howard Benson of the Estuarine Processes Branch (HE-P) supervised the execution of the field data collection. Messrs. Joseph W. Parman, Larry G. Caviness, Samuel E. Varnell, Billy G. Moore, and James T. Hilbun of the HE-P collected data in the field. Mr. Caviness performed laboratory experiments on deposition and erosion. Dr. Bufu Yu conducted the numerical estuarine modeling under the terms of an Intergovernmental Personnel Act agreement with Johns Hopkins University. The report was edited by Ms. Jessica S. Ruff of the WES Information Technology Laboratory.

The study was conducted during the period February 1986 to July 1987 under the general supervision of Messrs. Frank A. Herrmann, Chief, HL; Richard A. Sager, Assistant Chief, HL; William H. McAnally, Jr., Chief, Estuaries Division; and George M. Fisackerly, Chief, HE-P.

COL Dwayne G. Lee, EN, was Commander and Director of WES. Dr. Robert W. Whalin was the Technical Director.

This report should be cited as follows:

Teeter, Allen M. 1988. New Bedford Harbor Superfund Project, Acushnet River Estuary Engineering Feasibility Study of Dredging and Dredged Material Disposal Alternatives; Report 2, Sediment and Contaminant Hydraulic Transport Investigations," Technical Report EL-88-15, US Army Engineer Waterways Experiment Station, Vicksburg, MS.

CONTENTS

CONVERSION FACTORS, NON-SI TO SI (METRIC) UNITS OF MEASUREMENT

Non-SI units of measurement used in this report can be converted to SI (metric) units as follows:

Multiply	By	To Obtain
cubic yards	0.7645549	cubic metres
feet	0.3048	metres
horsepower (550 foot-pounds (force) per second)	745.6999	watts
yards	0.9144	metres

NEW BEDFORD HARBOR SUPERFUND PROJECT, ACUSHNET RIVER ESTUARY ENGINEERING FEASIBILITY STUDY OF DREDGING AND DREDGED MATERIAL DISPOSAL ALTERNATIVES

SEDIMENT AND CONTAMINANT HYDRAULIC TRANSPORT INVESTIGATIONS

PART I: INTRODUCTION

1. In August 1984, the US Environmental Protection Agency (USEPA) reported on the Feasibility Study of Remedial Action Alternatives for the Upper Acushnet River Estuary above the Coggeshall Street Bridge, New Bedford, MA (NUS Corporation 1984). The USEPA received extensive comments on the proposed remedial action alternatives from other Federal, state, and local officials, potentially responsible parties, and individuals. Responding to these comments, the USEPA chose to conduct additional studies to better define available cleanup methods. Because dredging was associated with all of the removal alternatives, the USEPA requested the Nation's dredging expert, the US Army Corps of Engineers (USACE), to conduct an Engineering Feasibility Study (EFS) of dredging and disposal alternatives. A major emphasis of the EFS was placed on evaluating the potential for contaminant releases from both dredging and disposal operations.

2. The technical phase of the EFS was completed in March 1988. However, as part of Task 8 of the EFS, the results of the study were compiled in a series of 12 reports, listed below.

a. Report 1, "Study Overview."

b. Report 2, "Sediment and Contaminant Hydraulic Transport Investigations."

c. Report 3, "Characterization and Elutriate Testing of Acushnet River Estuary Sediment."

d. Report 4, "Surface Runoff Quality Evaluation for Confined Disposal."

e. Report 5, "Evaluation of Leachate Quality."

f. Report 6, "Laboratory Testing for Subaqueous Capping."

g. Report 7, "Settling and Chemical Clarification Tests."

h. Report 8, "Compatibility of Liner Systems with New Bedford Harbor Dredged Material Contaminants."

i. Report 9, "Laboratory-Scale Application of Solidification/ Stabilization Technology."

j. Report 10, "Evaluation of Dredging and Dredging Control Technologies."

k. Report 11, "Evaluation of Conceptual Dredging and Disposal Alternatives."

l. Report 12, "Executive Summary."

This report is Report 2 of the series. The results of this study were obtained from conducting EFS Task 4, elements 1, 3, 4, and 5 (see Report 1). These study results are incorporated and used in the evaluation of conceptual dredging and dredged material disposal alternatives described in EFS Report 11.

Background

3. The study area is located on the northwestern shore of Buzzards Bay in Massachusetts, as shown in Figure 1. Upper New Bedford Harbor is that part of the Acushnet River Estuary upstream of the Coggeshall Street Bridge and downstream from the Wood Street Bridge (approximately the head of tide), as shown in Figure 2. The upper harbor is often referred to as the Acushnet River Estuary. Sampling initiated in the late 1970s determined that the upper harbor has received polychlorinated biphenyl (PCB) discharges and that upper harbor sediments exhibit the highest concentrations of PCBs in the New Bedford area. Malcolm Pernie, Inc. (1982), summarized the early PCB sampling data for the Commonwealth of Massachusetts and concluded that dredging programs to recover PCB-contaminated sediments would be technically feasible. Dredging and onsite disposal is one remedial measure being considered by the USEPA. A decision by the USEPA on cleanup alternatives is expected in 1989.

4. The USACE has been tasked by the USEPA with additional predesign studies for remedial dredging and disposal of contaminated sediments from the upper harbor. The EFS follows the USACE Management Strategy for the disposal of dredged materials (Francingues et al. 1985) and was conducted by the USACE New England Division (NED) and the US Army Engineer Waterways Experiment Station (WES). Report 1 of this series describes the scope of the EFS and outlines the other reports. The EFS was coordinated with the overall remedial assessments being made by USEPA and its contractors.

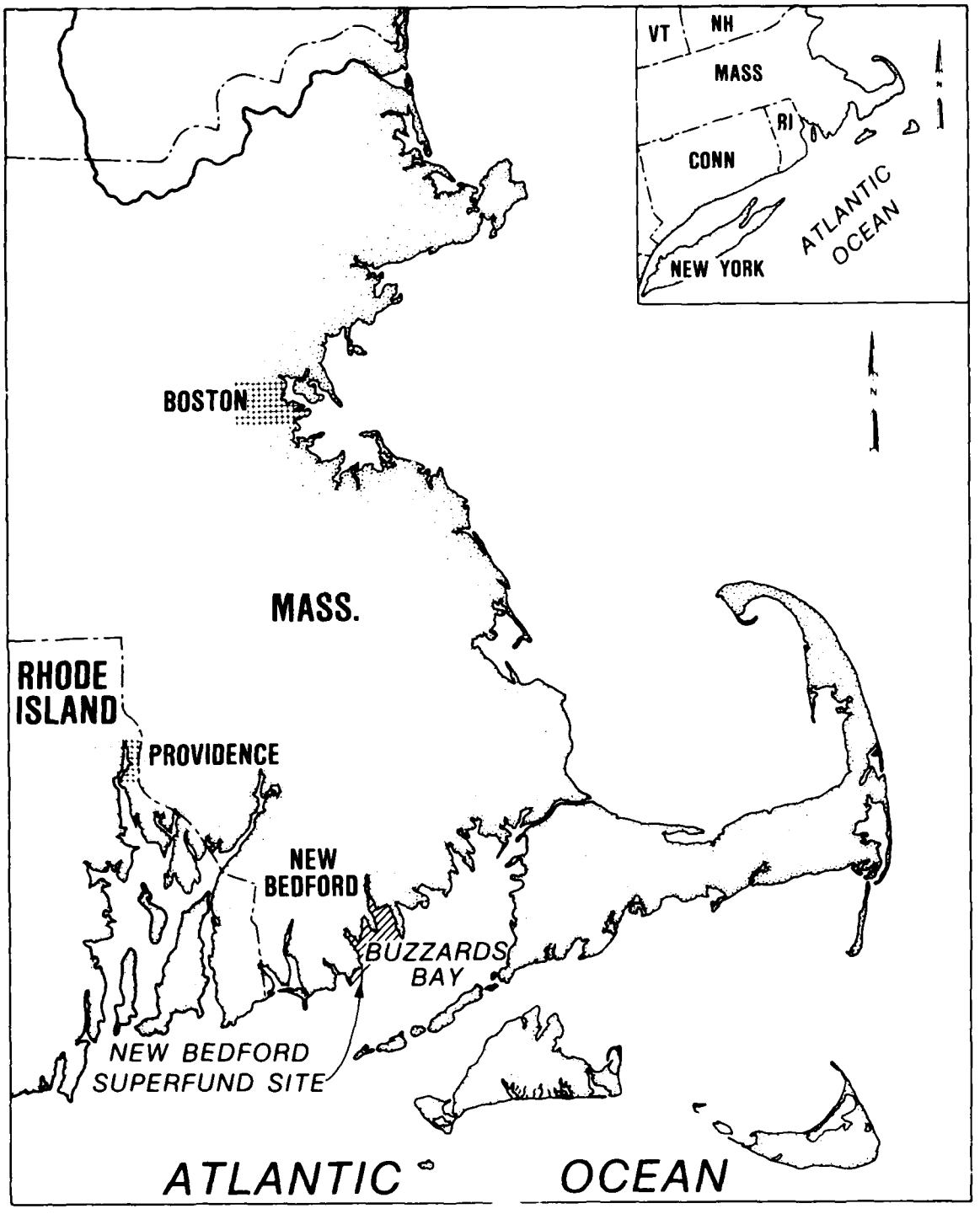

Figure 1. Location of New Bedford, MA

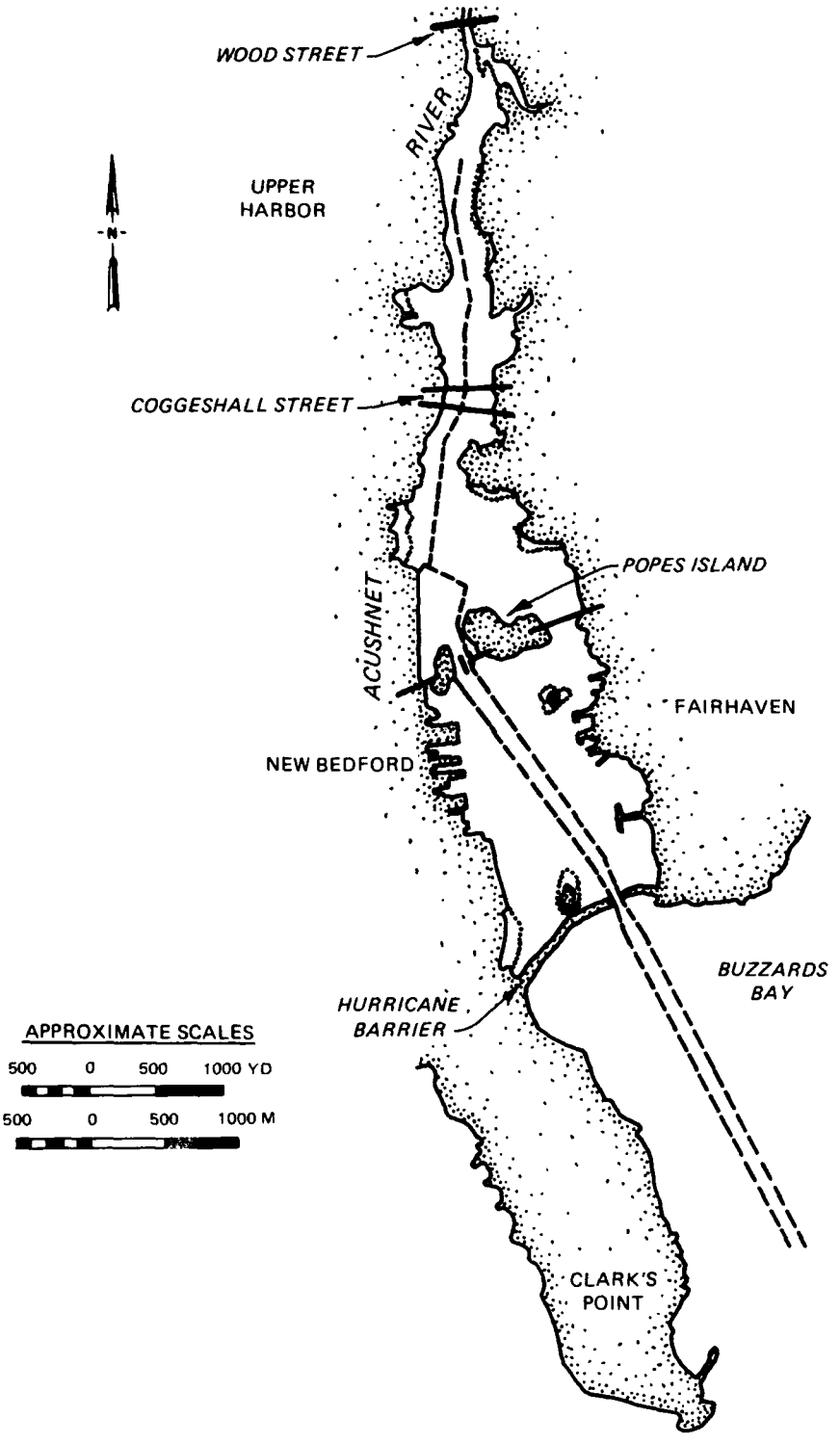

Figure 2. New Bedford Harbor and vicinity

EFS Overview

5. The EFS was divided into tasks and included components that:

   a. Performed suites of laboratory and bench-scale testing to predict the behavior of contaminants in New Bedford Harbor sediments during various dredging and disposal operations, and subsequently in various disposal environments.

   b. Assessed the migration of suspended sediments and PCBs in surface waters under present conditions, and predicted the releases and migration from various dredging and disposal operations.

   c. Detailed baseline sediment characteristics for the upper harbor to assess proposed dredging and disposal alternatives, and with which to make subsequent predesign/design studies.

   d. Combined the technically feasible dredging and disposal technologies into a set of alternatives, and provided concept design cost estimates for each.

The WES Hydraulics Laboratory (HL) evaluated hydraulic conditions and sediment migration as part of the WES Environmental Laboratory (EL) EFS. A prototype pilot study has been proposed to demonstrate the feasibility of some of the alternatives developed by the EFS (see Otis and Andreliunas 1987).

6. This report is a product of Task 4 of the EFS. Element 1 of Task 4 concerned contaminant release. Field portions of that element are reported in Parts II and III of this report. Other portions of element 1 are reported in Appendix A and in Report 3. Element 2 concerned controls for dredging, the results of which are given in Report 10. Work performed on element 3, hydraulic characterization, is summarized in Parts II, III, V, and VI. Work performed on element 4, erosion and deposition testing, is reported in Part IV. Element 5 concerned sediment migration analyses, and these results are reported in Parts VI and VII and in Appendix A of this report.

Purpose

7. The purposes of the studies described herein were to document present conditions with respect to sediment and contaminant migrations out of the upper harbor and to predict migrations and concentrations resulting from various potential dredging and disposal operations.

Scope

8. This report includes descriptions and results from three one-tidal-cycle prototype surveys to quantify sediment and contaminant migration, a prototype survey to assess sediment resuspension from box-corer dredging, laboratory studies of deposition and erosion characteristics of upper harbor sediments, near-field modeling of resuspended bed material plumes in open and confined aquatic disposal (CAD) sites, and estuarine hydrodynamic and transport modeling. Contaminant migration was assumed to be directly related to the transport of a soluble phase and phases adsorbed to various sediment fractions. The PCB phase partitioning and transformation kinetics were not modeled.

9. Methods are presented to assess the migrations from and concentrations in the upper harbor resulting from various dredging and disposal operations. Specific dredging scenarios are not assessed in this volume but are addressed in Report 11.

10. This report is divided into parts that describe specific aspects of the study. Descriptions of methods, assumptions, results, and discussions are contained within each part. Most parts are independent studies that feed information to other parts. Parts VII and VIII present the results from the other parts.

Study Approach

11. The approach of the study was to integrate prototype measurements, laboratory data, and model results to quantify present conditions and to predict dredging and disposal effects. Dredging and disposal effects addressed by modeling included contaminant and sediment migration away from the resuspension point and out of the upper harbor, the hydraulics of the present and dredged upper harbor, and concentrations of sediments and contaminants in the upper harbor during dredging and disposal releases. Most contaminants are bound to bottom sediments. The complexity of sediment/contaminant transport in the altered hydraulic system required numerical modeling to answer questions about specific dredging and disposal options as well as the overall feasibility of the dredging approach. Model sophistication and selection depended upon (a) the level of resolution required of the prediction, (b) the

amount and accuracy of available prototype data, and (c) resources available to complete the task. A general framework for remedial action modeling is given by Anderson-Nichols and Company, Inc. (1984).

12. Near-field analytical models were applied to the portion of the system within approximately 100 m of the point of release (the dredgehead, or disposal site outflow) for various combinations of ambient conditions. Several sediment fractions were included in the near-field models. Results were merged with a more comprehensive, estuarine model.

13. Estuarine modeling was performed to address certain specific hydraulic and sediment/contaminant transport questions that could not be answered by direct observation or experience because of the complexity of the site. Estuarine hydrodynamic and transport modeling used two-dimensional (2-D) numerical models. The 2-D horizontal models averaged currents and transport conditions in the vertical dimension. The model boundaries were located sufficiently far from the area of interest so that the planned dredging and disposal activities did not affect the boundary.

PART II: METHODS OF FIELD DATA COLLECTION

14. This part presents a summary of previous prototype studies in upper New Bedford Harbor, and the field data collection methods used for tidal cycle and sediment resuspension surveys by EFS Task 4.

Results of Previous Prototype Studies

15. New Bedford Harbor is located on the north shore of Buzzards Bay and is the estuary of the Acushnet River (Figure 1). The Acushnet River drains a small basin of only 47.7 sq km above the Saw Mill Dam, 700 m upstream from the Wood Street Bridge and the point of greatest freshwater inflow. The Wood Street Bridge is approximately the upstream limit of tidal influence. The New Bedford Harbor is about 6.4 km long from the Hurricane Barrier to the Wood Street Bridge. The upper New Bedford Harbor or the Acushnet River Estuary is about 2.5 km long from the Coggeshall Street Bridge to the Wood Street Bridge. The Coggeshall Street Bridge is the uppermost of three constrictions in the harbor and has a maximum opening width of about 33.5 m and a depth of 5.8 m. The Interstate 195 bridge also constricts the harbor about 100 m downstream from the Coggeshall Street Bridge. The Hurricane Barrier constricts the harbor entrance to a width of 45.7 m and a depth of 8.5 m.

Freshwater inflow

16. Discharge measurements are not routinely made in the basin. Based on the size of the basin and the characteristics of other New England basins of a similar type, the mean annual freshwater discharge has been estimated as 0.9 cu m/sec (Jason M. Cortell and Associates 1982). However, measurements over the 1972 to 1974 period made by the US Geological Survey indicate a maximum (monthly) flow of only 0.7 cu m/sec and a minimum (monthly) flow of 0.016 cu m/sec. According to the NED, the Standard Project Flood for the basin at the Saw Mill Dam is 37.7 cu m/sec peak flow. The 6-hr unit hydrograph for the Standard Project Flood peaks at 3.1 cu m/sec.* The NED has established a rating curve for the Saw Mill Dam. A staff reading taken on 11 April 1983 at the Saw Mill Dam indicated a flow of 14.2 cu m/sec. Storm ewers also drain into the upper harbor.

---

* US Army Engineer Division, New England. 1961. "New Bedford-Fairhaven Barrier," Waltham, MA.

Tidal conditions

17. The mean tide range at New Bedford Harbor is 1.13 m, and the spring range is 1.4 m. The tide, as measured at the Coggeshall Street Bridge during a mass transport study (USEPA 1983), appears to be very close to the predicted tide at New Bedford. Therefore, little tidal damping or phase shift appears to occur between the lower and upper harbor and Buzzards Bay, in spite of the harbor's three constrictions. Tides around the margins of Buzzards Bay show only small phase and amplitude differences.

Currents

18. Currents vary sharply over the harbor area because of the harbor constrictions. At the Hurricane Barrier, currents have been estimated at 1.22 m/sec (Ellis et al. 1977). At the Coggeshall Street Bridge, currents were about 1.83 m/sec maximum ebb, 0.91 m/sec maximum flood, 0.52 m/sec average ebb, and 0.34 m/sec average flood (USEPA 1983). Multiple current reversals were reported at the Coggeshall Street Bridge. Reversals during flood tides of between 2- and 26-min duration occurred, with those longer than 6-min involving reversal of the entire flow. Currents over 0.61 m/sec were reported to have opposed the flood tide (USEPA 1983). Current speeds measured over two tidal cycles averaged roughly 0.06 m/sec at two stations in the lower harbor, with a maximum of 0.18 m/sec (Summerhayes et al. 1977). Current speeds in the upper harbor averaged roughly 0.09 m/sec, with a maximum of 0.26 m/sec (USEPA 1983). Net current estimates have not been reported.

Salinities

19. Reported salinity conditions were nearly uniform over the harbor area. In the upper harbor, top-to-bottom differences of less than 1 ppt were common, with differences of as much as 18 ppt reported at the Coggeshall Street Bridge after a heavy rain. Salinities in the upper harbor were typically 26 to 30 ppt and have been reported as low as 12 ppt at the surface after a heavy rain (USEPA 1983). The lower harbor also appears to be vertically well mixed with generally 1- to 2-ppt top-to-bottom differences in salinity. Longitudinal gradients in salinities were also small (Ellis et al. 1977).

Suspended material

20. Suspended material measured in the New Bedford Harbor occurred at low concentrations. In the upper harbor, total suspended solids concentrations collected at all depths ranged from about 10 to 40 mg/ℓ. The former was

a more typical value; 40 mg/ℓ values occurred after the passage of a storm event. In that storm event, 1.27 cm of rain fell over a 4-hr period, and winds were from the south and strong, with gusts of 112.6 km/hr reported (USEPA 1983). The response of the system to this event was modest relative to the probably frequency of the storm occurrence, a three- or four-fold increase in total suspended solids. Routine monitoring of total suspended solids in the lower harbor showed concentrations generally less than 10 mg/ℓ, with a maximum of 26 mg/ℓ over a 2-year period (Ellis et al. 1977). After the passage of Hurricane Belle on 10 August 1976, the maximum concentration of suspended solids collected surface and bottom was 31.5 mg/ℓ at the Interstate 195 bridge. Again, the response of the harbor to a major storm event was a modest increase in total suspended solids. Studies have shown that the volatile suspended solids account for 30 to 50 percent of the total suspended solids at the bottom, while the bed sediments contain generally less than 10 percent volatile solids (Summerhayes et al. 1977). No suspended sediment concentrations have been reported for the freshwater inflow.

Flux of PCBs

21. The flux of PCBs out of the upper harbor had been studied once prior to 1986 (USEPA 1983). Samples were collected from nine stations at the Coggeshall Street Bridge at irregular intervals during three consecutive tidal cycles. Eight samplings were completed. Flux was estimated by multiplying average flows and average PCB concentrations. An open, vertical sample bottle was used to collect water samples. A single sample was taken that included the free surface, and that sample was found to have the highest PCB concentration for the survey. PCBs were found to be generally higher near the surface (average 0.98 µg/ℓ) and were not well correlated to suspended material concentration (USEPA 1983).

Bed sediments

22. Bed sediment characteristics of New Bedford Harbor have been the subject of a number of studies, usually in conjunction with pollutant evaluations. The physical properties of the near-surface sediments are important to the sediment migration task of the EFS. Hydrodynamically sized grain distributions were obtained in a previous study by Huidobro and DeLorenzo (1983) at eight stations in the upper harbor and 17 stations in the lower harbor. Surficial grabs for these stations were subsampled at 0 to 4 cm and 4 to 8 cm. Seven cores from the upper harbor were split into top and bottom 10-cm

sections and were analyzed for size gradation, water content, and oil and grease (Geotechnical Engineers, Inc. 1982). A settling test performed on a composite of the seven upper-harbor cores at 31-g/ℓ concentration showed the material to have a relatively high settling rate (~0.1 cm/sec) (Energy Resources Company 1982). Moisture contents for 10.16-cm core sections from the 0- to 30.48-cm depth were reported by Malcolm Pirnie, Inc. (1982). Fourteen samples were taken by grabs and corer from the upper and lower harbors of New Bedford. Variations of sediment properties (texture and visual classification) over 0- to 5-cm and 5- to 25-cm depths were reported (Ellis et al. 1977, Summerhayes et al. 1977). The clay fraction of the New Bedford Harbor sediments consists of chlorite, mica, and minor amounts of quartz (Ellis et al. 1977). Condike (1986) reported sediment physical and chemical characteristics for Task 2 of this EFS. A review of these results is included in Report 11 of the series.

Tidal Cycle Survey Methods

23. The WES HL collected field data in upper New Bedford Harbor as part of the USACE's EFS. This section summarizes the field data collection scope and procedures. Field data were reduced and analyzed; the results are presented in Part III.

Field sampling plan

24. In general, field data were collected during three synoptic boat surveys at nine stations, as shown in Figure 3. At each station, current speed and direction, total suspended material, and salinity were sampled at three depths intermittently over a period of 13.5 hr (27 samplings and 729 samples). The sampling interval was 30 min for stations 4 through 6, and 45 to 60 min for stations 1 through 3. Flow-proportioned samples were composited at 30-min intervals (25 samplings and 225 subsamples), and surface floatable samples were taken at hourly intervals (12 samples) at the Coggeshall Street Bridge (stations 4, 5, and 6) for PCB analysis. Tide gages were operated at Clark's Point, near Popes Island, and at the upstream side of the Coggeshall Street Bridge. A water level gage and automatic suspended material sampler were operated at the Saw Mill Dam.

25. Three boats were used for the surveys. Station locations for three stations above and three stations below the Coggeshall Street Bridge along the

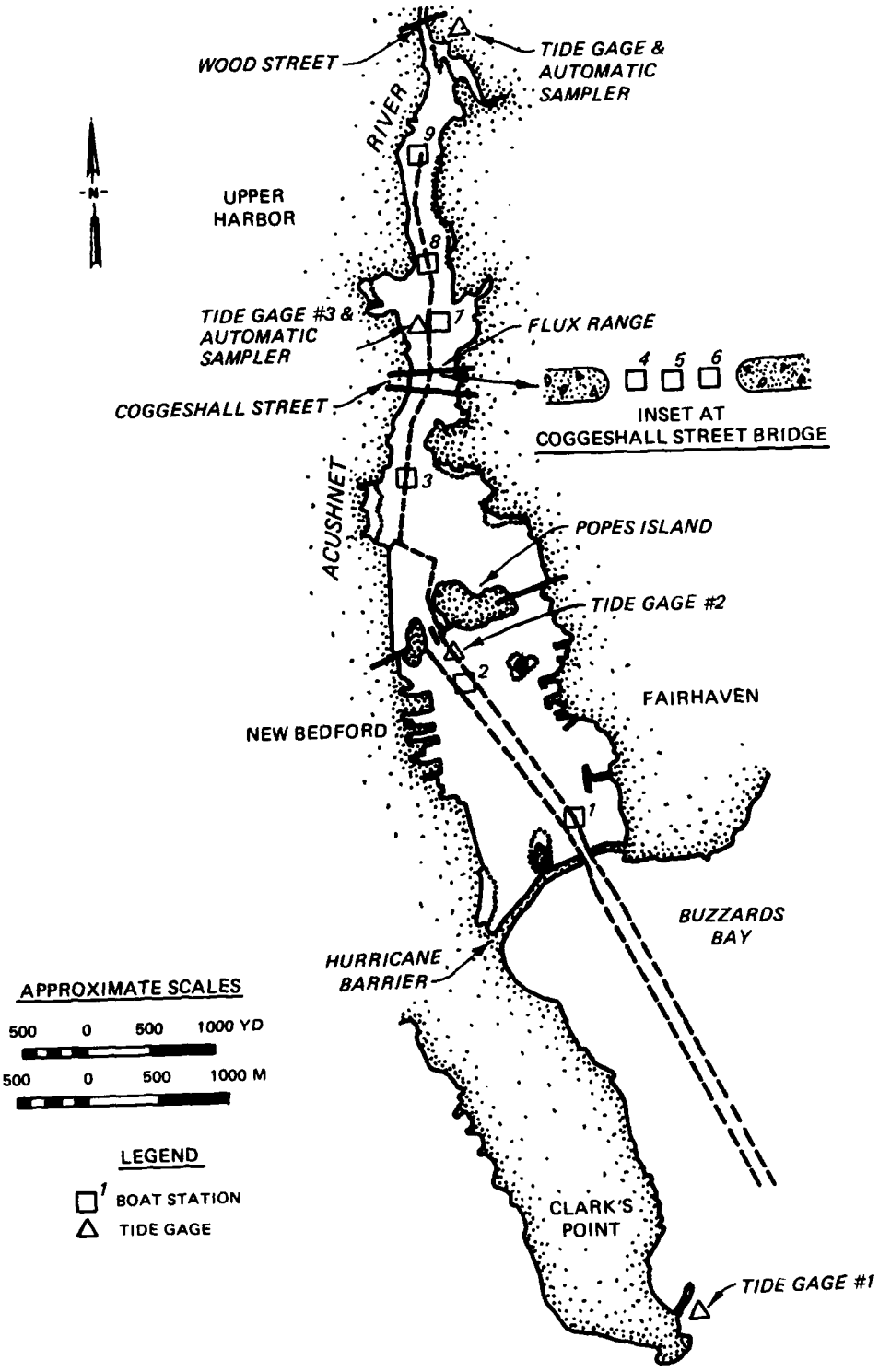

Figure 3. Sampling and gaging locations for New Bedford Harbor

waterway were marked with buoys and included three locations for which data bases exist. The survey boats moored to the buoys and held stationary during sampling. At the Coggeshall Street Bridge, two hand lines were stretched across the bridge opening above water. The survey boat was manually moved between sampling stations, marked on the bridge, by the hand lines. Stations at the bridge were located at the horizontal locations of 17, 50, and 83 percent of the cross-sectional area at mean tide level as calculated from cross-sectional information.

26. Current velocities were measured using Gurley Model 665 vertical-axis, cup-type impeller-meters in conjunction with a magnesyn directional indicator. These meters were calibrated before each survey. Water samples for total suspended solids and salinities were taken with a 12-V (d-c) pump using 15.24 m of 0.63-cm inside diameter plastic tubing attached to the current meter support. Pumps and tubing were flushed with three system volumes before individual samples were drawn. The samples and current measurements were taken at a depth of 0.6 m, middepth, and 0.6 m above the bottom. In addition, currents were measured at the 0.15-m depth, when practical. Pumped samples were stored in 227-ml plastic bottles. Large-volume water samples were taken at middepth using a 10-ℓ horizontal Niskin sampler and stored in 19-ℓ plastic sample containers. All suspended solids and salinity samples were kept cool (4° C) and dark and were analyzed within 7 days.

27. Samples for PCB analysis were collected with ISCO Model 2700 automatic samplers and on fiberglass cloth pieces. The sampler was fitted with 7.62-m Teflon lines. PCB samples were composited in 9.5-ℓ glass sample containers with Teflon lids. Two sample containers were used, one to composite ebb samples and one to composite flood samples. Sampling containers, lines, and pumps were washed with acetone, and intakes were covered with acetone-washed aluminum foil just prior to the beginning of sampling. Sampling intakes were located near the velocity meter, about 0.30 m above a 34-kg wire depressor, and faced into the flow. Once the sample intake was lowered through the water surface, the aluminum cover was removed and the sampler was not brought up through the water surface again until the end of the survey. During the survey, current speeds were measured, and a volume of sample equal to 40 ml per 1 fps* of current speed was drawn into the appropriate sample,

* A table of factors for converting non-SI to SI (metric) units is presented on page 5.

determined by the direction reading of the current meter. The ISCO sampler air-purged the sample intake line before and after each sample. After the survey, composite samples were packed in ice and transported in insulated containers by air to WES for immediate analysis. PCBs as Aroclors were assayed in the composites.

28. Surface-floatable samples were collected using pre-acetone-rinsed 0.093-sq m pieces of fiberglass cloth. The fiberglass cloths were stretched on a prerinsed aluminum frame and touched at random to the water surface away from the side of the boat at the center bridge station every hour during the surveys. The fiberglass cloths were carefully removed from the frame and placed in a prerinsed 3.8-ℓ, wide-mouth glass jar with a Teflon lid liner. Total PCBs as Aroclors were determined by hexane extraction of the fiberglass cloth samples.

29. Tide gages were installed at the three locations mentioned earlier and were operated for the duration of the field study. Fisher & Porter Model 1550 recorders were used. The timers were checked for accuracy before deployment. Datum planes were established for the gages by NED survey personnel. The difference between mean low water and National Geodetic Vertical Datum is 0.49 m. Tide gages were fitted with a hydraulic damper to eliminate wind-wave effects. Tide gages recorded every 6 min on foil-backed paper tape. The inflow gage used the same type recorder and recorded every hour. Automatic suspended sediment samplers were installed at the Saw Mill Dam overflow and upstream of the Coggeshall Street Bridge and were operated throughout the field study. Samplers were set to composite two slacks and two strength-of-flow samples into one bottle. Samplers and recording gages were serviced every 3 weeks.

Sample handling and analyses

30. The WES HL performed laboratory analyses on samples to determine total suspended solids and salinity concentrations. Total suspended solids were determined according to a standard nonfilterable solids method using Nuclepore 0.45-μm pore-size filters. Selected samples were also used to determine volatile solids, using glass fiber filters and a standard method. Salinities were determined by specific conductance, using a calibrated Beckman instrument. The accuracy of this instrument has been found by calibration with traceable standards to be ±0.3 ppt. The WES EL performed the required PCB analyses.

31. Specific analytical methods for PCBs were consistent with those established by EPA method 608 (40 Code of Federal Regulations Part 136), except that a capillary column, rather than a packed column, was used for the gas chromatograph. A random blank surface floatable sample was included in the analyses. The PCB samples were specially labeled immediately after the field surveys for chain-of-custody, and logs were kept of all transfers. The PCB samples were kept under lock at all times.

32. The three surveys were conducted on 6 March, 24 April, and 5 June 1986. Data from survey boat sheets were keyed into computer files. Listings and plots were made for each station and depth for salinity, suspended sediment, and current speed (ebb and flood direction).

33. Data were used in the adjustment of hydrodynamic models and as boundary conditions in Part VI. Data were analyzed by flux-decomposition methods to evaluate the fluxes of salinity, suspended sediment, and PCBs and to identify dominant processes responsible for these fluxes. Velocities and water levels were used to compute tidal volumes at the Coggeshall Street Bridge. Details and results of these analyses are presented in Part III.

Sediment Resuspension Survey Methods

34. As a part of Task 5 of the EFS, composite sampling in the upper harbor was conducted during the week of 31 March 1986. The composite sampling (collection at multiple sample sites to be combined into one representative sample) was carried out by an NED contractor who took box core samples. The opportunity to sample sediment disturbances during the composite sampling was used by the HL to collect and test samples of sediment and contaminant releases under actual field conditions. The magnitude of suspended sediment generated by dredging is related to the hydraulic and sediment conditions at the dredging site, as well as the characteristics of the dredging equipment utilized. Dredging equipment and techniques are reviewed in Report 10. The observations of composite sampling gave an indication of possible dredging resuspension rates for upper-harbor cleanup dredging. The objectives of the field data collection were to:

a. Obtain samples of suspended solids to determine sediment resuspension rates and the settling velocity characteristics of the material(s).

b. Capture water and floatable samples to determine contaminant release.

Location of sampling

35. Composite sampling was performed at a number of upper-harbor sites by the contractor using a 0.31-m square box corer rigged on a small, self-powered barge. During the coring operation, samples were collected at upper-harbor sampling grid cells G-17 and J-8 (Figure 4).

Sampling equipment

36. To minimize disruption of the water column in the vicinity of the test site, a single boat was used for sample collection. The boat was equipped with an over-the-side array consisting of a Teflon sampling tube, velocity meter, and 34-kg wire depressor. Collection equipment for floatable sampling and camera equipment (polarized filters, color, and color infrared films) were also carried onboard. Sample bottles for floatable and contaminant water samples were 3.8-ℓ acetone-rinsed glass jars with Teflon lid liners. Suspended solids and settling samples were stored in 227-ml and 19-ℓ plastic bottles, respectively. Three personnel operated the boat, collected samples, and recorded data. One other supervised. Personnel wore full protective gear while in close proximity (<92 m) to composite sampling activities.

Sampling procedure

37. Near-field samples were collected approximately 5 m from the actual coring site. Samples were taken very close to the point of sediment disturbance to avoid settling of particulates. Samples for settling velocity and suspended material testing were collected. Water and surface floatable samples were collected for PCB analysis. Samples were also collected at a radius of 46 m from the core site for suspended material analysis.

38. The sampling boat rendezvoused with the coring barge on the morning of 31 March 1986. The day was sunny, 10° to 18° C, with northwesterly winds 16 to 24 km/hr. The coring barge had to wait for the tide to increase depths before moving into position at the J-8 grid (Figure 4). The barge stirred up much material while moving into position, by direct contact with the bed and by prop wash. The depth was 1 m.

39. Near-field sampling, consisting of surface-floatable, 3.8-ℓ, 19-ℓ, and 227-ml samples (at about 1/4 and 3/4 depth), was performed between 1011 and 1018 EST. The composite coring started at 1030 and lasted until 1100 EST.

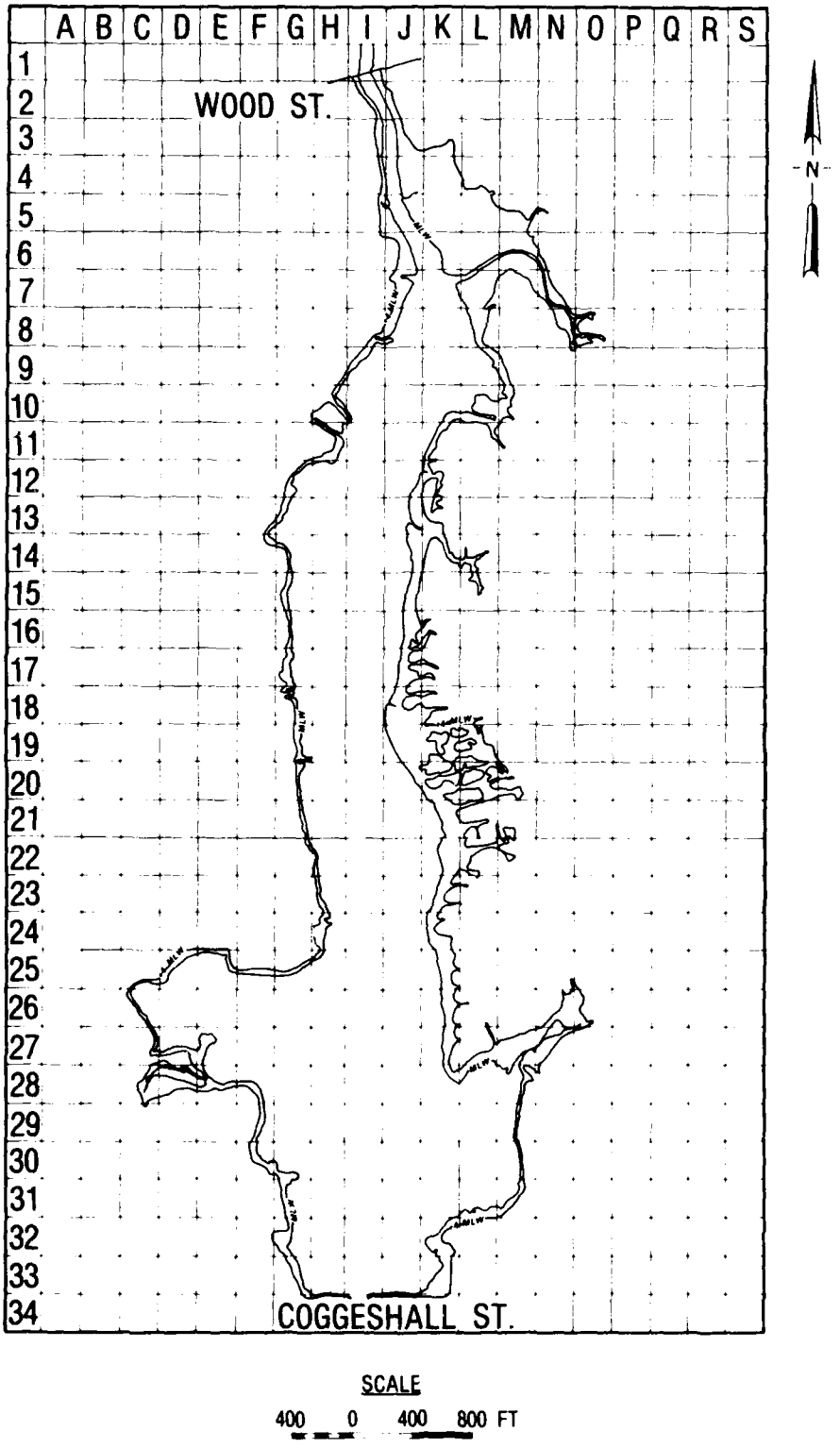

Figure 4. Sampling grid for upper New Bedford Harbor

Near-field samplings were again performed between 1044 and 1048 EST, and between 1051 and 1102 EST at 3/4 depth.

40. While the coring barge remained in position, the sampling boat moved to a distance of about 46 m from the coring site. Samples were collected in 227-ml bottles for suspended material analysis at intervals around the coring site between 1108 and 1117 EST at 3/4 depth.

41. At 1130 EST, the coring barge moved from J-8 grid and was in position at G-17 grid at 1205 EST. The sampling boat moved alongside and collected near-field background samples from 1222 to 1225 EST before coring began. Background samples for suspended material were at surface, middepth, and bottom. All other water samples were from 3/4 depth. The depth at position G-17 was 1.6 m.

42. Composite coring started at 1222 and lasted until 1250 EST. Near-field samplings were repeated at 1230-1232 EST and 1239-1241 EST. The sampling boat moved away from the coring site and collected 227-ml suspended material samples between 1255 and 1302 EST at a distance of 46 m at 3/4 depth.

Sample analysis

43. Samples for total suspended solids and settling velocity were analyzed by the HL. Total suspended material was determined by a standard method using 0.45-μm Nuclepore filters. Settling velocities were determined by using a 10-cm-diam by 2-m-high clear plastic settling column and pipette analysis. Samples were resuspended by shaking for 5 min prior to introduction into the settling column.

44. Contaminant samples consisting of six floatables samples and six water samples were analyzed by the EL, WES. Two floatable samples and one water sample were broken in shipment. PCB Aroclors were determined.

PART III: RESULTS OF PROTOTYPE SEDIMENT AND CONTAMINANT STUDIES

45. One of the objectives of the WES HL field data collection program in New Bedford Harbor was to establish baseline conditions. The baseline conditions were required to determine movements and migration of contaminants out of the upper harbor through an understanding of the physical processes active in the transport of PCBs from the upper harbor. The baseline also provides a gage for comparison of contaminant flux under existing conditions to contaminant fluxes for dredging and dredged material disposal alternatives.

46. Conditions/processes considered for the baseline included:

a. Fluxes of PCBs at the Coggeshall Street Bridge and fluxes of suspended material along the length of the estuary.

b. Estuarine flow and salinity conditions along the length of the estuary for the three field surveys performed.

c. Resuspension potential for bottom sediments, and transport mechanisms for suspended material.

d. Laboratory studies defining other important sediment behavior (these studies and methods are presented in Part IV).

47. Field data were collected during three surveys. Survey dates, tides, freshwater flows, and winds are given in Table 1. Nine stations were sampled repeatedly over three tidal cycles. Figure 3 shows station locations.

48. Three stations were located across the opening of the Coggeshall Street Bridge which forms the boundary between the upper and lower harbors. Current speed and direction, salinity, and suspended material were sampled. In addition, flow-proportioned composite samples and surface-floatable samples were collected for PCB analysis. Details of the data collection were previously given.

49. Analyses of the field data were performed, and the results are summarized below.

Fluxes at the Coggeshall Street Bridge

50. Survey data were used to calculate tidal volumes for ebb and flood tidal phases. Current velocities were integrated spatially over the bridge cross section, correcting for tide height, and were integrated in time to determine total discharge for each tidal phase. The upper harbor's surface area is about 800,000 sq m at mean tide. The cross-sectional area at the

bridge is about 141.6 sq m to mean tide level. Tables 2 and 3 show results expressed in billions of litres. Tables 4 and 5 list PCB-Aroclor sample concentrations.

PCB

51. Ebb and flood PCB Aroclor concentrations were multiplied by the tidal volumes to obtain ebb and flood PCB fluxes. The difference between ebb and flood fluxes is the tidal net flux.

52. The PCB flux results are summarized in Table 2. Note that the results for the second survey were revised in 1988, after a reexamination of previous analyses. Observed net fluxes were always seaward (negative) with a mean net flux of -1.25 kg per tidal cycle. A source of PCBs to the flow of the upper harbor was indicated, confirming the results of the USEPA (1983).

53. There are biases in the observed fluxes introduced by tidal asymmetry. If the ebb tide range and tidal volumes are greater than those of the flood tide, then the fluxes are biased toward the ebb phase and vice versa. To remove tidal bias, tide-corrected fluxes were calculated and are shown in Table 2. Tide-corrected fluxes were computed as the sum of net-flow fluxes (freshwater volume times mean concentrations) plus tidal-pumping fluxes (the difference between ebb and flood concentrations times the mean tidal volume). The two flux mechanisms included in the tide-corrected fluxes will be discussed later.

54. The tide-corrected net PCB fluxes were also seaward, with a mean net flux of -1.55 kg per tidal cycle. The dominant mechanism for PCB net flux out of the upper harbor is tidal pumping, which will be described later. PCB concentrations were generally lower on the flood than on the ebb tide, and the "to-and-fro" tidal motions effectively disperse contaminants seaward, either attached to particles or dissolved. Further discussion of the mechanisms responsible for seaward PCB flux is given in the section titled "Suspension/Bed Exchange of PCB" (paragraphs 80-81).

55. An EPA Response Team (USEPA 1983) studied PCB fluxes at the Coggeshall Street Bridge in 1983 using a slightly different method. Their results were similar in magnitude to the present study, and net fluxes were always seaward. In reviewing and comparing our results to USEPA's, a discrepancy was noted between tidal volumes and tidal prisms. The USEPA's computed cross-sectional area for the bridge was apparently too great, but the PCB fluxes can be easily corrected. The corrected average total-PCB net flux was -0.86 kg,

with a range of -0.77 to -0.98 kg per tidal cycle. Table 3 shows corrected USEPA results and tide-corrected USEPA results. Averaging these previous results with results from this study, the mean net PCB flux out of the upper harbor was -1.23 kg per tidal cycle.

56. Floatable material samples at the bridge were low in PCBs, mostly below analytical detection limits (0.01 µg/0.093 sq m). Fluxes of PCB in the floatable transport mode could not be accurately estimated but were at least several orders of magnitude less than that carried by the flow.

Suspended material

57. Fluxes of total suspended material (TSM) at the bridge stations were estimated by integrating discrete measurements of velocity and TSM over space and time. Results are shown in Table 2, along with tide-corrected net fluxes. Flow-proportioned TSM concentration values for ebb and flood phases were calculated based on the tidal volumes and are included in Table 2. Results from the USEPA study are shown in Table 3.

58. The net flux of TSM was always found to be landward or upstream, although fluxes in either direction were at least twice net values. About one third of the sediment that enters the upper harbor on the flood tide settled there during that tide. Average net flux of TSM into the upper harbor was about 2,200 kg per tidal cycle. The freshwater inflow adds some additional sediment, on the order of a several hundred kilograms per tidal cycle.

59. Shoaling resulting from the deposition of 2,500 kg of sediment per tidal cycle amounts to 3 mm per year when spread over the entire surface area of the upper harbor at a bulk wet density of 1.5 g per cubic centimetre (775 dry g/ℓ). Actual sedimentation rates will vary widely over the upper harbor, depending on current, wave, and depth regimes. Summerhayes et al. (1977) estimated sedimentation rates in the lower harbor to be about 40 mm per year in previously dredged areas and 2 to 3 mm per year for Buzzards Bay.

Estuarine Conditions

Conditions near the proposed diked disposal site

60. The proposed diked disposal site for the pilot study is located on the west side of the upper harbor, about 0.4 km upstream from the Coggeshall Bridge, on the downstream side of a cove (Figure 2). Wave and current

information were requested from NED for dike protection design purposes. No source of specific information exists for the proposed site; however, the surveys are a source of general information for this area.

61. The HL tidal-cycle survey made 24 April 1986 was relatively extreme with respect to both waves and currents. Tidal range was 1.65 m, and freshwater inflow was 1.53 cu m/sec. Winds at the beginning of the survey were 12.9 to 19.3 km/hr but increased to 32.2 to 48.3 km/hr from the northeast.

62. The proposed site is closest to survey station 7 (see Figure 3), and numerical hydrodynamic model results indicate that the currents are very similar at those two locations. Maximum current speeds for station 7 were 0.37 m/sec on the flood tide and 0.31 m/sec on the ebb tide at the surface. The root-mean-square of the instantaneous depth-averaged component of the tidal currents was 0.19 m/sec.

63. Waves were not estimated for the site at the time of the survey. Observations were made at the Coggeshall Bridge of waves reaching 0.92 m during the flood phase of the survey. However, the region of high wave heights was restricted to the deeper channel area upstream from the bridge and dropped off rapidly in shallow, more sheltered areas with lower current speeds.

64. Figure 5 is a photograph taken during the April survey. It was taken from under the bridge looking upstream into the cove area. Station 7 was located to the right of the small structure (on which a tide gage was mounted) in the photograph. This photograph and recollections of general conditions indicate that wave heights at the proposed site on that day were less than 0.31 m.

Suspended material fluxes

65. Suspended material concentrations were found to be lower in the most seaward stations and to increase upstream. Figure 6 shows the longitudinal distribution of TSM concentration averaged for the April and June surveys. There was very little TSM variation between these surveys. The most dominant flux mechanism for suspended material was tidal pumping at depth.

66. Three important estuarine transport processes for suspended material were evaluated along the length of the estuary using the data--transport by net flow, vertical circulation, and tidal pumping. Descriptive estuarine parameters were also calculated from the field data. Results are presented in Tables 6-11 and are discussed in the paragraphs that follow. Negative signs applied to fluxes or velocities indicate movement in the seaward direction.

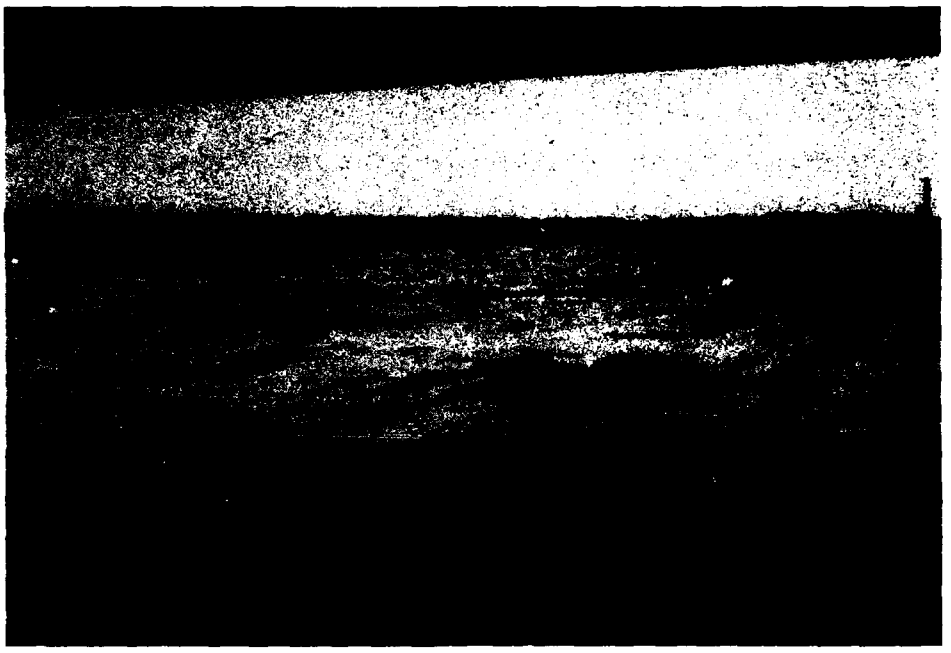

Figure 5. Wave conditions on 24 April 1986 upstream of the Coggeshall Bridge

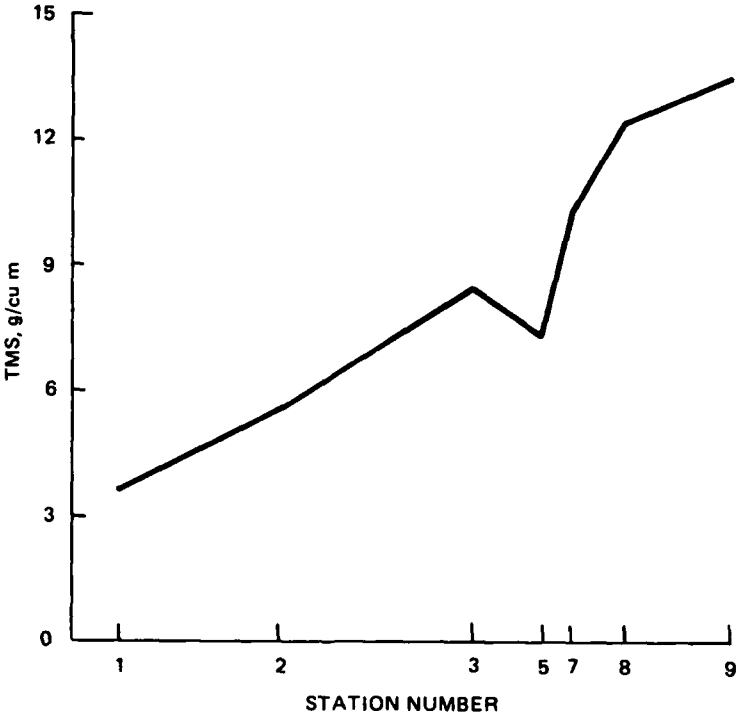

Figure 6. Longitudinal distribution of TSM concentration

67. Net-flow transport is quasi-steady with respect to the tide and is produced by freshwater inflow, long-period oscillations, or tidal asymmetry. Over a period of a week or more, freshwater inflow makes up the greatest fraction of the net flow. Over a single tidal cycle, however, tidal asymmetry and long-period oscillations represent the largest component of net flow and can mask the net flow produced by freshwater inflow. For instance, a -0.85-cm/sec freshwater flow produces a net flow velocity of -0.0061 m/sec at the Coggeshall Street Bridge, while a tidal asymmetry of 0.15 m (difference between sequential high or low waters) produces a residual or net-flow velocity of +0.019 m/sec.

68. Vertical circulation is produced primarily by density differences resulting from freshwater inflows. Vertical circulation is often pronounced in stratified estuaries. Residual flows produced by geometry or by tidal wave deformation can also contribute to vertical circulation.

69. Tidal pumping is a process that transports material in the horizontal direction, often upstream in estuaries. If at a station the overall suspended sediment concentrations are higher on the flood than on the ebb tide, and if the tidal flows are equal in both directions, then depth-averaged tidal pumping in the upstream direction is indicated. If near-bed suspension concentrations are higher on the flood than on the ebb tide (typical), and especially if the near-bed flood currents are greater than currents on the ebb tide (also typical), then tidal pumping of suspended sediments at depth in the upstream direction will occur.

70. A datum at some station, time (t), and depth (z) can be decomposed into a series of components representing depth-means, time-means, instantaneous values, and vertical deviations from depth-means. For example, suspended concentration (C) can be decomposed as

$$C(z,t) = \bar{C}o + Cov(z) + Ci'(t) + Civ'(z,t) \qquad (1)$$

where

o = steady (tidal-averaged)

v = vertical deviation from the depth mean

i = instantaneous component

and where the overbar indicates depth averaging and prime (') indicates time-varying components. Velocity and salinities can be decomposed in the same manner, except that two additional steady-velocity components arise from Stokes drift. Stokes drift arises from the mass transport by waves. It is a steady Lagrangian component (with vertical deviations) that is not directly measurable at a single fixed point. It was calculated from the data as the time mean of flow displacement times the horizontal velocity gradient. Stokes velocities were not calculated for the Coggeshall Street Bridge stations (4, 5, and 6).

71. Tables 6, 8, and 10 show estuarine characteristics as velocity and salinity components for the three surveys. Incomplete tidal cycle data, caused by freezing equipment, prevented analysis of all but the bridge stations from the March survey. Instantaneous components were time-averaged by the root-mean-square method. Thus, $\langle \bar{U}i \rangle$ and $\langle \bar{S}i \rangle$ are the root-mean-square of the depth-averaged instantaneous component and are characteristic of the strength of the tidal flow. The time-averaged top-to-bottom salinity difference is twice the $\bar{S}ov$ value.

72. Tidal fluxes of suspended material and salinity were decomposed. Over a tidal cycle, the flux of suspended material was expressed as

$$\text{Flux of } C = A(\bar{U}o\bar{C}o + \overline{UovCov} + \bar{U}so\bar{C}o + \overline{UsvCov} + \overline{UiCi} + \overline{UivCiv}) \qquad (2)$$

where

A = cross-sectional area

$\bar{U}so$, $\bar{U}sv$ = depth-averaged Stokes drift and vertical deviations, respectively, from the depth mean

73. Tables 7, 9, and 11 show flux components for suspended material. Components $\bar{U}o\bar{C}o$, $\bar{U}so\bar{C}o$, and $\overline{UiCi}$ are depth means. Terms $\bar{U}o\bar{C}o$ and $\bar{U}so\bar{C}o$ represent suspended material transport by depth-mean flows. Term $\overline{UiCi}$ is the cross correlation between depth-mean velocity and suspended material concentrations and is the depth-mean tidal pumping described earlier.

74. Flux components $\overline{UovCov}$, $\overline{UsvCov}$, and $\overline{UivCiv}$ are vertical deviations from depth means. Terms $\overline{UovCov}$ and $\overline{UsvCov}$ represent suspended material transport by steady vertical shear. They are the vertical circulation components described earlier. Component $\overline{UovCov}$ is closely associated

with transport by gravitational circulation. Component $\overline{UivCiv}$ is the cross correlation between vertical deviations in the depth-mean velocity and suspended material concentrations and is the depth-varying tidal pumping described earlier. Figure 7 shows the longitudinal distribution of total TSM flux and dominant flux components.

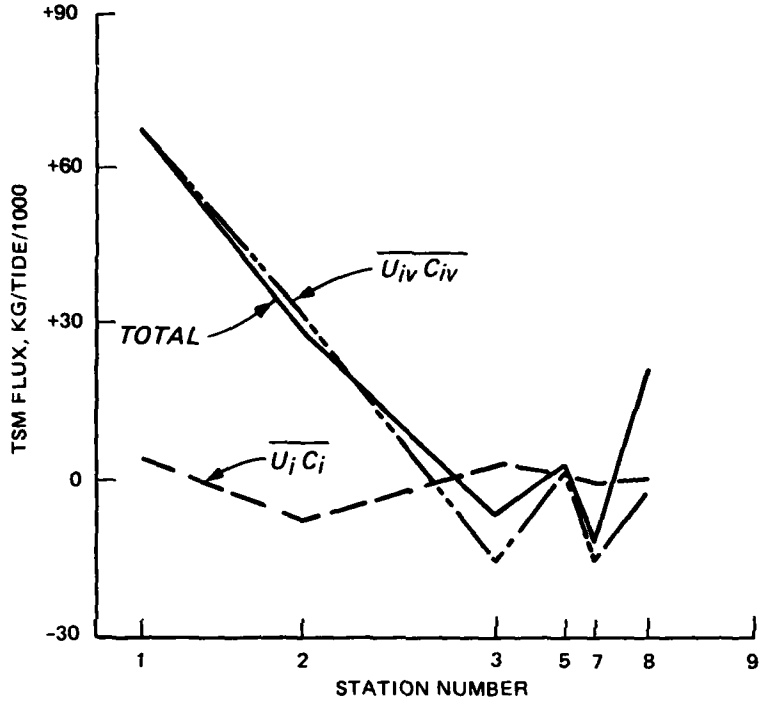

Figure 7. Longitudinal distribution of total TSM flux and dominant flux components

Mechanisms for TSM Transport

75. Postma (1967) described how the processes of settling and scour lags can lead to upstream suspended transport. At New Bedford, lags in settling and redispersion of TSM and tidal variations in vertical TSM stratification produced upstream transport. Both mechanisms depend on some asymmetry in the tidal flow conditions and are described in the following paragraphs.

Time scales for settling and redispersion

76. Fine-grained suspensions have vertical distributions dependent on particle Peclet number (P_e) defined as

$$P_e = \frac{HW_s}{K_z} \tag{3}$$

where

H = depth

W_s = settling velocity of the sediment

K_z = vertical diffusivity

During periods of slack water, turbulence in the flow subsides, and suspended material settles toward the bed. The time for an average particle to settle fully to the bed, $T_s = H/2W_s$, is relatively long due to the small settling velocities of fine-grained sediments. Redispersion time scale for TSM depends on the vertical diffusion time scale for passive matter, $T_m = H^2/4K_z$, and P_e. The redispersion time scale is defined as $T_r = T_m(1 + P_e/2)$.

77. Data from the April (spring tide) and June (neap tide) surveys were used to calculate settling and redispersion time scales. Since the time scales are relatively long, averages of root-mean-square tidal-fluctuating components ($<\bar{U}i>$) were used to estimate shear velocity using a Manning's coefficient of 0.02. A median W_s of 0.1 mm/sec is representative of aggregate size analyses and settling tests and was used to characterize TSM. Results were:

	Time Scales, thousands of seconds			
	April Survey		June Survey	
Location	T_s	T_r	T_s	T_r
Lower Harbor	43.5	6.5	43.5	5.5
Upper Harbor	18.5	1.8	18.5	3.7

Both time scales, but particularly T_s, are long with respect to the time scales for tidal currents (~22,000 sec) and thus produce phase differences between tidal velocities and TSM concentrations (tidal pumping). Redispersion time scales were much shorter than settling time scales. Maximum redispersed TSM produced by the highest tidal currents, generally near low water in New Bedford, is transported in the flood direction, producing upstream tidal pumping.

Tidal variations in TSM stratification

78. The effects of TSM stratification on longitudinal transport were quantified by calculating vertically averaged TSM transport velocity as

$$U_{tsm} = \frac{\int CU \, dZ}{\int C \, dZ} \tag{4}$$

In a completely vertically mixed system, U_{tsm} would equal $\bar{U}$. The ratios of U_{tsm} to $\bar{U}$ were calculated for flood and ebb tidal phases and found to be on average 1.8 percent higher on the flood tide phase. Ratios of U_{tsm} to $\bar{U}$ ranged from 0.95 to 1.0. Given equal tidal velocities on the flood and ebb tidal phases, the difference between flood and ebb U_{tsm} values would be sufficient to pump TSM upstream against the very small freshwater net velocities.

79. Vertical mixing was found to be more intense during flood tidal phases. The Munk-Anderson vertical diffusivity function based on the gradient Richardson number was evaluated at each sampling time and gives an indication of vertical mixing as the ratio K_z/K_{zo}. Term K_{zo} is the vertical mixing under homogeneous density conditions. The plot of the ebb and flood averages for the April and June surveys (Figure 8) shows that vertical mixing is more complete for the flood tidal phase.

Suspension/Bed Exchange of PCB

80. The migration of PCB contaminants from the sediments in upper New Bedford Harbor is a complex process involving the physiochemical behavior of the sediments and the contaminants, and possibly biological factors. The continued release of PCBs in the presence of ongoing general deposition implies that contaminant material is able to migrate by some mechanism to the surface of the sediment bed. From this point, contaminants could be released into the overlying flow by diffusion of a soluble phase, by biological action, by desorption, by erosion, or by a particle exchange mechanism. The scope of the WES HL work included only physical migration of sediments and associated contaminants, normally thought of as involving erosion of bed sediments. However, erosion in upper New Bedford Harbor is normally very slight and produces flux primarily in the upstream direction.

81. PCBs attached to sediment particles at the surface of the bed in upper New Bedford Harbor could be exchanged into the overlying sediment suspension, along with sediment particles by a physical particle exchange mechanism, and thus would be mobilized for possible escape from the upper harbor.

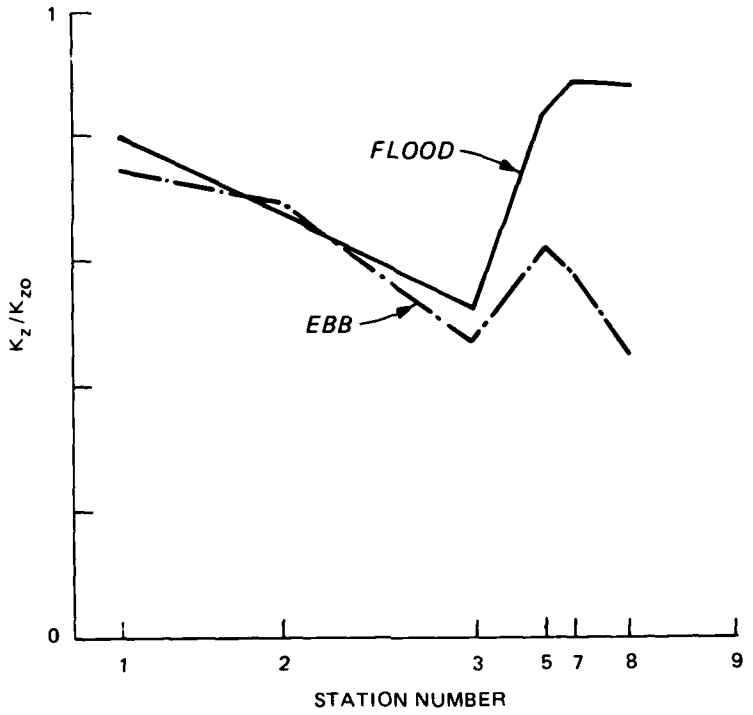

Figure 8. Vertical mixing for flood and ebb tides

The net vertical transport of contaminant resulting from particle exchange would be in the direction of reduced concentrations. A more complete description of a physical particle exchange mechanism is presented in Appendix A, not as the only or most dominant mechanism for the escape of PCBs from the sediments in upper New Bedford Harbor but one that is known to operate in fine, cohesive sediments and suspensions. That analysis indicated that particle exchange could be an important transport mechanism.

Resuspension During Composite Sampling

82. Figures 9 and 10 show schematically the suspended material results at J-8 and G-17 grid cells, respectively, during composite sampling.

83. The coring barge stirred up a considerable amount of material while moving into position at J-8 grid. The barge touched bottom, and the engine was run at full power to maneuver into and alter position slightly during coring operations. The coring operation was therefore relatively "dirty" in generating suspended material.

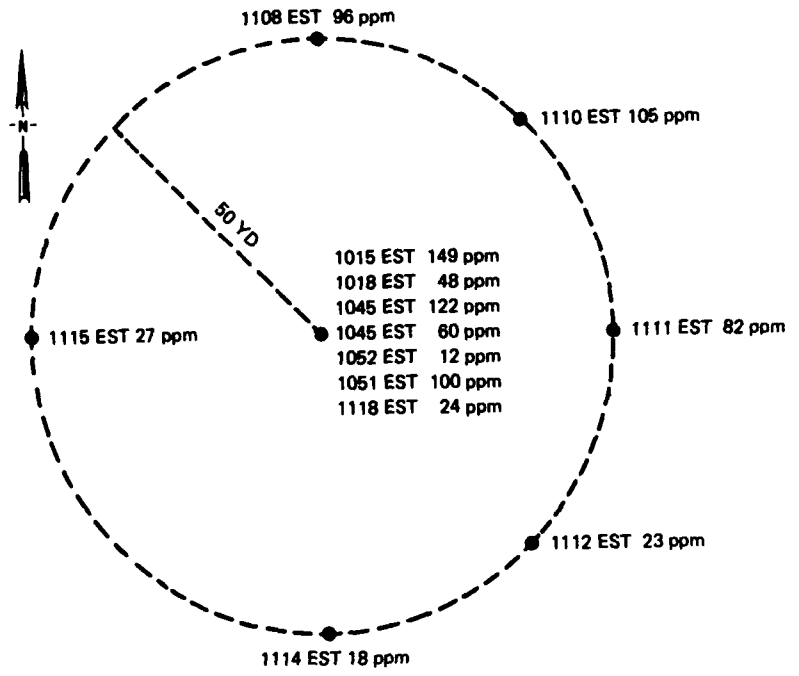

Figure 9. Suspended material concentrations around J-8 grid, 31 March 1986

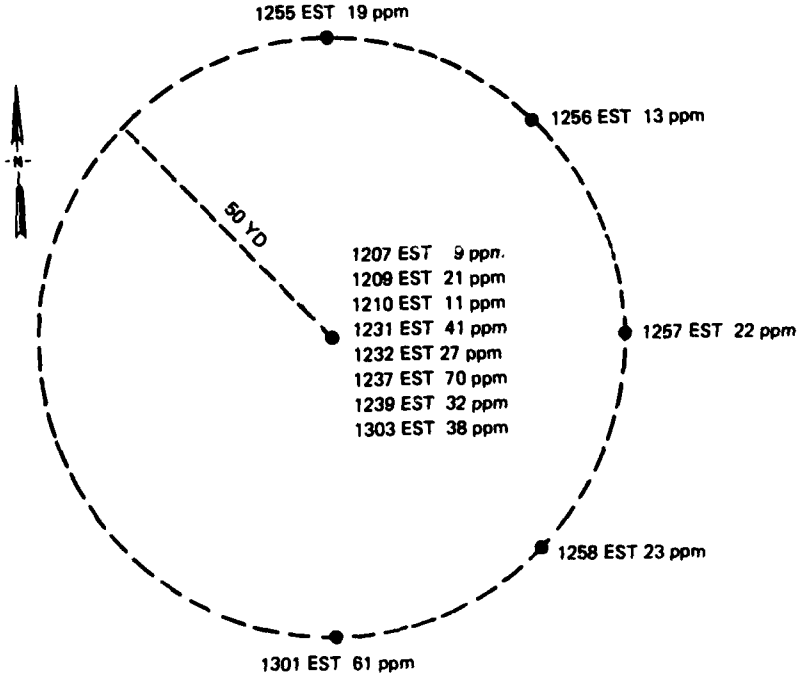

Figure 10. Suspended material concentrations around G-17 grid, 31 March 1986

84. The average suspended material at the center of the J-8 grid was 112 mg/ℓ, excluding the spurious sample taken at 1052 EST. The background suspended material concentration was 23 mg/ℓ. The plume was detected at three of the 46-m-radius sampling points and averaged 94 mg/ℓ.

85. The average suspended material concentration at the center of G-17 grid was 43 mg/ℓ, and the average background was about 17 mg/ℓ. The plume from composite coring was only detected at one station at 46 m, and that sample had a higher concentration (61 mg/ℓ) than the average of the center samples.

86. Table 12 shows settling velocity results for two of the sampling periods at the J-8 grid. All other samples were low in concentration and contained stringy material that prevented reliable analysis. Settling rates were used to characterize the suspended material and to calculate resuspension rates. Settling rates of the suspended material sampled were relatively high for fine-grained material.

87. Resuspension rates were calculated from the data by several methods, as shown in Table 13. Median settling velocities were used to characterize the settling of the resuspended material. Concentrations near the coring sites and out 46 m were fit with a 2-D vertically averaged plume model to estimate resuspension rates. A description of that model is included in Part V. Also, concentrations around J-8 were directly integrated over the sampling area observed at 46 m to obtain another estimate of resuspension transport rate a short distance from the coring site. The J-8 resuspension rate estimates should be considered most reliable, since they are based on greater numbers of plume samples. The average resuspension rate was about 15 g/sec if the high value (based on a single sample) at G-17 is excluded, or about 20 g/sec if the low value at J-8 is also excluded.

88. Tables 14 and 15 contain PCB analysis results for water and floatables. The sum of the columns is the total Aroclor concentration. The second and third columns from the left indicate the sampling time and the grid cell. Floatable concentrations are in units of micrograms per 0.093 sq m (micrograms per square foot).

89. The mass of particulates in these samples was too low to fractionate them by particle size, and only total Aroclor PCBs were determined. No surface floatable patch or sheen could be distinguished.

90. Floatable material PCB-Aroclor concentrations were small compared

to that carried in suspension. The lowest total PCB concentration measured for a water sample (0.0025 ppm) corresponds to 232 µg per 0.093 sq m, assuming that the sample was representative of the 1-m depth, compared to the highest floatable concentration of 1.55 µg per 0.093 sq m.

91. Another sampling of resuspended bed material was taken 4 June 1986. While proceeding by small boat north of grid cell J-8 (Figure 4) to sample sediments in shallow water, the boat struck bottom and resuspended material with its propeller. Suspended sediment blackened the water and an oily sheen was observed to form a 3- by 5-m patch on the water's surface. A floatable sample and a suspended sample-of-opportunity were taken using the procedures previously described. Tables 16 and 17 show the results of the PCB analysis of those samples, which indicated the highest surface-floatable and suspended PCB concentrations measured during the EFS Task 4 study. The exact location of this sample was not determined.

PART IV: SEDIMENT WATER TUNNEL TESTING

92. Migration of resuspended sediments from the upper harbor depends on their settling and depositional characteristics, and to some extent on erosion characteristics. Dredged material in confined aquatic disposal cells will be subjected to tidal currents and possible erosion prior to capping; therefore, the erosion characteristics of dredged material deposited in the CAD must be known. Unsteady tidal hydraulics make cyclic deposition/erosion a possible mode of transport for fine sediment material to escape the upper harbor. Therefore, both deposition and erosion information were needed to evaluate sediment-associated contaminant migration.

93. Depositional and erosional characteristics of fine-grained sediments vary greatly and are critical to the prediction of sediment and contaminant migration. Direct testing on sediments from the study area was therefore necessary. Testing was complicated by the nature of the sediments, which were highly contaminated with PCBs, heavy metals, and aromatic hydrocarbons.

94. This part presents findings of laboratory studies on deposition and erosion of New Bedford Harbor bottom sediments. Further details of the testing procedure are given in Teeter (in preparation). Information developed in this study was intended to meet requirements for numerical sediment-associated contaminant migration predictions, and for planning and controlling dredging and disposal operations.

95. A total of 12 tests in four test series were performed. All tests included a deposition test phase and at least one erosion test phase. Ten tests included settling test phases. The process description, materials and equipment, test procedures, data analysis, and results are presented in the sections that follow.

Process Description

96. Sediment released into suspension by dredging and disposal operations would represent some specific fraction of the bed material in the upper harbor. Sediment is physically sorted or fractionated during dredging and disposal operations and during the subsequent suspended transport. The objective of the deposition and erosion tests was to characterize the more mobile,

fine-grained New Bedford Harbor sediment, less than 74 μm (silts and clays) and greater than 0.45 μm (colloids), which is hydraulically transported almost entirely in suspension rather than as bed load. Because of the differences in cohesion, settling characteristics, etc., for silts and clays, fine-grained sediment was characterized as a sum of several fractions or components. The fine-grained material can also contain an organic fraction that behaves similarly to cohesive sediments.

Settling

97. Settling is that component of suspended particle or aggregate motion caused by the balance between gravity and viscous drag forces. Settling rates are therefore defined in quiescent native fluid. Settling characteristics affect rates of deposition and the vertical distribution of suspended material.

98. Aggregation is very important to cohesive sediment settling rates and is responsible for clay deposition in estuaries and marine environments. Aggregation of a particular sediment-particle suspension depends primarily on suspended sediment concentration, current shear or velocity gradients, and salinity. Current shear and salinity effects on New Bedford sediments have not been studied. However, previous experiments on the effects of current shear on settling found impacts at shear rates above those encountered within most natural flows (Hunt 1982). Salinity effects on aggregation are greatest between zero and 4 ppt concentration and are not an important factor in New Bedford Harbor, which is almost entirely above this range.

99. Three ranges of concentration-dependent settling usually occur. At low concentrations, aggregate and particle interaction is minimal, and settling is independent of concentration. At intermediate concentrations, settling is enhanced by concentration because of increased aggregation and particle interaction. At high concentrations, aggregate and particle interaction hinders settling.

100. Resuspended sediment concentrations from dredging and disposal operations are expected to initially be in the enhanced settling range. The dependence of settling velocity in the enhanced settling-concentration range has the functional form (Ariathurai, MacArthur, and Krone 1977)

$$W_s = A1\ C^n \tag{5}$$

where

W_s = settling rate or velocity

Al = constant

C = suspended sediment concentration

n = exponent

The exponent n is usually found to be close to 1.33. The concentration range over which Equation 5 applies varies with the cohesive properties of the sediment. Generally, the lower bound is in the range of 10 to 200 mg/ℓ, and the upper bound is in the range of 2,000 to 75,000 mg/ℓ.

101. Fine grained sediment suspensions usually have a range or distribution of W_s. Clay and fine silt fractions form a relatively uniform settling aggregate at a given concentration. Medium and coarse silt fractions settle at higher rates and are less dependent on concentration than the clay fraction. The objective of the settling tests was to determine the magnitude and distribution of W_s at various suspended sediment concentrations for the finer fractions of the material.

Deposition

102. Deposition (D), or flux of sediment material to the bed, is the sum over a number of fractions of settling flux times deposition probability (Mehta et al. 1986):

$$D = \sum_{i=1}^{k} P_i W_{s_i} C_i \tag{6}$$

where

k = number of fractions

i = subscript, indicates a sediment fraction

P = probability that an aggregate reaching the bed will remain there

W_s = settling velocity

C = concentration just above the bed

The value of P varies linearly from 0 at a critical shear stress for deposition, τ_{cd}, to 1 at zero bed shear stress, $\tau_b = 0$. The functional form $1 - \tau_b/\tau_{cd}$ where $\tau_b < \tau_{cd}$ is used for P (Krone 1962). The objective of the

deposition testing was to determine τ_{cd} and the magnitude of the product PW_s for each sediment fraction identified.

103. A suspension of uniform material in a steady, uniform flow will either deposit completely or remain entirely suspended, depending on whether the bed shear stress is below or above τ_{cd}, according to Equation 6. The consequence of the presence of multiple sediment fractions in a suspension is that, under a given flow condition, some sediment fractions may deposit while others may remain in suspension. The suspension may therefore transport an equilibrium concentration (some fraction of the source concentration) indefinitely.

104. The values for W_s inferred from deposition tests are smaller than those obtained from quiescent settling tube tests. The cause for this is not known. However, shear in the flow is greatest just above the bed and could cause disaggregation, and produces lift forces counteracting settling at this point.

Resuspension

105. The mode of resuspension (used synonymously with erosion) considered important to potential contaminant migration at New Bedford Harbor is particle erosion. At τ_b above a critical value, particles are individually dislodged from the sediment bed as interaggregate bonds are broken. Particle resuspension (E) is related to the shear stress in excess of a critical value and to an erosion rate constant (M). Thus,

$$E = M\left(\frac{\tau_b}{\tau_c} - 1\right), \qquad \tau_b > \tau_c \tag{7}$$

where τ_c is the critical erosion shear stress (Ariathurai, MacArthur, and Krone 1977). Observed erosion does not follow Equation 7 indefinitely. Suspension concentrations above experimental eroding beds often reach equilibrium values that depend on the bed shear stress. Equilibrium suspensions form as erosion rates decrease with time to zero, while the flow remains constant. Equilibrium suspensions have been found not to be related to the transport capacity of the flow (as for sand) but have been related to vertical differences or inhomogeneity in the bed (either particle characteristics or bed density) or to armoring by selective erosion at the bed surface. The purpose of the resuspension tests was to determine the magnitude of M and τ_c for

representative sediment fractions and to detect the formation and nature of equilibrium suspension.

Materials and Equipment

Test material

106. The test material consisted of sediment from the composite sample collected as Task 5 of the EFS. The composite sample was taken from a number of locations in the upper harbor and is representative of moderately contaminated (in a relative sense) sediments. The composite sample has been used for a number of laboratory tests in the EFS. The grain size distribution of the composite sample is shown in Figure 11. The solids concentration, total exchangeable cations, and oil and grease content of the composite sample are given in Table 18. The principal mineral groups for New Bedford sediments have been reported to be chlorite and mica (Ellis et al. 1977).

107. The composite sample was prepared for erosion and deposition testing by passing it through a US standard No. 200 sieve, with an orifice diameter of 74 μm. Figure 12 shows the grain size distribution for the sieved composite sample reconstructed from Figure 11. About 32 percent of the composite sample was coarser than 74 μm. Seawater was used in the sieving operation and reduced the bulk density or concentration of the material to 1.17 g/cu cm or 250 g/ℓ, respectively.

108. Tests were performed as a sequence of sediment additions to a closed system, the sediment water tunnel, as described later. Sediments resuspended from the bed of the sediment water tunnel at the beginning of each test became incorporated into the test material. In some cases, only resuspended material was tested. This resulted in the test material being different from, and finer than, the original sieved composite sample.

Sediment water tunnel

109. A special testing device was developed for this study to safely test contaminated sediments. The testing device was a closed-conduit sediment water tunnel, open to the air only at a small expansion chamber. The water tunnel had a uniform cross-sectional area, which changed from rectangular in the horizontal, deposition/resuspension sections to circular in the vertical settling and pumping sections. See Figure 13 for the configuration of the sediment water tunnel.

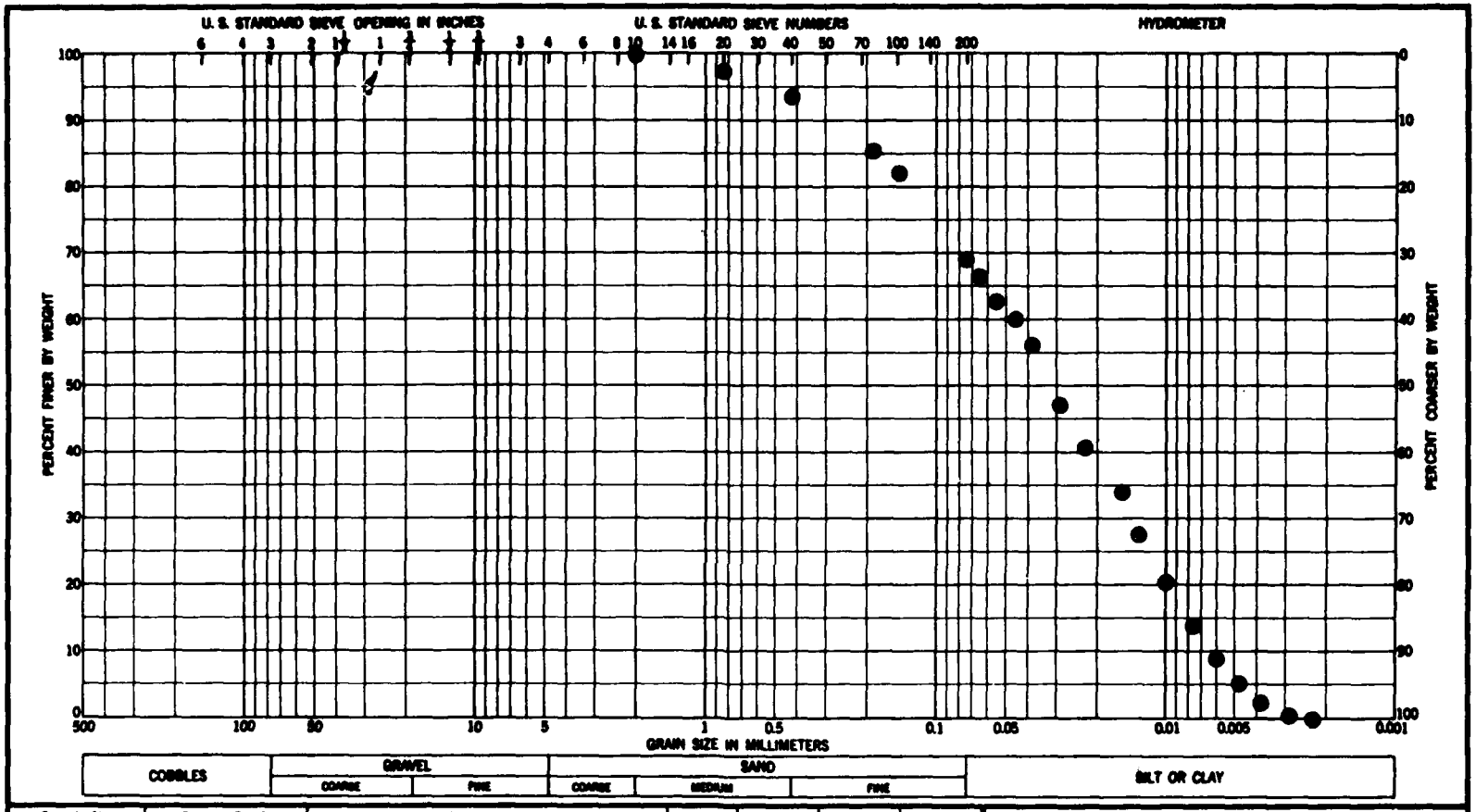

Sample No.	Elev or Depth	Classification	Nat w %	LL	PL	PI
27		dark gray-sandy organic SILT (OH)				

Project: New Bedford Harbor, Mass.

Area: Composite

Boring No.: Lab ser no 100-452-27

Date: 29 Jan 87

GRADATION CURVES

ENG FORM 1 MAY 63 2087

Figure 11. Grain size distribution of the composite sample

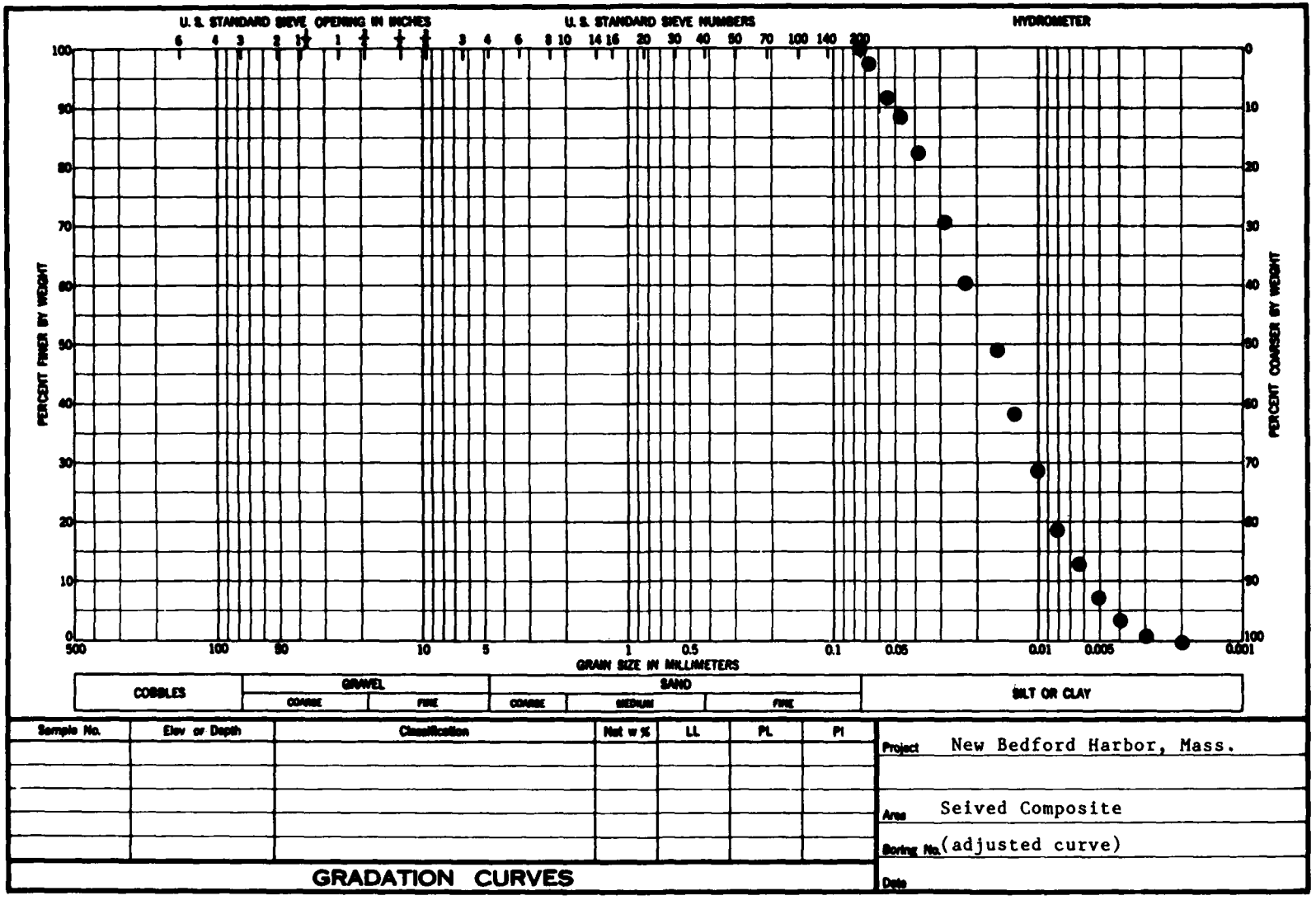

Figure 12. Adjusted grain size distribution for the sieved composite sample

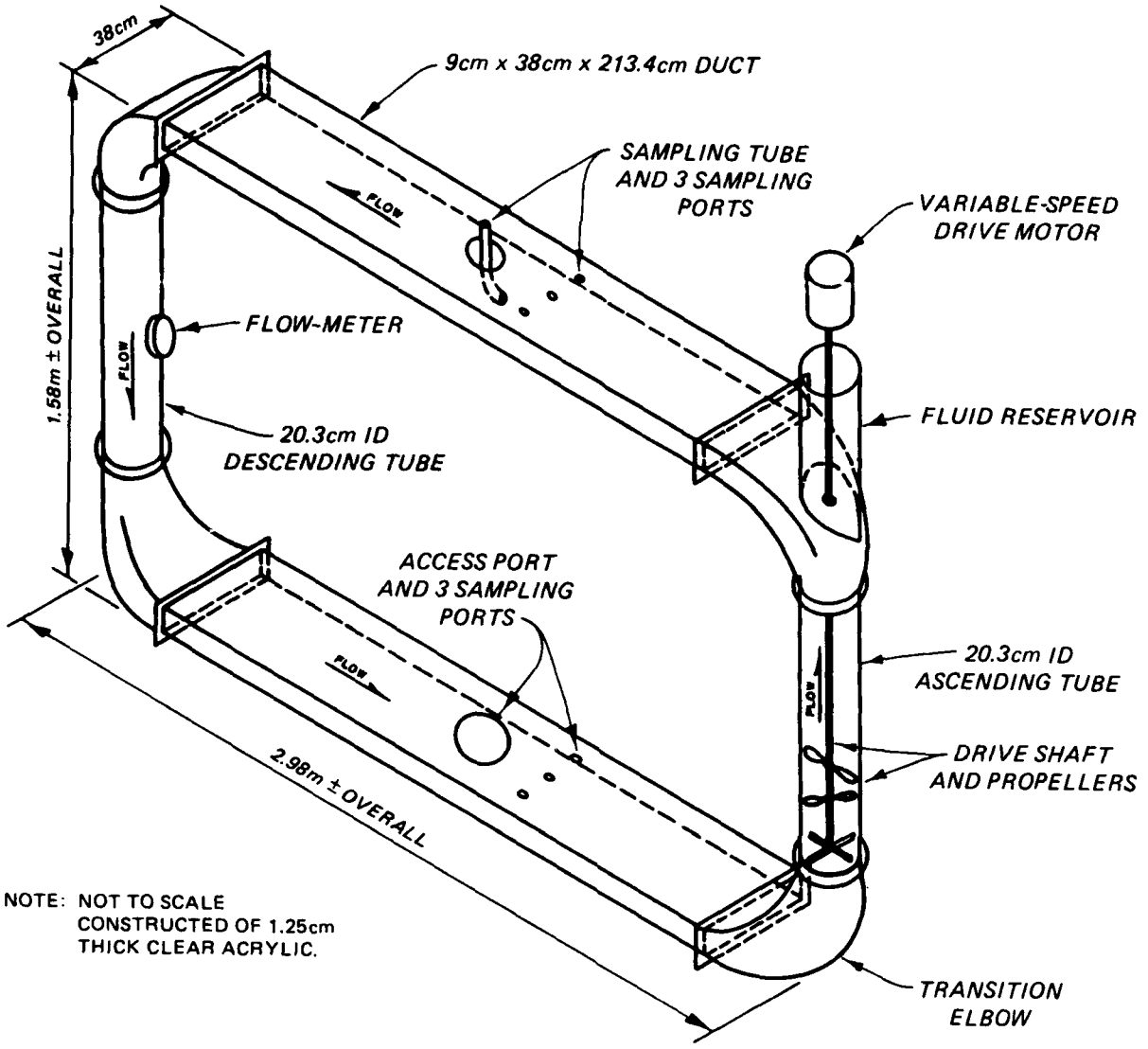

Figure 13. Isometric view of sediment water tunnel

110. The water tunnel was calibrated so that propeller speed could be related to average velocity and bed shear stress (Table 19). Calibration curves were developed using the tachometer, a flowmeter, and a hot-film shear stress sensor. The seawater used for the tests was reconstituted from Instant Ocean salt mix to a salinity of 25.8 ppt. Water temperature for the tests was between 22.2° and 22.6° C and varied less than 0.3° C during any test.

Test Procedures

111. Four test series (designated I through IV) were performed to provide deposition and resuspension data over ranges of conditions and to allow

estimation of the coefficient described earlier. Three tests were performed in each series, and each test had combinations of erosional, depositional, and settling test phases. An initial water tunnel sediment bed was established by the addition of 75 g of sediment during two preliminary deposition periods. Tests were performed by additions of sediment to the water tunnel without removal of material from previous tests.

112. Table 20 shows the chronology for all tests. Samples from the sediment water tunnel were analyzed for total nonfilterable solids by a standard method. Settling tests were performed in the descending tube, as shown in Figure 13, with the flow in the sediment water tunnel stopped. After establishment of the deposition test speed, samples were taken at 0, 2, 4, 6, 10, 15, 20, 30, 45, 60, and 90 min. Samples were drawn by syringe from the 3.2-cm depth in the center of the upper rectangular tunnel section. Resuspension of deposited sediment was studied in the water tunnel by subjecting deposits to a range of current shear stresses. Resuspension periods were observed and sampled at the beginning of each test.

Data Analysis

Settling

113. Settling velocities were calculated from test data by the pipette method. The change in concentration at the sampling depth was equal to the fraction of material settling greater than h/t, where h is the height of the suspension above the sampling point and t is the sampling time. The settling test data were transformed into percent removed and natural log of sampling time. A second-order polynomial was fit through the data by least-squares regression. Settling velocity distributions were reconstructed from the regression coefficients.

114. In addition to cumulative distributions, some statistical parameters were calculated descriptive of the settling velocity distributions similar to those used to characterize grain size distributions (Inman 1963), including the geometric mean, standard deviation, skewness, and kurtosis (Table 21). The geometric mean is a better descriptor of the central tendency of the distribution than the simple average, which was also calculated, and is commonly used. The geometric standard deviation is a dimensionless indicator of the spread of the distribution. Skewness indicates the degree of

asymmetry and the direction of distribution shift. Kurtosis indicates the peakedness of the distribution.

Deposition

115. Deposition was determined by monitoring suspended sediment concentration of a steady flow. The equation expressing mass balance for the water tunnel suspension is

$$\frac{\partial(CV)}{\partial t} = -APW_s C \tag{8}$$

where

C = average suspended sediment concentration

V = suspension volume

A = depositional area of the water tunnel

116. Assuming that W_s depends on a power of C, as expressed by Equation 5, then one solution to Equation 8 is

$$C^{-n} - C_o^{-n} = nA1P\frac{t}{h} \tag{9}$$

where

n = enhanced-settling exponent

C_o = initial concentration

A1 = coefficient in the settling velocity equation

h = effective depth V/A

The value of A1 is expected to be different (smaller) for the deposition tests than for the settling tests. The power n was assumed to have the value 4/3. Equation 9 was rearranged and used as a regression equation to determine A1 from the raw data.

117. Deposition data were further analyzed as the superposition of a number of fractions, as in Equation 6. Plots of $C^{-4/3}$ versus t/h were used to differentiate the test data into three depositional components or fractions, as indicated by straight-line segments and inflections. The initial concentrations of these fractions and the time at which half the fraction was deposited (t*) were estimated from the data. The slopes (deposition rates) for the deposition fractions were then estimated from

$$\frac{4}{3} Al_i P_i = \frac{h}{t^*} \left[\left(\frac{C_{o_i}}{2} \right)^{-4/3} - C_{o_i}^{-4/3} \right] \quad (10)$$

Deposition rate slopes ($4/3Al_iP_i$) were calculated for each shear stress and fraction. By plotting the slopes versus τ_b, intercepts at $4/3Al_iP_i = 0$ defined τ_{cd} for each fraction. Using τ_{cd} to calculate P_i, Al_i values were calculated.

Resuspension

118. Resuspension was determined by monitoring the suspension concentration in a steady flow. The constancy of E was determined by inspection of concentration/time data. The magnitude of equilibrium suspension concentrations and of the fraction of total mass in suspension was compared to bed shear stress.

Results and Discussion

119. The equilibrium suspensions formed during resuspension and deposition test phases and the variability in deposition results between resuspended versus the directly added sediments indicated the presence and importance of multiple sediment fractions to sediment behavior. Table 22 shows that the values of τ_{cd} and τ_c varied about an order of magnitude between sediment fractions. Values of W_s and Al varied by greater than an order of magnitude.

Fraction quantification

120. Sediment fractions were designated as 1, 2, and 3 based on their deposition and erosion characteristics. The fractional composition of material in the depositional tests, resuspension tests, and in the sediment additions to the water tunnel was estimated using the following approach. The most easily eroded fraction (fraction 3) was first identified as 39 percent of the total sediment deposit, as discussed later in this section. At the end of resuspension test phases, 39 percent of the total material suspended in the sediment water tunnel was fraction 3 material. The remainder of the material resuspended was assumed to be in fraction 2. This quantified sediment fractions for resuspension test phases and for series II and IV deposition tests.

121. Series I and III deposition tests were preceded by sediment additions and also had resuspended bed material incorporated into test suspensions. The test material in fractions 2 and 3 was determined by evaluating the $C^{-4/3}$ versus t/h curves, as discussed later in this section. Fraction 3 could be assumed to be the same percentage of the test material as for the resuspended material, 39 percent. Fraction 1 was identified as the most rapidly depositing fraction from $C^{-4/3}$ versus t/h curves. The fractional makeup of the sediment material added to the water tunnel during test series I and II was determined by subtraction of the resuspended fraction composition from the deposition test fraction composition. Fraction 3 averaged 41 percent of the added material, confirming the magnitude of this fraction. Considering all results, the approximate composition of the sieved composite sample was 30, 30, and 40 percent for fractions 1, 2, and 3, respectively, as shown in Table 23.

Settling

122. Table 21 shows individual settling test results and composite results for series II and III. Composites were calculated by averaging the percent-removed curves from the test series when results indicated that analytical variation was probably larger than the true variation between the tests. Generally, between 70 and 85 percent of the suspended material was removed by settling during the 300 min of the settling test phases. A plot of the power law settling function (Equation 5) is shown as Figure 14.

123. Measured settling velocities were representatives of the finer sediment fractions, because the test material was sieved and further sorted by other test phases. Series I, II, and III settling test phases were performed after deposition phases. Test IV-1 was conducted after mixing and before deposition testing, to initiate the test at a high concentration. Settling test IV-1 also contains fractions of silt that were not present in other settling test phases.

124. Field suspended samples were taken in the proximity of a coring operation in the field. Results were reported in Part III. Those results for median W_s were higher by a factor of 5 to 10 than the results presented here and are shown in Figure 14. The earlier tests may be more representative of bulk sediments from the upper harbor, while the present tests represent the finer, more slowly depositing fraction of the sediment.

125. A uniform sediment material that exhibits concentration-dependent

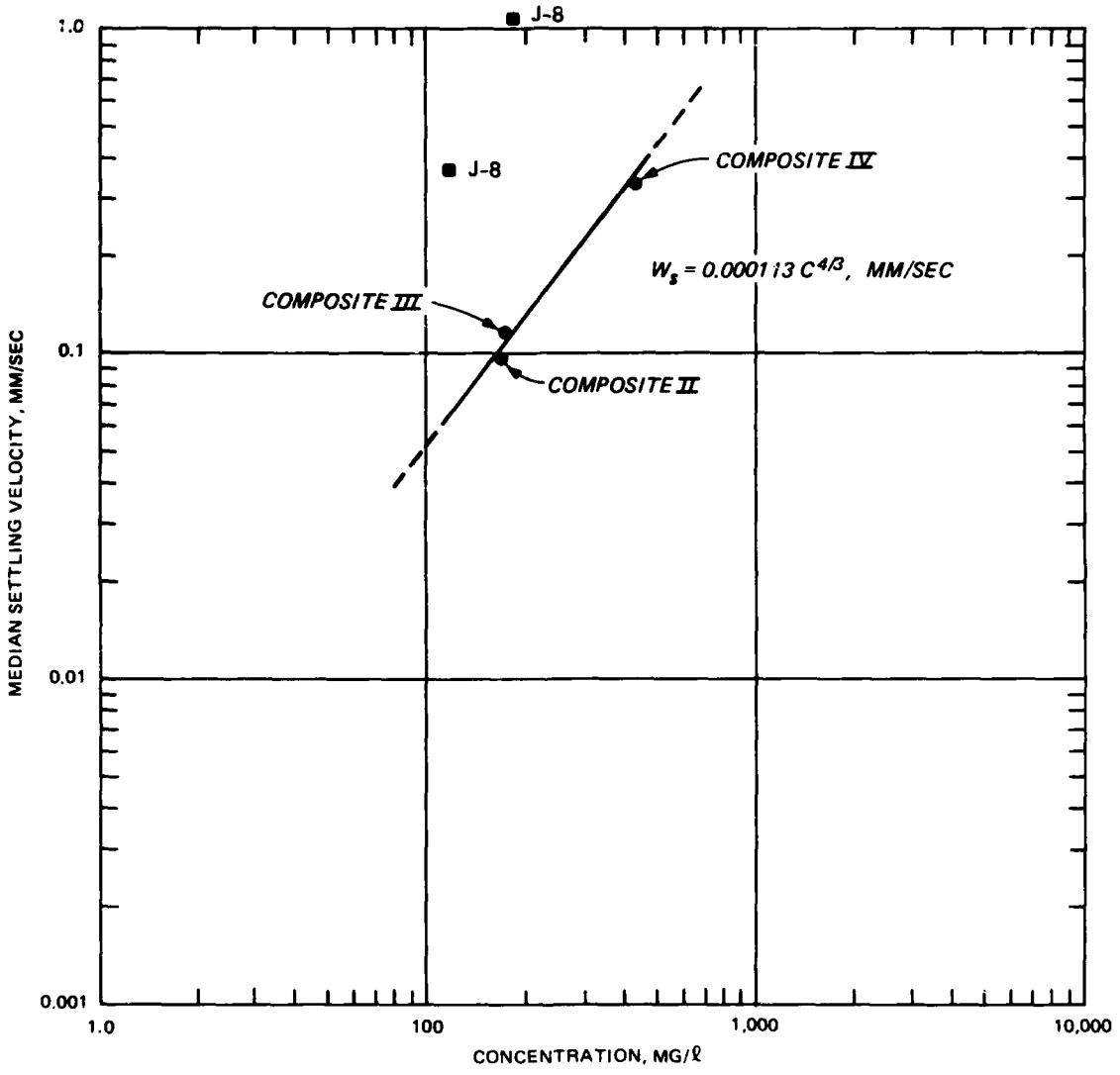

Figure 14. Median settling velocity/concentration relationship for settling test phases and previous field samples at grid cell J-8

settling rates will also exhibit an apparent W_s distribution when tested, because concentration decreases during testing. Concentration dependence can be identified by plotting W_s from the distribution against a concentration equal to the initial concentration times twice the corresponding percent exceeded. The 50-percentile W_s therefore plots at the initial concentration.

126. Figure 15 shows the W_s distribution obtained from composite series II and test IV-1 plotted as concentration dependence relative to their initial concentration. Both tests show that the settling distributions diverge from the enhanced settling curve at about 100 mg/ℓ. The lowest W_s values are equivalent to about 75 mg/ℓ on the enhanced-settling curve. Thus, 75 mg/ℓ is a reasonable lower limit of application of Equation 5 and the coefficients obtained from the settling and deposition tests.

Deposition

127. Analysis of the $C^{-4/3}$ versus t/h plots suggested that the test material could be described by the superposition of three components or fractions. Not all tests displayed all three fractions, due to variations in the composition of the test material and to sorting. Weight percentages found for the three depositional fractions are given in Table 23 for the various tests and the sieved composite. The τ_{cd} and Al values developed from the analysis of the data for the deposition fractions using Equation 10 are given in Table 22.

128. Results for τ_{cd} for the slowest deposition fraction (fraction 3, τ_{cd} = 0.043 N/sq m) were about 25 percent lower than Krone's (1962) result for San Francisco Bay sediments but in the general reported range of 0 to 0.15 N/sq m (O'Connor and Tuxford 1980). Equation 5 applies to the enhanced concentration-dependent settling concentration range above 75 mg/ℓ, as indicated earlier in this section. At concentration below 75 mg/ℓ, Equation 9 and constant W_s values should be used to calculate deposition. Appropriate W_s values are shown in Table 22 for the three sediment fractions.

Resuspension

129. Resuspension rates were not constant for test periods, and equilibrium suspensions occurred. Erosion was rapid during the first few minutes after the application of or increase in bed shear stress. Sediments were picked up by the flow as small clouds, which formed windrows above the bed like blowing snow on a frozen lake. Erosion decreased rapidly as the tests

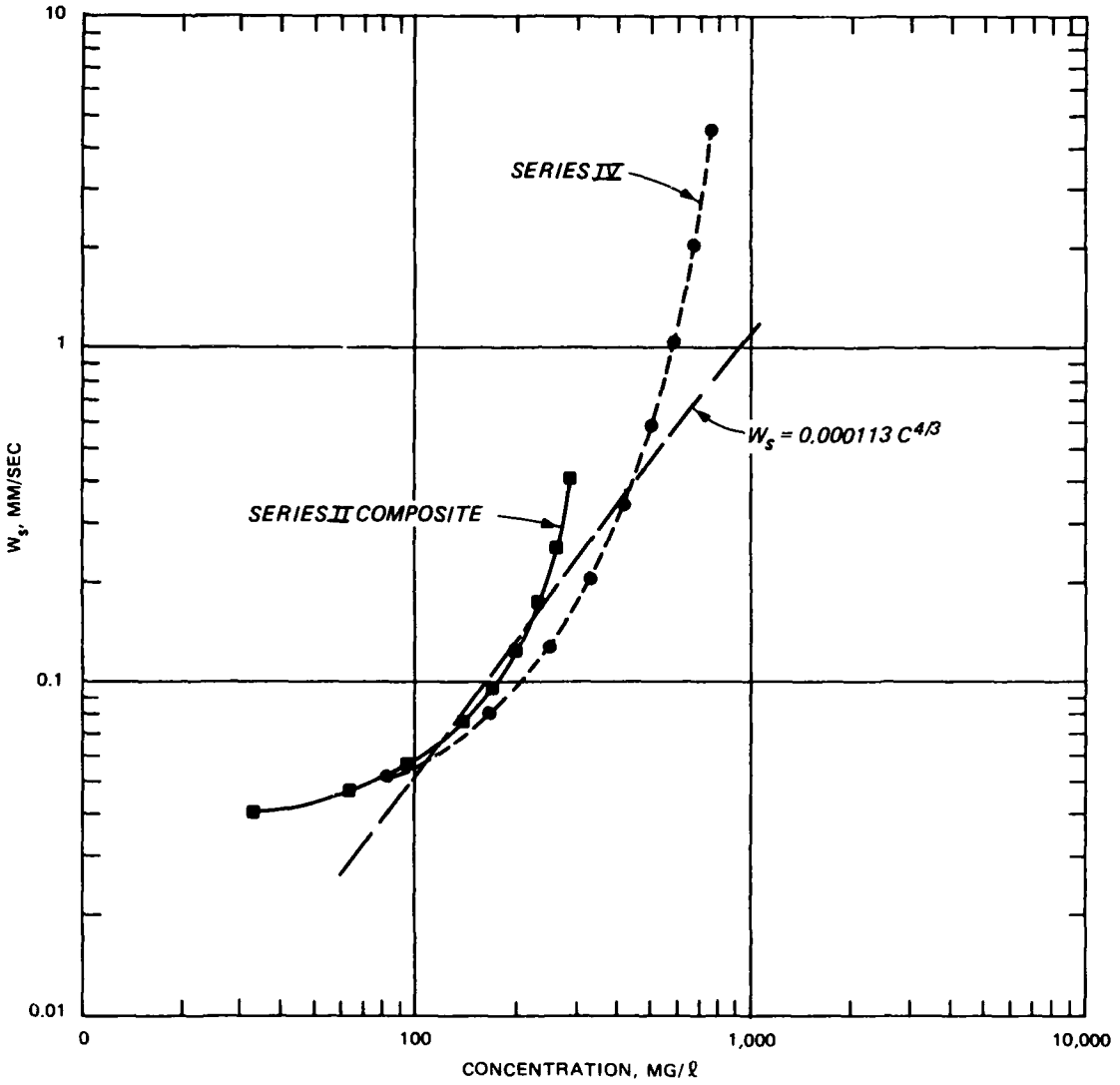

Figure 15. Settling velocity distributions from 10 to 90 percentiles plotted as concentration dependence

progressed, and suspended concentrations reached an equilibrium value. Thus, Equation 7 applied only to the beginning of the resuspension test phases.

130. The fraction of material eroded from the bed was found to be within a narrow range (37 to 64 percent) for the entire shear stress range. A number of test results at the lower end of this range showed that there was an easily erodible fraction. The average percent eroded was 39.0, with a standard deviation of 1.8 percent. Resuspension test results identified the characteristics of the most easily eroded fraction of sediment (Table 23).

131. The value of τ_c for the most erodible fraction was taken as 0.06 N/sq m. The most easily eroded fraction is the same fraction identified as the slowest to deposit (fraction 3). Both were about 40 percent of the sieved composite. The τ_{cd} for this fraction was 0.043 N/sq m, while τ_c was 0.06 N/sq m. The critical shear stresses τ_c and τ_{cd} for fraction 3 were therefore similar.

132. Only about an additional 15 percent of the total bed material, or half of fraction 2, eroded between 0.06 and 0.6 N/sq m, and the remainder of the material had critical shear stresses greater than 0.6 N/sq m.

133. Resuspension tests were performed after a range of bed consolidation times from 1 hr to 2 weeks. Results were similar for all tests. The implication was that bed sediment consolidation or hardening was very slow for New Bedford sediments and would not affect application of these experimental results to similar time periods in the prototype.

PART V: NEAR-FIELD PLUME AND CAD MODELS

134. Near-field mathematical analyses of two sediment release problems were made. Suspended sediment plume calculations were performed to evaluate the escape of sediments and contaminants from proposed dredging and disposal site outfalls in upper New Bedford Harbor. Near-field analyses of the escape of sediments from a confined aquatic disposal area during the filling phase were also performed. Both plume and CAD near-field analytical models were applied to predict the escape and concentrations of suspended sediments near point sources. These relatively simple models were used to provide estimates of impacts on water quality and to provide information on sediment behavior with more spatial detail than the more comprehensive estuarine model.

135. This part describes the near-field plume and CAD models and the application of the near-field models to the proposed dredging and disposal operations. Results were developed for the migration of sediment and pore fluid only, and not specifically for contaminants. The association between sediments and contaminants will be made in Report 3 of the EFS report series.

136. Dredging resuspends some amount of sediment at the point of contact between the dredge and the bed sediments. The rate of sediment resuspension, sediment characteristics, and ambient conditions control the amount of sediment that will escape from the proximity of the dredge and from the upper harbor during dredging. Resuspension rates vary widely depending on the mechanics of the dredging method, the nature of the sediments, and the ambient hydraulic conditions. Suspended sediments will also be discharged with effluent from confined disposal facilities (CDF) and released during CAD filling. Resuspension rates for dredging and the release rates from CDF and CAD sites will be discussed in Part VII.

Plume Model

Description

137. The analytical plume model used for the evaluation was recently developed at WES and was two-dimensional in the horizontal plane. It is based on straightforward extensions to established principles and methods. Since documentation for this model has not been published, a short description of the model follows.

138. The model assumes a vertical line suspended sediment source. Suspended sediments are advected away from the source in the arbitrary X-direction, spread or diffused in the Y-direction, and allowed to settle. In place of a diffusion coefficient for lateral spreading, a non-Fickian diffusion velocity approach was used in the model. Near-field mixing scales for dredge plumes generally include small- as well as large-turbulence components. The diffusion velocity formulation introduces a length scale-dependence into model plume spreading, similar to that observed in field experiments. Okubo (1980) discussed the concept of diffusion velocity and presented results for plumes of conservative material. Spreading rates have been found to be about 11 percent of the advective rates for two-dimensional plane jets and about the same for plumes (for example, see Launder, Reese, and Rodi 1985).

139. In the near-field, travel times are expected to be much shorter than the tidal period, and time variations are assumed to be negligible. The steady governing equation for a dynamically passive suspended sediment plume, advecting away from a source (at X = 0, Y = 0) in the X-direction and spreading only in the Y-direction, and settling is

$$U \frac{\partial C}{\partial X} = YV_s \frac{\partial^2 C}{\partial Y^2} - \frac{PW_s C}{H} \tag{11}$$

where

U = current speed in the X-direction

C = depth-averaged suspended sediment concentration

V_s = horizontal diffusion velocity

P = depositional probability

H = depth

The solution for the governing equation becomes

$$C(X,Y) = \frac{Q_s}{2HV_s X} \exp\left[- \frac{UY}{V_s X} - \frac{PW_s X}{HU} \right] \tag{12}$$

where

Q_s = release rate of suspended material at the source

$V_s = 0.11U$

140. Equation 12 and the computer algorithm used to solve it were tested for consistency and accuracy. The diffusion velocity (V_s) was reduced in steps and the results compared to one-dimensional analytical solutions to settling. Results compared favorably for small V_s. Mass conservation was checked by reducing W_s, integrating the concentration field across the flow at some distance from the source, and verifying that the flux matched the input sediment release rate. Tests confirmed that concentration and flux results could be scaled by the sediment release rate (Q_s).

141. Model output included an echo of input data, a list of center-line concentrations at 5-m intervals to 100 m, integrated fluxes at 50 and 100 m, and a plot of concentration contours. Fluxes were calculated by trapezoidal area integration of U times C with 0.5-m interval spacing from the center line to 45 m perpendicular to the flow. Another model module compiled results from a test matrix of four current speeds and four settling classes into a statistical summary.

Application

142. The required data for the plume model were Q_s, H, U, and W_s. The ratio of Q_s at the dredging site to the flux of sediment passing 50 and 100 m from the site was used to evaluate the suspended sediment migration away from a dredging site. Thus, the results are independent of Q_s. A site depth of 1 m was assumed, the average depth of the upper harbor. The remaining two variables, U and W_s, were assigned distributions.

143. A velocity time-history from a two-cycle mean tide numerical simulation (see Part VI) at station 7 (see Figure 3) was used to obtain current speed values and frequencies. Current speeds were divided into four ranges, and the frequency of occurrence for each range was determined.

144. Depositional classes from Part IV of this report were used for plume simulations. An additional fraction was added to represent the fine sand removed from the composite before laboratory testing. The distribution was therefore divided in four classes, and the frequency (by mass) in each class was specified according to the observed distribution. Settling velocities were assigned values based on the low concentration results of Part IV (less than 75 mg/ℓ).

145. Results for the matrix of plume calculations are shown in Table 24 for 50 and 100 m, along with the values and probabilities of variables used. The test matrix formed by the four values of current speed and

four values of settling velocity was simulated with 16 plume runs. The joint probability for each run was calculated as the product of the two corresponding frequencies for U and W_s. The sum of the weighted results is the average sediment predicted to escape from 50 and 100 m of the dredging site for the set of conditions tested.

146. Figure 16 shows an example plot of plume concentration contours for a current speed of 0.03 m/sec and a settling rate of 0.01 mm/sec, representative of the finest sediment class. These calculations were made for a Q_s of 5 g/sec. Plume concentrations scale by Q_s. For example, concentrations for a $Q_s = 40$ g/sec made up of the lowest settling class would be eight times greater than those in Figure 16.

147. Plume predictions for dredging in upper New Bedford Harbor indicate that, on average, about 35 and 29 percent of the material released at the dredgehead will escape from 50 and 100 m of the site, respectively. The remainder will settle within this radius. As shown in Table 24, most of the sediment escaping does so at the highest current speed and has the lowest settling rate. However, the weighted totals were highest for the moderate current speeds and for the lowest settling rate. Moderate current speeds had the greater frequencies of occurrence.

148. Peak concentrations at the plume center line averaged about 1.1 mg/ℓ per g/sec Q_s at 50 m and 0.4 mg/ℓ per g/sec Q_s at 100 m. Coefficients of variation (standard deviation divided by the mean) were 0.5 to 0.88 for the range of conditions considered in the plume calculations. Average concentrations would be about one third as great as peak concentrations, based on the assumed concentration distribution in the plume model. Conservative plumes (with little or no settling) representative of the lowest settling class or released pore fluid averaged about 2.9 and 1.1 mg/ℓ per g/sec sediment on pore water released at 50 and 100 m, similar to Figure 16.

149. Natural plumes have spatial and temporal variability not displayed by plume models in general, but average plume properties are expected to be characterized by the models.

CAD Escape Model

Description

150. During the filling phase of CAD operations, slurries of

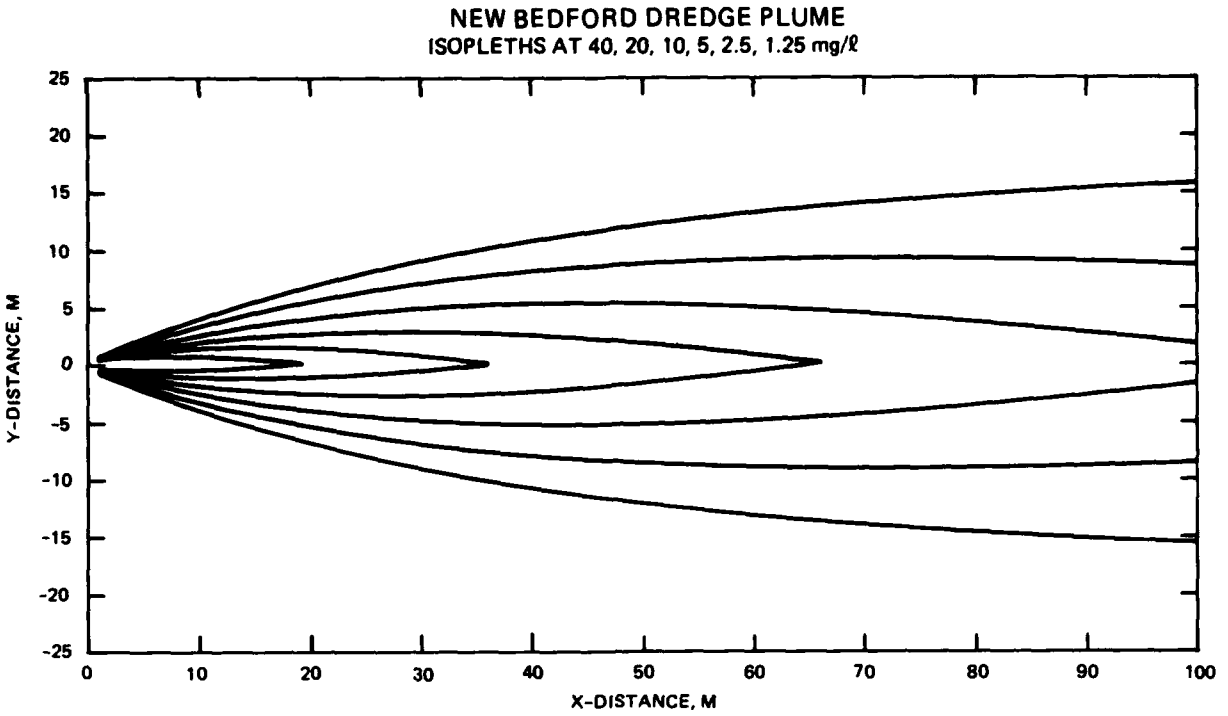

Figure 16. Example New Bedford dredge plume concentration isopleths for Q_s = 5 g/sec , U = 0.03 m/sec , and W_s = 0.01 mm/sec

hydraulically dredged sediment will be pumped into one of a series of previously excavated depressions or cells. The slurries will be distributed within a cell by a manifold and diffuser system to minimize entrainment of additional ambient water and escape of sediments. Shortly after entering a CAD cell, slurries will begin to separate into two components--a turbid supernatant and a dense, high-concentration suspension. The dense suspension will undergo zone settling and expel pore water. Water expelled from the dense suspension may carry some sediments into the supernatant. Suspended material in the supernatant will either be carried away from the CAD cell by ambient currents or will settle and deposit onto the dense suspension. The dense suspension will remain in the CAD cell as long as ambient currents are insufficient to entrain or erode the material.

151. The model developed in the following paragraphs addresses the question, how much of the suspended sediment in the CAD cell supernatant will escape from the site? Model calculations identified the nature of the sediment material that would escape from the CAD cell.

152. The amount of solids that would be carried into the supernatant by the expulsion of slurry pore water can be estimated from zone settling or

elutriate tests. It should be noted that the amount of solids expelled is a function of the concentration of the dense suspension and the settling characteristics of the solids. The lower the concentration of the dense suspension, the greater the amount of solids that potentially could escape into the supernatant. At some higher concentration, the escape of solids from the dense suspension will decrease to zero. Pore spaces and pore fluid flows decrease markedly at higher dense-suspension concentration. By the same process, the escape of solids will decrease with time as a dense suspension undergoes zone settling or hindered settling consolidation in a CAD cell. The concentration at which escape of solids ceases can also be identified from settling tests.

153. An analytic model of the transport of suspended material out of a CAD cell was developed to estimate the ratio of the amount and concentration of suspended material escaping from the cell to the amount released from the dense suspension. The release rate of solids, $Ro = C_o fQ$ where C_o is the initial suspended concentration (kilograms per cubic metre) of the turbid supernatant at the center of the cell or the location of the diffuser ($X = 0$), f is the fraction of pore water leaving the slurry, and Q is the slurry inflow rate (cubic metres per second). The parameter f is the difference between water fraction in the slurry and the water fraction at which solids escape ceases. The purpose of the analysis is to determine the fraction of sediment escaping from the cell site (R/R_o and C/C_o).

154. Escape of sediment from the CAD was modeled as a one-dimensional settling process. Suspended sediments were assumed to originate at $X = 0$ and advect toward the edge of the CAD cell at $X = L$. The depth outside the cell is h, and the cell has a depth of H below h (see Figure 17). The vertical velocity of the sediment particles is equal to their settling velocity, W_s, reduced by the upward flow from the slurry discharge, Q/A, where A is the area of the cell.

155. The governing equation for the deposition process within the CAD cell and resulting decrease in suspended concentration is

$$(H + h) \frac{\partial \bar{C}}{\partial t} = -PW_s C_b \qquad (13)$$

where

$\bar{C}$ = depth-averaged supernatant concentration

t = time

P = deposition probability

C_b = supernatant concentration at the bottom or bed

The following additional assumptions or substitutions were made:

a. The vertical distribution of suspended sediments obeys the analytical law (Teeter 1986)

$$C_b = \bar{C} + \bar{C}\left[\frac{W_s\,(H + h)}{K_z\left(1.25 + 4.75\,P^{5/2}\right)}\right]$$

b. The vertical eddy diffusivity is that of a homogeneous shear flow and can be expressed by (Fischer 1973)

$$K_z = 0.067U^*\,(H + h)$$

where U^* is the shear velocity and is defined in terms of the depth-averaged flow inside the cell, U_i, as

$$U^* = 0.04U_i$$

c. Time is defined by

$$t = \frac{X}{U_i}$$

d. The flow is steady and the slurry discharge relatively small so that by continuity U_i can be defined by

$$U_i = \frac{Uh}{(H + h)}$$

where U is the current speed outside the cell.

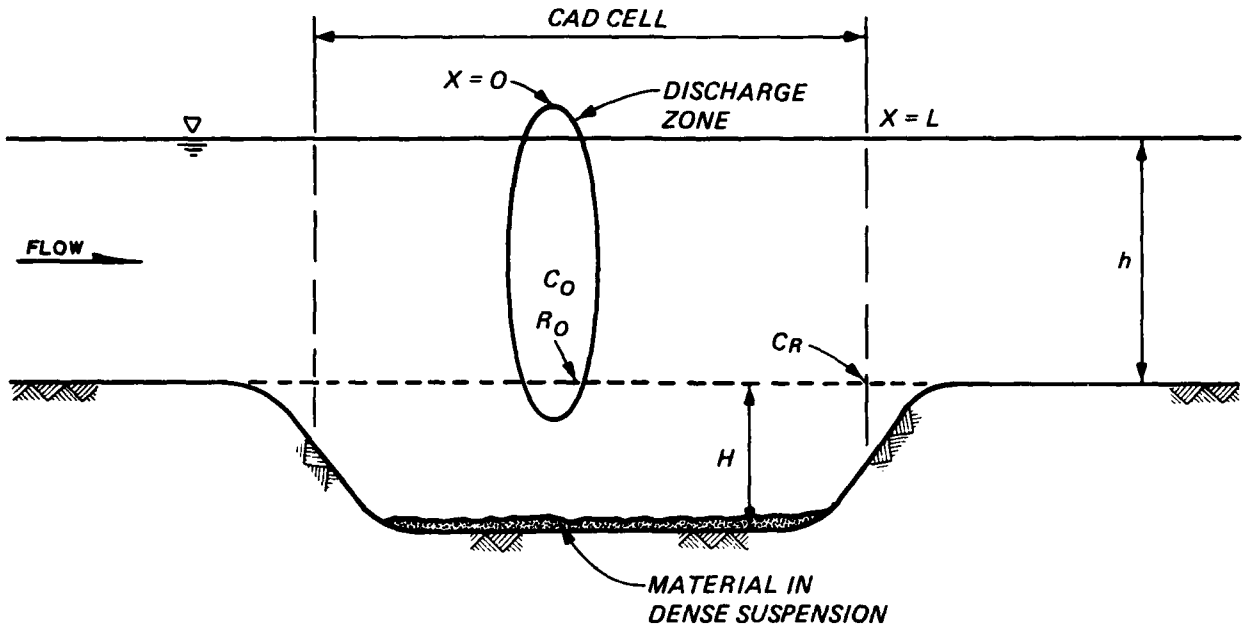

Figure 17. Cross section of CAD cell

156. Using the above expressions, the analytic solution to the governing equation at X = L becomes

$$\frac{\bar{C}}{C_o} = \exp\left\{ - \frac{P(W_s A - Q)L}{AUh} \left[1 + \frac{P(W_s A - Q)(H + h)}{0.003AUh\left(1.25 + 4.75P^{5/2}\right)} \right] \right\} \qquad (14)$$

Equation 14 expresses the ratio of the suspension concentration leaving the cell to the initial concentration of solids in the supernatant resulting from settling and deposition to the bottom of the cell. Assuming that only those suspended sediments above the level of the surrounding bed will escape from the CAD,

$$\frac{\bar{R}}{R_o} = \exp\left\{ - \frac{P(W_s A - Q)HL}{AUh^2} \left[1 + \frac{P(W_s A - Q)(H + h)}{0.003AUh\left(1.25 + 4.75P^{5/2}\right)} \right] \right\} \qquad (15)$$

Equation 15 expresses the ratio of the rate of sediment settling below the level of the surrounding bed (h) to the total settling and deposition on the bottom of the cell. Equation 14 is a more conservative (higher) estimate of escape than Equation 15.

Application

157. A three-dimensional matrix for test conditions U, W_s, and H was used to calculate average CAD release ratios using R/R_o and C/C_o. Four depositional classes and current speed ranges (for station 7) identical to those used in the plume calculations were used. The third test condition was the depth of the CAD below the bed level, H. The value of H was assumed to range from 0.92 to 2.92 m, and the natural water depth was assumed to be 1.0 m. The characteristic length from the point of discharge to the edge of the CAD was assumed to be 50 m. Confined aquatic disposal configurations are discussed in Report 11 of the EFS report series.

158. The assumed value for the ratio Q/A (8.4 E-06 m/sec) was based on an assumed 100 cu yd/hr (76 cu m/hr dredging rate or 400 cu yd/hr (304 cu m/hr) slurry inflow rate (0.085 cu m/sec) and an area equivalent to 100 by 100 m. This parameter is not critical to model results as long as it is small in comparison to W_s. Note that the assumed Q/A was larger than the lowest settling W_s class, causing this entire fraction to escape from the CAD.

159. Results are shown in Tables 25 and 26 for R/R_o and C/C_o, respectively. Results for R/R_o and C/C_o were similar, with C/Co results only slightly higher. Results indicate that only the finest or slowest settling fraction escaped from the CAD and that the escape of this fraction was almost complete. Settling rates for other sediment fractions prevented much escape for the range of current speeds tested.

160. The results can be compared to plume results at 50 m. For $H = 0.92$ m, escape from the CAD was 29 to 30 percent, while the average plume escape was 35 percent. Therefore, the escape from a CAD was estimated to be about 80 percent of the escape from a plume for the same conditions except the CAD depth.

161. If the solids suspended at the CAD were representative of the bed sediments, then only the finest fraction would have a chance to escape. However, as discussed in Part VII, the elutriate tests suggested that the released sediment would be made up predominantly or completely by the finest sediment fraction. The escape of that fraction from the CAD was predicted by the model to be high, about 100 percent.

162. Some sensitivity tests were performed varying the CAD size, and therefore also Q/A. By doubling the length of the CAD side to 200 m and

maintaining the same inflow rate, the escape of sediments was predicted to decrease by only 1 percent. By halving the length of the CAD side to 25 m and maintaining the same inflow rate, the escape of sediments was predicted to increase only by about 4 percent, and the escape of sediment from a CAD cell is not predicted to increase greatly when the diffuser is near the edge of the cell. Therefore, the escape of sediment was always nearly the same as the fraction of the slowest settling sediment (28 percent) and was relatively insensitive to other conditions.

PART VI: ESTUARINE NUMERICAL MODELING

163. The major objective of the EFS estuarine numerical modeling was to calculate tidal currents for the upper harbor and to predict the movements of sediments within and out of the upper harbor during dredging using schematic two-dimensional numerical modeling. This part summarizes the results obtained for the numerical hydrodynamic and sediment transport modeling. Emphasis will be on the migration of various sediment fractions out of the upper harbor. The association between sediments and contaminants is discussed in Report 3 of the EFS report series.

164. Computer codes RMA-2V and RMA-4 of the TABS-2 numerical modeling system (Thomas and McAnally 1985) were used to model vertically averaged hydrodynamics and sediment transport, respectively. These models are implicit finite element solvers for the two-dimensional shallow-water Reynolds form of the Navier-Stokes equations and the advection-diffusion transport equation. Sediment migration modeling was a two-step process, with hydrodynamic model calculations performed first and used to drive sediment transport calculations. Analyses of the sediment transport runs were then made to estimate the escape of resuspended sediments from the upper harbor.

Numerical-Hydrodynamic Modeling

165. Hydrodynamic modeling was performed to characterize hydraulic conditions and to generate data required for sediment transport modeling. The area of interest was above the Coggeshall Street Bridge (see Figure 2). However, to properly describe boundary conditions, the model domain was extended downstream to the Hurricane Barrier. A numerical mesh of 219 elements was developed to cover the study area for use by both RMA-2V and RMA-4 (Figure 18).

166. The numerical hydrodynamic modeling required specification of the seaward boundary as a time-varying water surface elevation and the upstream boundary as a time-varying inflow velocity. A mean tide water level sequence observed during WES's 5-7 March 1986 survey at the tide gage on the end of Clark's Point (tide gage 1) was applied to the seaward boundary of the model. At the upper boundary of the model, velocities were specified which changed

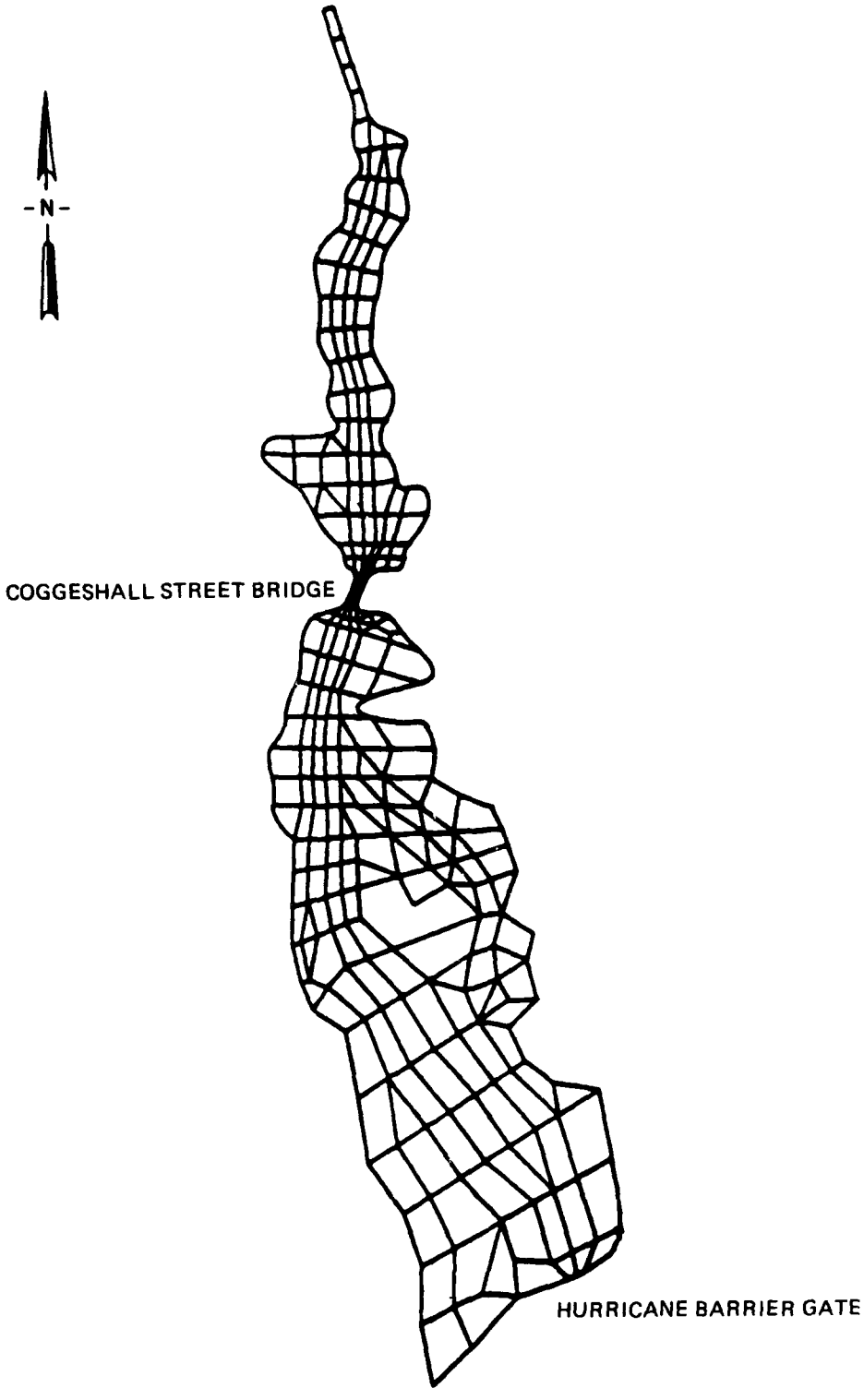

Figure 18. Finite element mesh for RMA-2V and RMA-4

with the tide to correspond to a constant freshwater inflow of 0.85 cu m/sec at all time steps.

167. The hydrodynamic model was verified to field data. Two element types were specified over the mesh--one type along the main channel and the other type covering areas close to the banks. Manning coefficients of 0.015 and 0.02, respectively, were specified for the two element types to obtain the best agreement with field data. A turbulent exchange coefficient of 244 kg-sec/m^2 was used.

168. Field versus model water surface elevation comparisons at tide gage 3, and velocity comparisons at boat stations 5, 7, 8, and 9 are given in Figures 19-23. Figure 3 shows the station locations, and Figure 24 shows the node locations used for the comparisons. Figures 25a and 25b are computed vector plots representative of the velocity field above the Coggeshall Street Bridge during flood and ebb tidal phases, respectively.

169. Hydrodynamic computations were performed by "spinning up" the model from a steady, flat water surface condition. Results from model-time hour 7 through hour 29 were repeated four times to generate an eight-tidal cycle input file for sediment transport modeling.

170. The original mesh geometry was modified for sensitivity testing by lowering bed elevations by 1 m in two areas, one in the lower and one in the upper portion of upper New Bedford Harbor (above Coggeshall Street Bridge). These two modified geometry conditions tested the effects on hydrodynamics of lowered bed elevations due to dredging.

Sediment Transport Modeling

171. Sediment transport modeling was performed to estimate escape probabilities from the upper harbor for various sediment materials that might be resuspended as a result of pilot dredging. Transport of resuspended sediment was modeled as a steady sediment mass loading at specified points. Boundary concentrations were set to zero at the upper and lower boundaries of the mesh at all times when inflow occurred. Initial concentrations were set to zero at all mesh locations. Therefore, only sediments released at the mass loading point were included in computations.

172. An arbitrary mass loading (15 g/sec) was specified at node 66 in the vicinity of proposed pilot dredging (Otis and Andreliunas 1987).

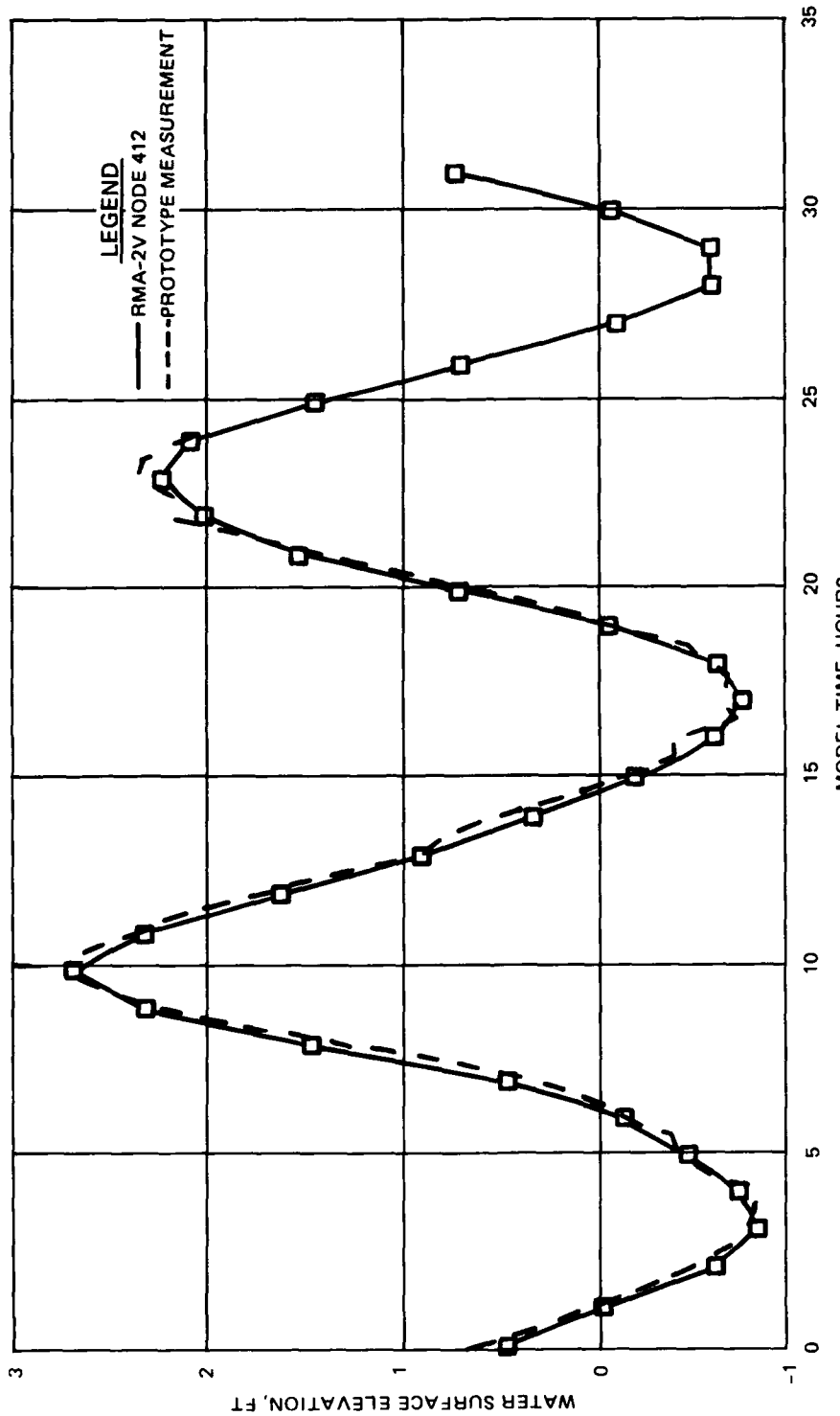

Figure 19. Model/prototype tide height comparison at tide gage 3

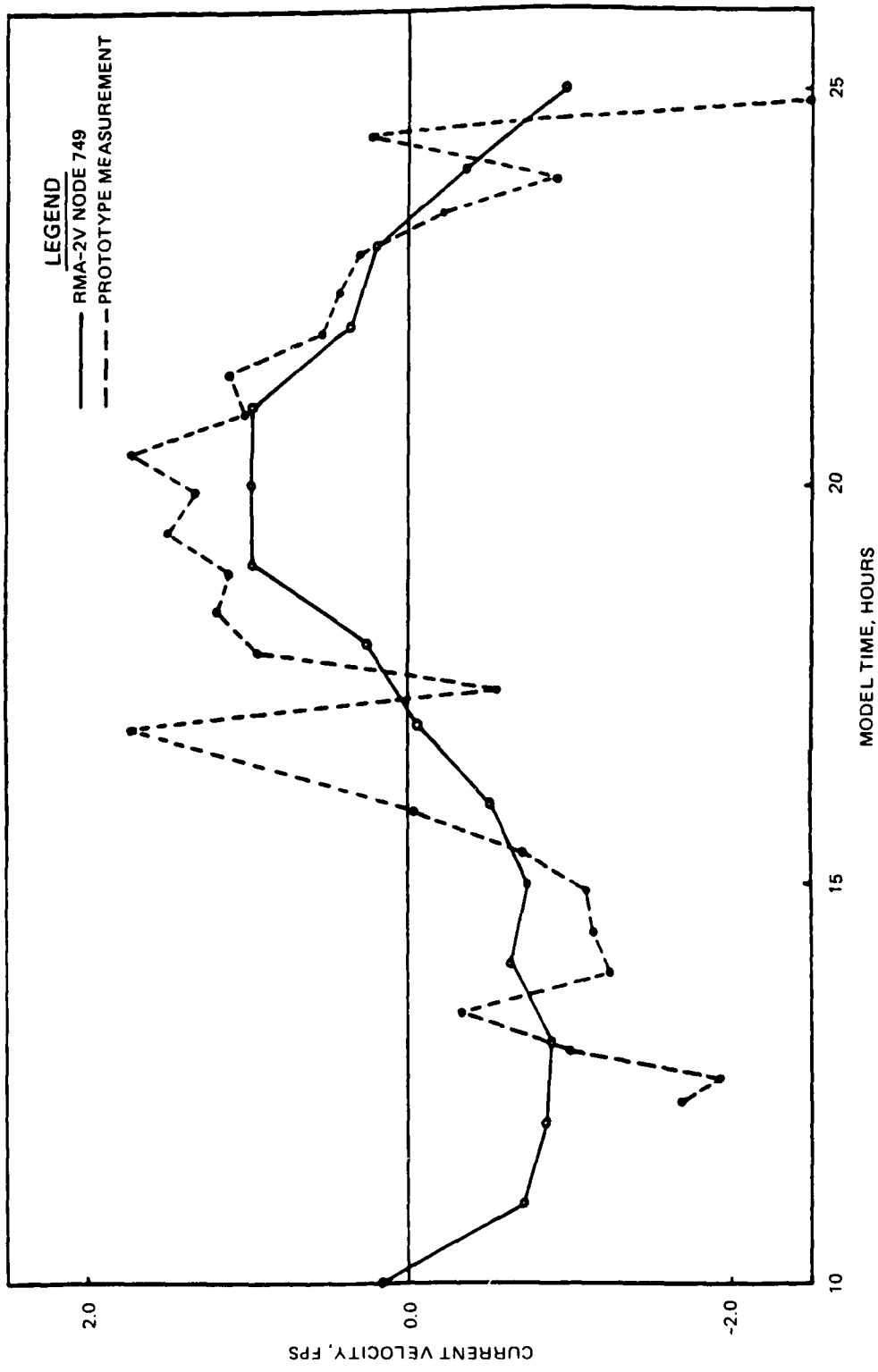

Figure 20. Model/prototype velocity comparison at station 5

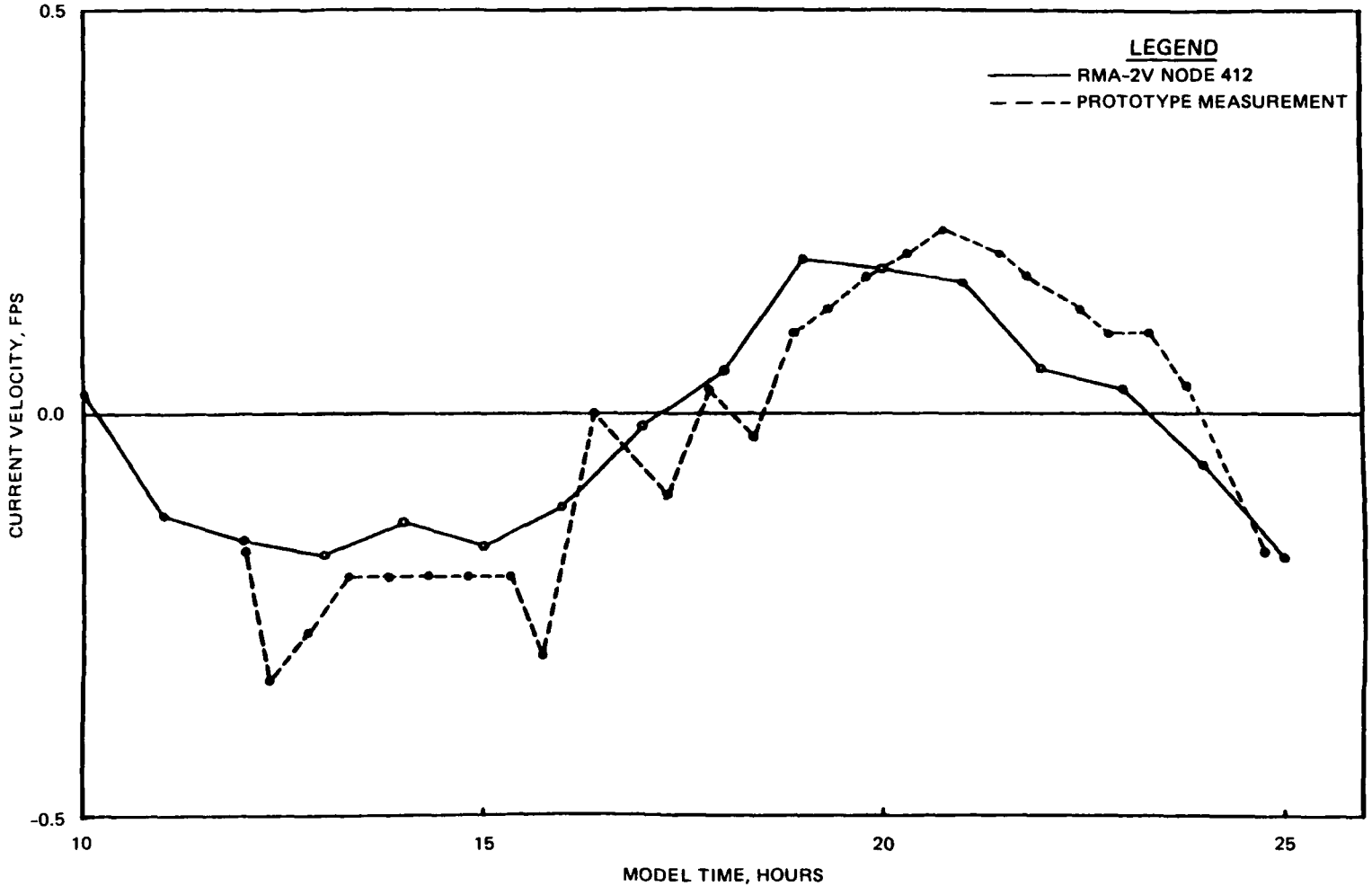

Figure 21. Model/prototype velocity comparison at station 7

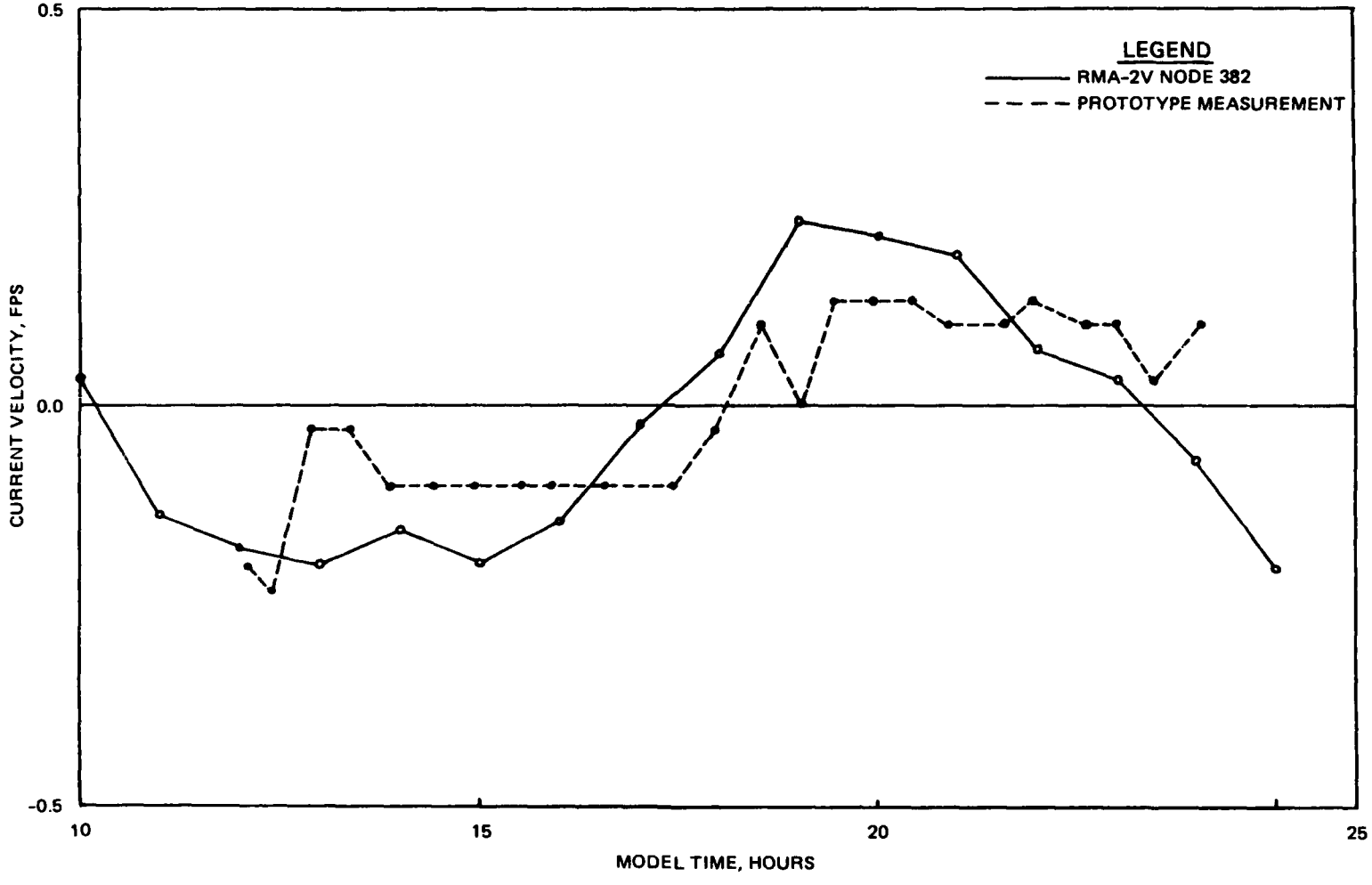

Figure 22. Model/prototype velocity comparison at station 8

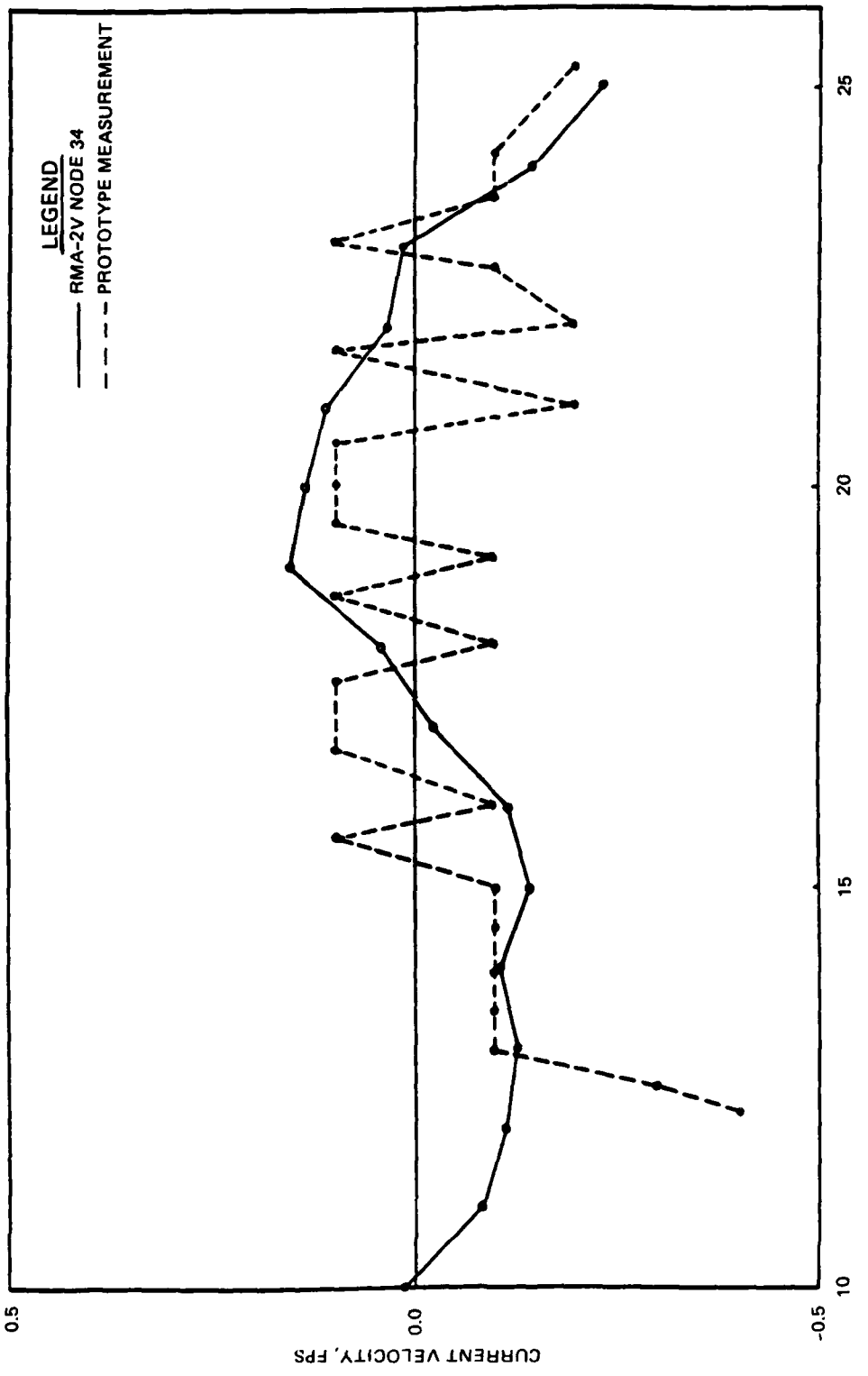

Figure 23. Model/prototype velocity comparison at station 9

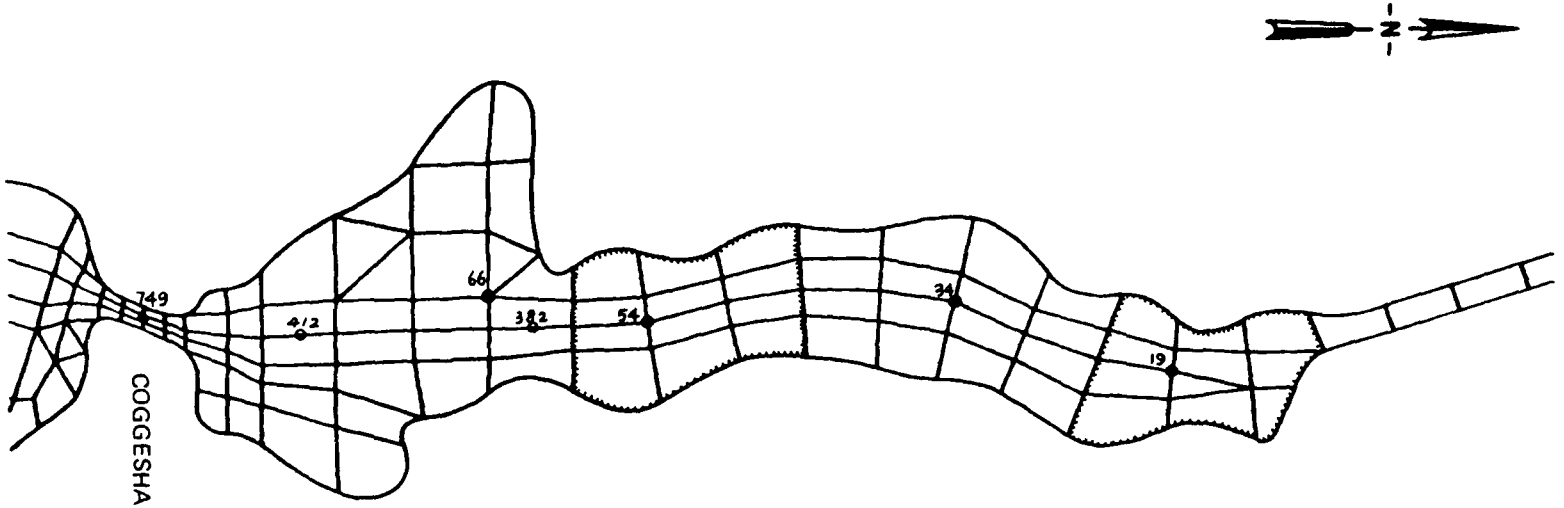

NODE 66: MASS LOADING (LOCATION OF PILOT DREDGING)
NODE 54: MASS LOADING WITH REDUCED BED ELEVATION (LOWER)
NODE 19: MASS LOADING WITH REDUCED BED ELEVATION (UPPER)

NODE 749: STATION 5
NODE 412: STATION 7 & TIDE GAGE NO. 3
NODE 382: STATION 8
NODE 34: STATION 9

Figure 24. Locations of field stations and mass loading points in the upper harbor

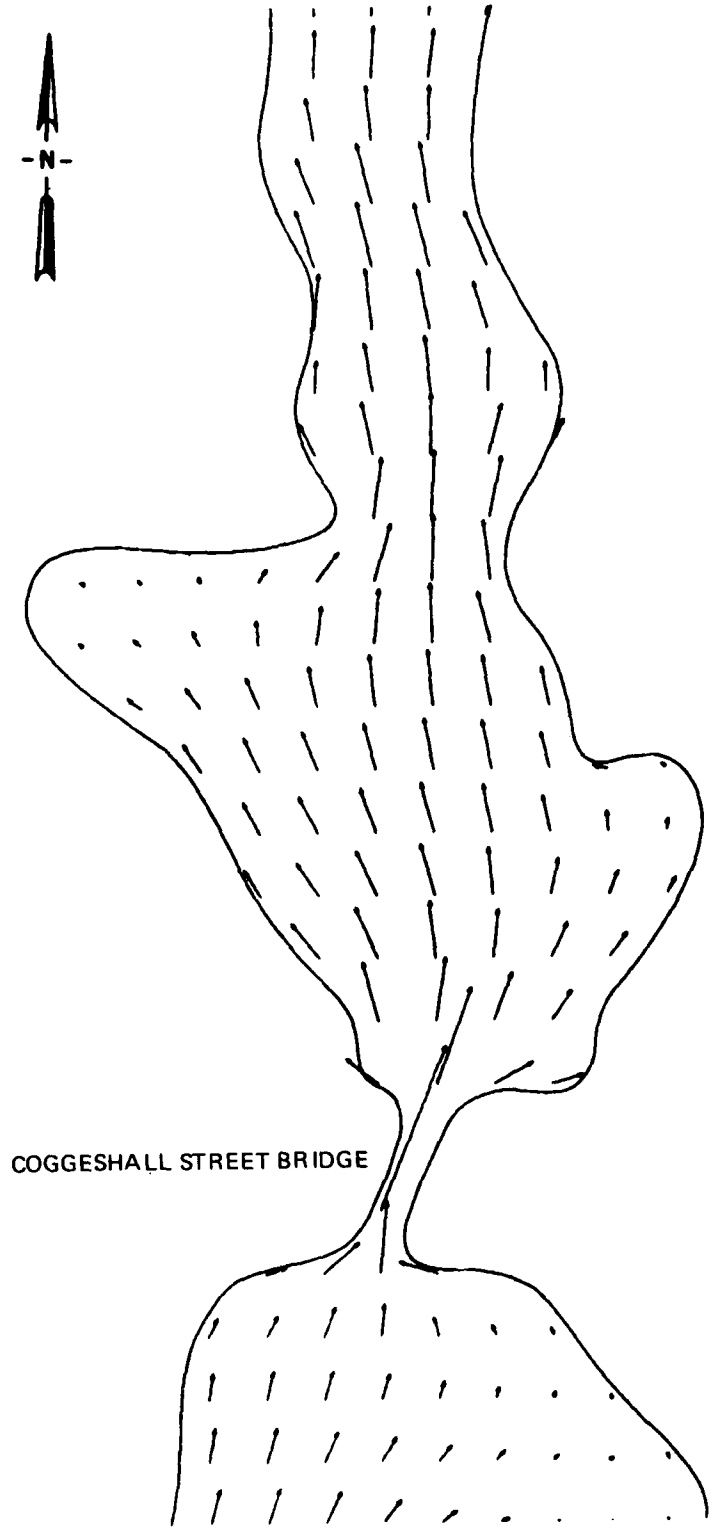

a. During flood

Figure 25. Computed local velocity field (Continued)

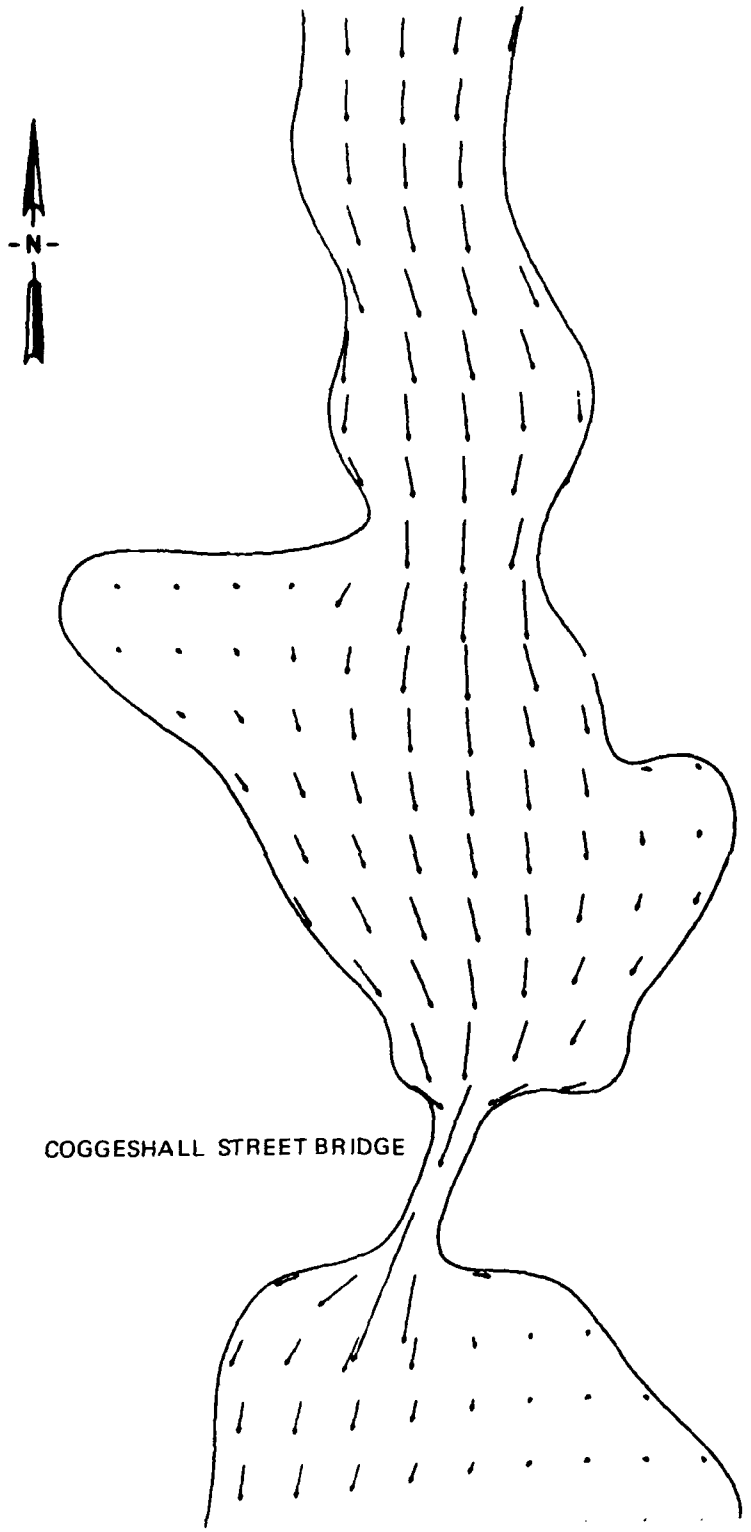

b. During ebb

Figure 25. (Concluded)

Additional transport computations were performed for resuspended sediment source areas upstream from the pilot area at nodes 54 and 19 (Figure 24). A dispersion coefficient of 5.0 sq m/sec was selected after some sensitivity tests and was used in all computations.

173. Deposition of sediments from suspension was included in sediment modeling as a sink term in the advection-diffusion transport equation. Five settling components or fractions were used to characterize a range of sediments that (a) are resuspended at the dredgehead, (b) are released with effluent from the proposed confined disposal area, and (c) escape from CAD sites. The settling characteristics of resuspended sediments from each of these sources are expected to vary and were independently evaluated in Parts IV and VII. The effective sediment deposition coefficient used in the sink term of the transport equation was

$$\alpha = \frac{W_s P}{H} \tag{16}$$

where P is the probability of remaining on the bed after settling. The five depositional fractions or components were specified over the range

$$0.10 < \alpha < 25.6$$

where α has the units of 1/day. The sediment deposition coefficient of a sixth component was set to zero to represent a conservative substance and to normalize results from other deposition coefficients. Normalization of results was necessary to accurately define mass loading because, in the RMA-4 computer code, mass loading magnitude was found to be somewhat sensitive to release location, dispersion coefficient, and other conditions. Mass loading magnitude was also tested separately using steady-state RMA-4 solutions.

174. Contour plots of the concentration field with zero deposition coefficient during flood and ebb (Figures 26a and 26b) show that maximum concentration around the source area was about 3 mg/ℓ for a release rate of 15 g/sec. However, numerical model results overestimated spreading (and underestimated peak concentrations) near the source. (Refer to Part V for near-field predictions.) Concentrations were proportional to release rates. For

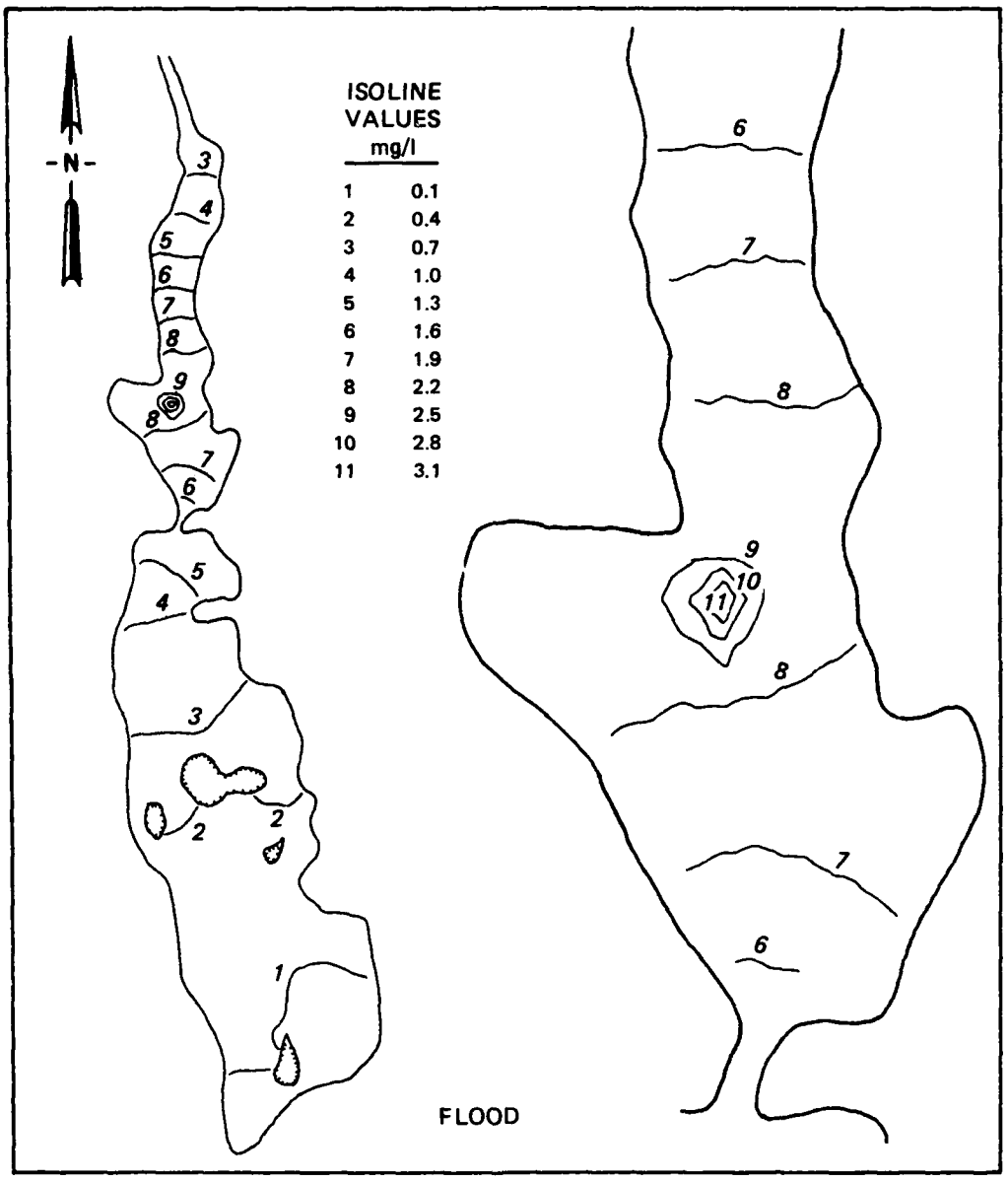

a. Flood tide

Figure 26. Sediment concentration field (Continued)

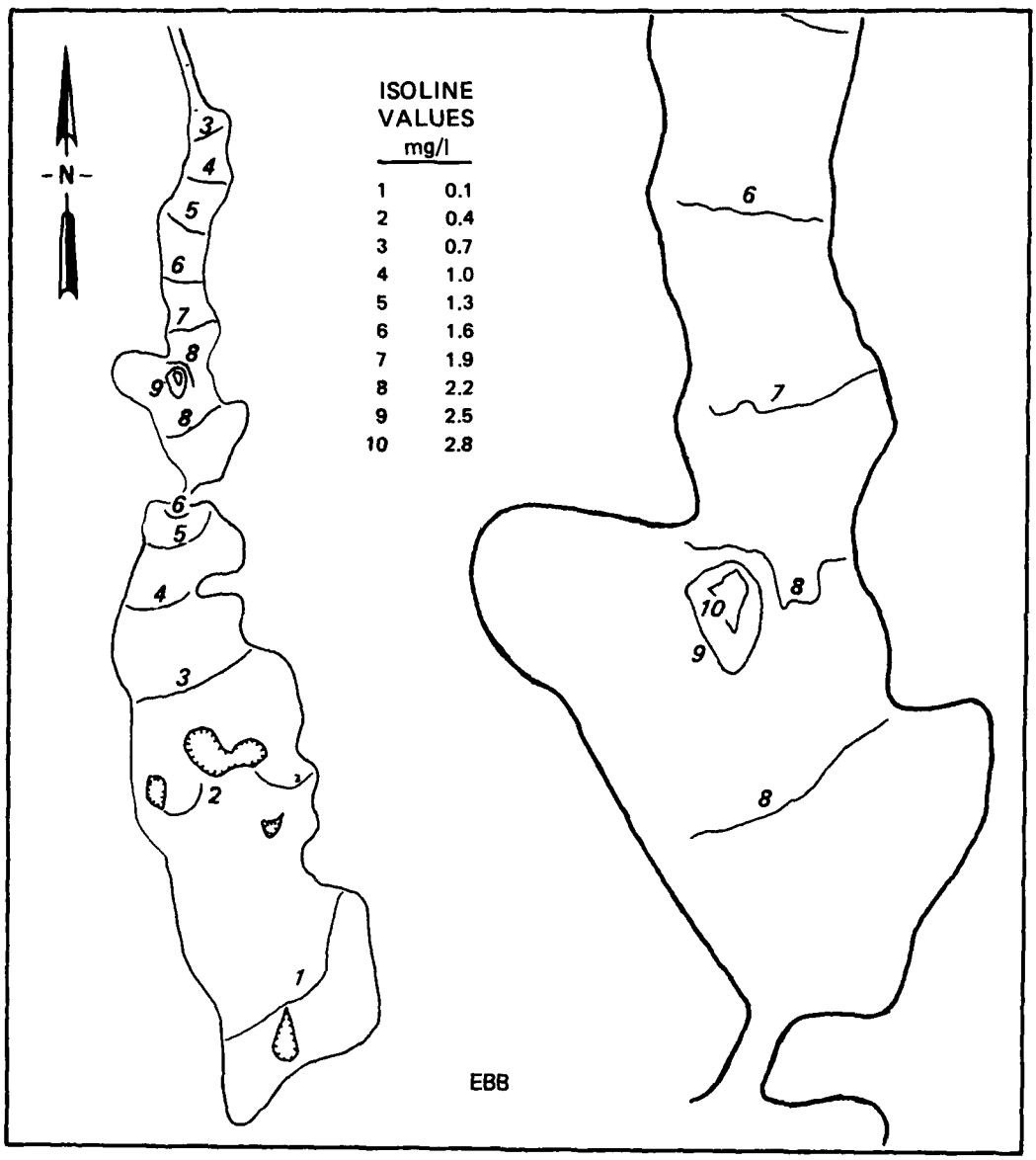

b. Ebb tide

Figure 26. (Concluded)

instance, a release of 30 g/sec would have doubled the concentrations shown in Figures 26a and 26b.

Sediment Migration Analysis

175. Sediment transport model results were analyzed to determine the escape probabilities of resuspended sediments released in the upper harbor and permanently leaving the upper harbor. Average transport rates under Coggeshall Street Bridge during flood and ebb were computed after a spin-up time of from four to seven tidal cycles. This was done because the smaller the deposition coefficient, the longer the spin-up time required to reach repeating tidal-averaged sediment transport rate. Mean sediment transport rate during flood (L_f in grams per second) was calculated by averaging over the flood portion of the tidal period and over the cross-sectional area under the bridge:

$$L_f = W\left[< \overline{CVH} > \right] \tag{17}$$

where

W = width

C = sediment concentration

V = current velocity

H = water depth

and where the overbar indicates area averaging and the brackets indicate averaging over a flood tidal phase. The ebb transport rate, L_e , was calculated similarly. The escape probability as a percent of the mass loading was calculated as

$$\frac{|L_e| - |L_f|}{\text{Mass loading}} \times 100\%$$

Escape probabilities were calculated for each settling fraction, for the three resuspension source locations, and for the three geometries tested.

176. A plot of escape probabilities versus sediment deposition coefficient for mass loadings at the three source locations is shown in Figure 27.

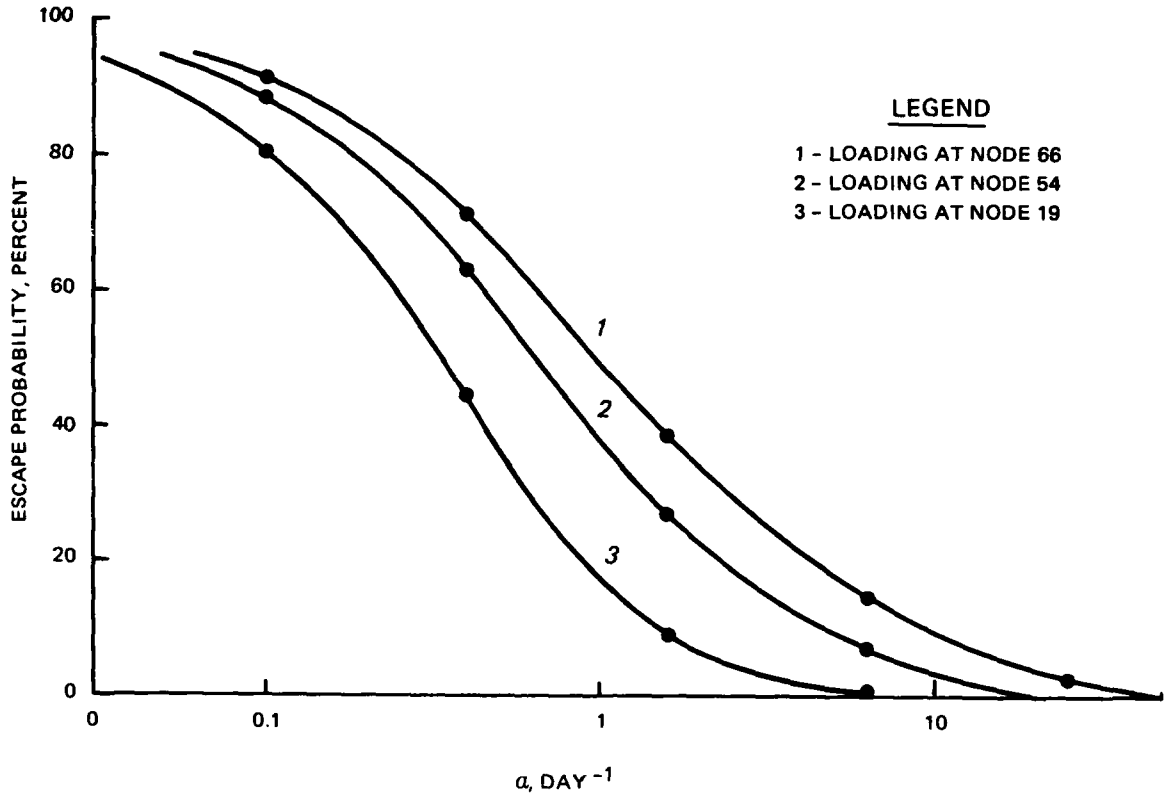

Figure 27. Escape probabilities for sediments released at three points along the upper harbor (see Figure 24 for locations)

The most important factor determining sediment escape probability from the upper harbor was the sediment deposition coefficient, α . The escape probability decreased appreciably when the source area was moved upstream away from the bridge, as shown in Figure 27. Results for lowered bed elevation showed only a very slight decrease in escape probabilities (about 2 percent) and will not be presented.

177. Results shown in Figure 27 were used to estimate the escape of specific sediments from various sources for proposed dredging and disposal operations (Part VII).

PART VII: MIGRATIONS AND CONCENTRATIONS DURING DREDGING AND DISPOSAL

178. In this part, results from other parts will be combined and used to predict various aspects of sediment and contaminant escapes and concentrations during possible dredging and disposal operations. Parts III and IV defined the behavior of sediments in the prototype and under specific hydrodynamic conditions. Parts V and VI described the concentrations and the escape of sediments near their sources and from the Coggeshall Street Bridge predicted by near-field and estuarine models. This part will describe how those characteristics and predictions can be used to make estimates for some broad categories and combinations of proposed dredging activities. Specific dredging scenarios will not be addressed here but will be covered in Report II of this series.

Sediment Releases

179. Both the magnitude of initial sediment releases and the composition of those releases must be predicted or assumed to make estimates of sediment migrations during dredging. Dredging activities that contribute to the mobilization of sediments and contaminants, and which are considered here, included dredging, discharges from CDFs, and from CAD sites during filling operations.

Dredging

180. Dredging equipment has been evaluated and is reported in Report 10. The results of that evaluation with respect to equipment sizing suggested that dredge production rates can be assumed to be about 100 cu yd/hr (0.021 cu m/sec). The slurry flow rate will be much higher than the production rate, due to the entrainment of water, and can be assumed to be about 400 cu yd/hr (0.084 cu m/sec). Slurry sediment content would be about 125 g/ℓ.

181. Dredging equipment selected for use in possible upper-harbor cleanup will be evaluated on its ability to minimize the resuspension of bottom sediments during dredging operations. Many specialized pieces of equipment have been developed and used for this purpose and are described in Report 10. Testing this equipment under field conditions is particularly difficult and has not been performed with the detail necessary to predict

resuspension rates for a given set of conditions. Tests have shown that resuspended concentrations are low around special dredging equipment. However, the situation is that there is no existing data base with which to estimate the sediment resuspension and release rates for a specific dredge and for a general set of conditions.

182. Only a few measurements have been made of resuspension rates for typical cutterhead dredging (not dredging performed to minimize resuspension). The hydraulic dredging, fine-grained sediment resuspension rates reported by Nakai (1978) ranged from about 5 to 45 kg/cu m sediment dredged for the conditions tested. Results were normalized to 7 cm/sec ambient current speed. Other test conditions included a range of dredge sizes from 2,000 to 4,000 hp (1.5 to 3 MW), deep-water depths (about 10 m), sediments with about 35 to 50 percent clay, and a 0.30-m suction pipe. Nakai's (1978) results would extrapolate to 100 to 950 g/sec for the assumed New Bedford dredging rate, but such an extrapolation would not be warranted because hydraulic, sediment, and dredging conditions were not comparable to proposed cleanup dredging. There would be little similarity between the dredging reported by Nakai (1978) and the cleanup dredging performed in upper New Bedford Harbor.

183. Field measurements made by WES in the vicinity of box core dredging were reported in Part III. Those observations showed that resuspension by the vessel was substantial, possibly greater than the resuspension by the actual box corer. Releases averaged about 30 g/sec and were representative of a disturbance of bottom sediments by a vessel and machinery similar to a small dredge, site sediments, and ambient currents.

184. Dredge resuspension rates for proposed upper New Bedford Harbor cannot be estimated with certainty. For estimating sediment and contaminant escape from the proposed pilot dredging, a value of 40 g/sec was used (Otis and Andreliunas 1987). The dredging pilot study will be the best opportunity to estimate resuspension rates for dredges operating in upper New Bedford Harbor.

185. The composition of dredgehead resuspended material will be similar to the in situ sediments. Sediments tested in Part IV were from the composite sample collected from Task 5 of the EFS, and escape estimates were based on that material. The slowest settling fraction identified in Part IV corresponded to that fraction less than 14 μm in the sediment tested. The magnitude of this size fraction varied from 1 to 60 percent by weight for EFS

samples taken at 0- to 0.6-m depth in upper New Bedford Harbor (Condike 1986). Therefore, resuspended sediment composition would be highly variable during actual dredging, while the predictions made in the following section were for the average sediment composition. Results could be adjusted to site-specific sediment composition if necessary.

Confined disposal facility

186. Confined disposal facilities would be constructed and used to accept contaminated dredged materials. The volume of CDFs would be large and would give sediments ample opportunity to settle by gravity. The CDF retention times would be on the order of a couple of days. The pilot CDF will have a secondary cell attached, wherein flocculants will be added to promote settling of fine sediments (Otis and Andreliunas 1987). Similar systems may be used for a full-scale cleanup.

187. The magnitude of suspended sediment released with CDF effluent will depend on the slurry flow rate and the efficiency of the CDF in removing settleable solids. Laboratory tests indicated that, with flocculant addition, effluent suspended solids would be about 70 mg/ℓ (Otis and Andreliunas 1987).

188. The effluent suspended sediments from the CDF would consist entirely of the slowest settling sediment fraction identified in Part IV. The relatively rapid settling of the next slowest fraction (fraction 2 from Part IV) would trap that fraction and all other more rapidly settling fractions in the CDF.

Confined aquatic disposal

189. The CAD cells would be excavated in the bottom of the upper harbor, filled with contaminated sediments to within about 1 m of the natural bed level, and capped with clean material to return the bed to its original level. A submerged diffuser would be used to fill and cap CAD cells, minimizing the entrainment and resuspension of contaminated sediments. During the filling process, pore water and some suspended sediments would be expelled from the slurry and escape from the CAD cell.

190. Release from the CAD during filling was assumed to be 1 percent of the sediment flow rate in the pilot dredging study plan (Otis and Andreliunas 1987). Results of elutriate tests performed at 125 g/ℓ suggested about 500 mg/ℓ suspended solids in slurry supernatant (see EFS Report 3), indicating a release rate much less than 1 percent. Pilot dredging and disposal studies will provide the best opportunity to estimate actual CAD releases.

191. Part IV erosion testing determined τ_c of the most easily eroded fraction of newly deposited sediment to be 0.06 N/sq m. This value of τ_c defines areas unsuitable for CAD filling because of the potential for sediment release and migration from the site. Numerical hydrodynamic model results were used to define areas where τ_c would be exceeded. Model computations for a 1.13-m tide range were extrapolated to a 1.53-m spring tide. The CAD exclusion zones are shown in Figure 28.

Sediment Escape from the Upper Harbor

192. Sediment fractions identified and characterized in Part IV were representative of bulk in situ sediments. Escape of sediments past 50 and 100 m of their release points was calculated in Part V. The characteristics of the three sediment fractions identified in Part IV plus an additional fraction representative of the fine sand removed from the composite sediment before deposition and erosion testing were used. Sediment fractions in Part IV were designated 1 to 3 by decreasing settling rate. Fraction 0 is the designation for fine sand.

193. Table 27 lists the composition and depositional characteristics for the various releases and sediment fractions. Depositional probabilities (P) for the sediment fractions were calculated using the τ_{cd} values from Part IV and prototype hydraulic data. Data from stations 7 and 8 of the WES June 1986 survey were used to calculate average P values for the channel for fractions 3 and 2. Results for the two stations were similar, with P values of 0.31 and 0.89 for fractions 3 and 2, respectively. Since these values were for the higher current areas of the channel, they were averaged with P = 1, which is representative of the outer edges of the estuary. The P values for fractions 0 and 1 were assumed to be the same as for fraction 2.

194. Another estimate for deposition coefficient (α) for natural suspended sediments was made using the prototype data presented in Part III. Using average deposition rate per unit area, suspension concentration, and Equation 6, the result was $\alpha = 1.0$. However, the more conservative value for fraction 3 from Table 27 ($\alpha = 0.34$) was used to estimate sediment escape for the finest fraction.

195. Table 27 also shows the composition of sediment material released from the dredge, CDF, and CAD, as discussed in the last section. Deposition

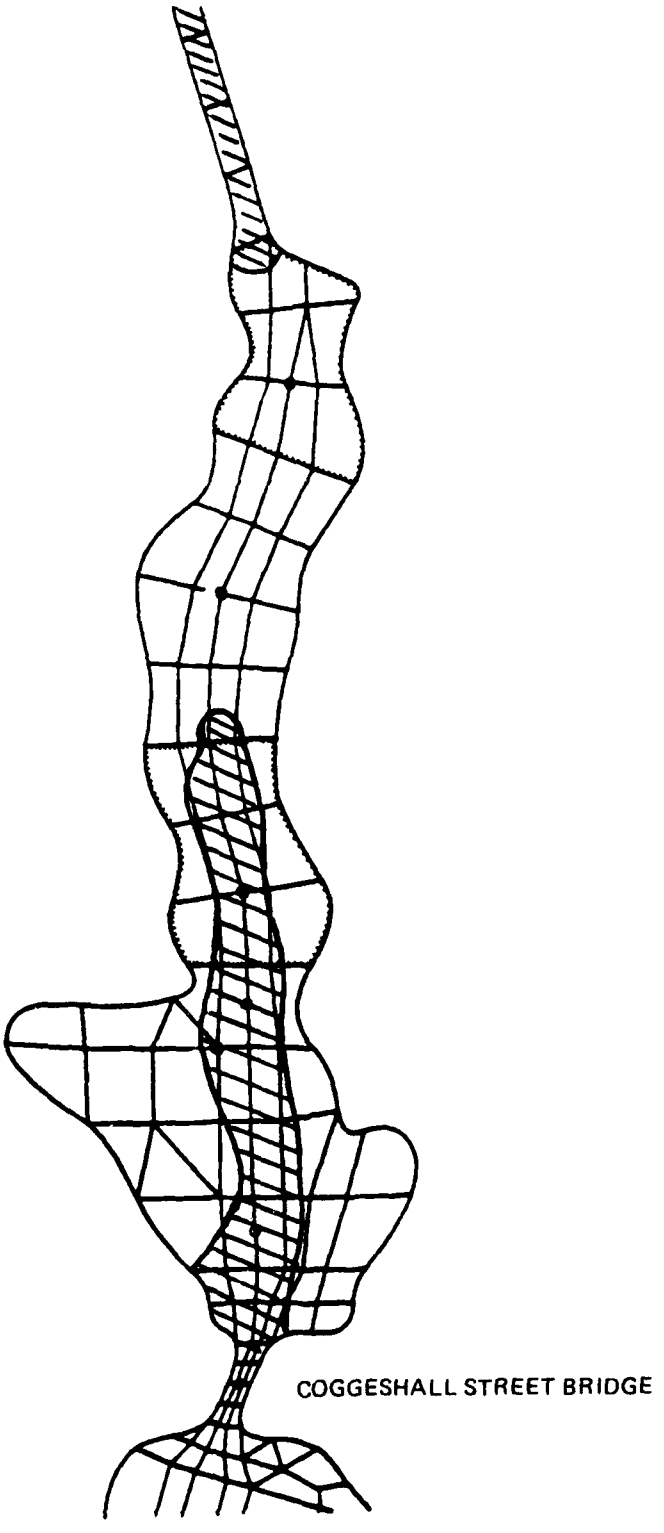

Figure 28. New Bedford upper harbor CAD exclusion zone (hatched) for 1.53-m spring tide on numerical mesh

coefficients, α in units of 1/day, shown in Table 27 were calculated from τ_{cd} and W_s characteristics determined in Part IV, H = 1 , and Equation 16.

196. Table 28 shows the escape probabilities for sediment fractions from the upper harbor. Results from Figure 27 (Part VI) were used to compile this table. Fraction 3 will be the only mobile sediments released to the upper harbor according to these results.

197. Escape probabilities in Table 28 are for specific sediment fractions. For example, if 40 g/sec sediment were resuspended by dredging in the middle portion of the estuary, then the escape would be about 7.6 g/sec at the Coggeshall Street Bridge (40 g/sec (× 0.28 g-fraction 3)/g-sediment × 0.68 escape probability for fraction 3). Examples for CDF and CAD escapes are given in Table 29 for the release rates discussed above.

Concentrations in the Upper Harbor

198. Two methods can be used to incorporate information from the previous parts into estimates for general increases in concentrations in the upper harbor and at the Coggeshall Street Bridge resulting from cleanup dredging and disposal. The first method is a tidal compartment model using field data as input; the second is a method to scale numerical results. Part V presented near-field concentration results from plumes within 100 m of their source. Only estuary-wide concentrations will be considered here.

199. Concentrations (C) of suspended material or contaminant can be calculated from field data using a tidal compartment model. The mass balance for the system above the Coggeshall Street Bridge is

$$\frac{d(CV)}{dt} = Q_s - \Phi CV \qquad (18)$$

where

CV = mass of material suspended in the upper harbor

Q_s = source of material in units of mass per tide cycle (about 44,712 sec)

Φ = flushing rate

At steady state, the mass of material is

$$CV = \frac{Q_s}{\Phi}$$

where

$$\frac{1}{\Phi} = \frac{(V) + 1/2T_p}{\varepsilon T_p}$$

and where

(V) = mean-tide volume of the upper harbor

T_p = tidal prism

ε = fraction of new water in T_p

For the WES surveys, average T_p was 1.1 E+06 cu m/tide. Concentration would be highest at high-water slack tide and thus, for the ebb tide (C_e), is

$$C_e = \frac{Q_s}{\varepsilon T_p} \tag{19}$$

The factor ε can be evaluated using concentration field data for a source in the upper harbor, such as the PCB data presented in Part III. The PCB contaminants have their source within the upper harbor, while suspended sediments were found to have their source downstream in Buzzards Bay. Therefore, the fraction of new water in the tidal prism can be estimated from PCB data using:

$$\varepsilon = 1 - \frac{C_f}{C_e}$$

where the subscripts e and f refer to ebb and flood tidal phases, respectively.

200. Using total PCB-Aroclor concentrations, ε values averaged 0.47 for two WES tidal surveys and three EPA tidal cycles. Numerical transport calculations reported in Part VI indicated that ε was dependent on α, and not on the location of the source loading. The power law fit using ε calculated from both upper and lower loading points was

$$\varepsilon = 0.56\alpha^{0.25} \qquad 0.1 < \alpha < 6.4 \tag{20}$$

Thus, for an α for fraction 3 of 0.34, ε was estimated as 0.43, in reasonable agreement with the estimate based on PCB field data.

201. The numerical results presented in Figures 26a and 26b can be scaled to concentrations resulting from other suspended sediment releases in the upper harbor. The concentration values in these figures are for $\alpha = 0$ and a 15-g/sec release from the lowest loading point. Concentrations for nonsettling or soluble fractions would be scaled by the release rate. Concentrations for settling fractions were found to scale by the square of the escape probability of the sediment fraction. Thus, the scaling factor is

$$\frac{Q_s}{15} \text{ (Escape Probability)}^2 \tag{21}$$

where Q_s is in grams per second for the specific sediment fraction considered. Scaled concentrations from Figures 26a and 26b may vary by 50 percent or more from concentrations of other numerical simulations, since the calculated concentrations shown in these figures are for a specific tidal phase and loading point. However, scaled concentrations away from the loading point may be accurate enough for water quality evaluation purposes.

202. Assuming a continuous resuspended sediment source of 30 g/sec (1,340 kg/tide) in the lower section of the upper harbor, and that the sediment was composed of fraction 3, the concentration on the ebb tide would be 2.6 mg/ℓ at the Coggeshall Street Bridge according to Equation 19. The scaling factor for the numerical results from Equation 21 would be 1.2, and according to Figure 26b, the concentration at the Coggeshall Street Bridge would be about 2.2 mg/ℓ on the ebb tidal phase. Concentrations calculated are in excess of background or natural TSM concentrations. The two methods are in reasonable agreement for a point loading in the lower portion of the upper harbor.

PART VIII: CONCLUSIONS AND RECOMMENDATIONS

Baseline Conditions - Conclusions

203. Upper New Bedford Harbor was found to be a vertically well-mixed, shallow estuary with little vertical circulation and generally low current velocities. Concentrations of TSM were generally below 10 mg/ℓ and increased in the upstream direction. Suspended materials were found to be generally migrating from Buzzards Bay upstream in the estuary, settling in the upper harbor (estuary) at about 2,500 kg per tidal cycle. However, much of the suspended sediment entering the upper harbor on the flood tide was flushed out on the next ebb tide.

204. Very few indications of erosion of bed material were found during field surveys. The variation in TSM concentration between spring- and neap-tide surveys and within tidal surveys was slight. Tidal pumping was the dominant transport mechanism for suspended material. Suspended material settled and redispersed with the tide and tended to migrate upstream.

205. Escape of PCBs seaward from the upper harbor was documented by WES field surveys at an average of 1.55 kg per tidal cycle and was linked to contamination of "new" suspended sediments entering the upper harbor or to soluble releases. A source of PCBs to the flow in the upper harbor was therefore confirmed. When averaged with estimates from a previous study, PCB escape was 1.23 kg per tidal cycle. The PCBs associated with suspended sediments or dissolved in the flow dispersed seaward by the action of "to-and-fro" tidal flushing, and horizontal PCB concentration gradients, away from their source in the upper harbor. Exchanges of uncontaminated for contaminated sediment particles between sediment flocs or aggregates in suspension and on the bed could have been one mechanism contributing to the mobilization of PCBs from bed sediments in the upper harbor. The PCB fluxes as floatable material were found to be relatively unimportant under normal conditions.

206. Laboratory tests on the settling, deposition, and erosion characteristics of the fine-grained component of upper-harbor sediments were performed in a new sediment water tunnel. Three sediment fractions were identified by testing. One sediment fraction was by far the slowest to settle and deposit, and easiest to resuspend. This mobile fraction comprised 28 percent

of the EFS composite sample and could vary from 1 to 60 percent at various sites in the upper harbor.

Possible Dredging and Disposal - Conclusions

207. Current velocities and in situ sediment properties could provide the setting for a low-resuspension dredging operation, if proper care is given to equipment selection and operation. Upper-harbor tidal hydraulics will not be altered appreciably by large-scale dredging. Vessels operating in the upper harbor were found to resuspend bottom sediments when under-keel clearances were low. The average depth of the upper harbor is only about 1 m at mean tide. In certain areas of the upper harbor, vessel impact on bottom sediments may include the release of oily sheens high in PCBs.

208. Management of dredging and disposal activities would play an important role in controlling contaminant migration. Resuspension rate estimates were the greatest source of uncertainty in the evaluation of sediment and contaminant migrations. Prototype experience and judgment guided estimates for resuspension and release rates used in this study and in the pilot study plan (Otis and Andreliunas 1987). The pilot study results will provide the best estimate for resuspension and release rates.

209. Resuspension and release rate estimates used in this study suggested that releases from the CAD during filling would be the largest suspended sediment source and would produce most of the material escaping from the upper harbor. Estuarine hydrodynamic modeling identified portions of the upper harbor where CAD filling could most probably result in resuspension of deposited dredged sediment.

210. Coarser sediment fractions comprised 72 percent of the EFS composite and will not migrate far from sources in the upper harbor. Near-field models indicated that only a very small fraction of the coarser sediments was predicted to escape 100 m beyond their source or from CAD cells. Estuarine model results indicated that the escape of the coarser sediment fractions from the upper harbor will be about zero.

211. Most mobile-fraction suspended sediments will escape beyond 100 m of resuspension points and from CAD cells. Typical concentrations at a radius of 100 m from the dredgehead would be about 12 mg/ℓ above background for a bulk-sediment release rate of 40 g/sec. Escape probabilities for

mobile-fraction sediment from the upper harbor will range from 0.76 to 0.52 for the lower and upper portions of the upper harbor, respectively.

Recommendations

212. To minimize escape of contaminants and sediments from upper-harbor cleanup dredging and disposal, operations should be well planned and limited. Vessel movements in shallow areas should be limited. Vessels should keep to the deep areas inside the channel to the extent possible. Equipment used for dredging and disposal (such as a hydraulic dredge or submerged diffuser) should rely on cables for movement instead of conventional propulsion systems to reduce propwash resuspension of bed sediments or dredged material. This is especially true near CADs during filling, when contaminated dredged material will be most vulnerable to resuspension.

213. The pilot study is highly recommended to confirm resuspension and release rate estimates. Pilot study water monitoring should determine release rates, not just concentrations, by measuring currents and concentrations at a large number of points. Monitoring during the pilot study should be of such detail that contaminant or suspended sediment problems occurring at the Coggeshall Street Bridge can be traced to their source.

214. Slurry densities or solids content should be maintained as high as practicable during CAD filling to reduce solids release and migration.

REFERENCES

Anderson-Nichols and Company, Inc. 1984. "Remedial Action Modeling, Vols 1-4," prepared for EPA under Contract No. 68-03-3116, Palo Alto, CA.

Ariathurai, R., MacArthur, R. C., and Krone, R. B. 1977. "Mathematical Model of Estuarine Sediment Transport," Technical Report D-77-12, US Army Engineer Waterways Experiment Station, Vicksburg, MS.

Condike, B. J. 1986. "New Bedford Superfund Site, Acushnet River Estuary Study," US Army Engineer Division, New England, Materials and Water Quality Laboratory, Hubbardston, MA.

Ellis, J. P., et al. 1977. "Data File: New Bedford Harbor, Massachusetts," Technical Report WHOI-77-73, Woods Hole Oceanographic Institution, Woods Hole, MA.

Energy Resources Company. 1982. "Results of Sedimentation Test on Sediment from the Acushnet River Estuary," Cambridge, MA.

Fischer, H. B. 1973. "Longitudinal Dispersion and Turbulent Mixing in Open-Channel Flow," Annual Review of Fluid Mechanics, Vol 5, pp 59-78.

Francingues, N. R., Jr., et al. 1985. "Management Strategy for Disposal of Dredged Material: Contaminant Testing and Controls," Miscellaneous Paper D-85-1, US Army Engineer Waterways Experiment Station, Vicksburg, MS.

Geotechnical Engineers, Inc. 1982. "Dredging of PCB-Contaminated Sediments, New Bedford Harbor/Acushnet River Estuary, Massachusetts," Winchester, MA.

Huidobro, P., and DeLorenzo, D. 1983. "New Bedford Environmental Investigation - Hydrodynamic Grain Size Measurements of Selected Harbor Sediments," GCA-TR-82-102-G(2), GCA Corps, GCA/Technology Division, Bedford, MA.

Hunt, J. R. 1982. "Self-Similar Particle Size Distributions During Coagulation: Theory and Experimental Verification," Journal of Fluid Mechanics, Vol 122, pp 169-185.

Inman, D. L. 1963. "Sediments: Physical Properties and Mechanics of Sedimentation," Submarine Geology, 2d ed., Caren Cronier, ed., Harper and Row, New York, pp 100-152.

Jason M. Cortell and Associates. 1982. "Waterfront Park, New Bedford - Draft Environmental Impact Report," prepared for Massachusetts Division of Waterways.

Krone, K. B. 1962. "Flume Studies of the Transport of Sediment in Estuarial Shoaling Processes, Final Report," Hydraulic Engineering Laboratory and Sanitary Engineering Research Laboratory, University of California, Berkeley, CA.

Launder, B. E., Reese, G. J., and Rodi, W. 1985. "Progress in the Development of a Reynolds - Shear Turbulence Closure," Journal of Fluid Mechanics, Vol 168, Part 3, pp 537-566.

Malcolm Pirnie, Inc. 1982. "Acushnet River Estuary PCB Study," White Plains, NY.

Mehta, A. J., Hayter, E. J., Parker, W. R., and Teeter, A. M. 1986. "Cohesive Sediment Transport Processes," Proceedings, Sedimentation Control Committee, National Research Council, Washington, DC.

Nakai, O. 1978 (Sep). "Turbidity Generated by Dredging Projects," Management of Bottom Sediments Containing Toxic Substances, Proceedings of the Third U.S.-Japan Experts Meeting, S. A. Peterson and K. K. Randolph, eds., Research Report EPA-600/3-78-084, pp 31-47, Corvallis Environmental Research Laboratory, US Environmental Protection Agency, Corvallis, OR.

NUS Corporation. 1984. "Draft Feasibility Study of Remedial Action Alternatives, Acushnet River Estuary Above Coggeshall Street Bridge, New Bedford Site, Bristol County, Massachusetts," Pittsburg, PA.

O'Connor, B. A., and Tuxford, C. 1980. "Modelling Siltation at Dock Entrances," Proceedings, Third International Symposium on Dredging Technology, Paper F2, pp 359-371, BHRA Fluid Engineering, Cranfield, Bedford, England.

Okubo, A. 1980. Diffusion and Ecological Problems: Mathematical Models, Springer-Verlag, New York.

Otis, Mark J., and Andreliunas, V. L. 1987. "Pilot Study of Dredging and Dredged Material Disposal Alternatives: Superfund Site, New Bedford Harbor, Massachusetts," Waltham, MA.

Postma, H. 1967. "Sediment Transport and Sedimentation in the Estuarine Environment," Estuaries, G. H. Lauff, ed., Publication No. 83, pp 158-179, American Association for the Advancement of Science, Washington, DC.

Summerhayes, C. P., et al. 1977. "Fine-Grained Sediment and Industrial Waste Distribution and Dispersal in New Bedford Harbor and Western Buzzards Bay, Massachusetts," Report 76-115, Woods Hole Oceanographic Institute, Woods Hole, MA.

Teeter, A. M. 1986. "Vertical Transport in Fine-Grained Suspension and Newly-Deposited Sediment," Estuarine Cohesive Sediment Dynamics, A. Mehta, ed., Springer-Verlag, New York.

Teeter, A. M. "Deposition and Erosion Testing of the Composite Sediment Sample from New Bedford, Massachusetts," Technical Report (in preparation), US Army Engineer Waterways Experiment Station, Vicksburg, MS.

Thomas, W. A., and McAnally, W. H., Jr. 1985. "User's Manual for the Generalized Computer Program System, Open-Channel Flow and Sedimentation, TABS-2, Main Text," Instruction Report HL-85-1, US Army Engineer Waterways Experiment Station, Vicksburg, MS.

US Environmental Protection Agency. 1983. "Aerovox PCB Disposal Site; Acushnet River and New Bedford Harbor, Massachusetts; Tidal Cycle and PCB Mass Transport Study," Environmental Response Team, Edison, NJ.

Table 1

Summary of Survey Conditions

Survey Date	Freshwater Inflow cm/sec	Tidal Range at Tide Gage 3 m	Wind Direction, Speed km/h	Water Temperature
6 Mar 86	1.17	1.04	S, 24-32	4° C
24 Apr 86	1.50	1.65	NE, 8-12 then 32-48	11° C
5 Jun 86	0.25	1.04	SW, 16-24	17° C

Table 2

Fluxes of PCBs and TSM at the Coggeshall Street Bridge

Survey Date	Tidal Phase	Tidal Volume*	PCB-Aroclor ppb	TSM** ppm	PCB/TSM Aroclor ppm†	PCB Flux kg	TSM Flux kg	Tide-Corrected†† PCB flux kg	Tide-Corrected†† TSM kg
6 Mar 86	Ebb	-1.13	1.3	3.9	333	-1.47	-4,400		
	Flood	0.89	1.3	7.2	180	1.15	6,400		
	Net	-0.25				-0.32	2,100	-0.07	3,100
24 Apr 86	Ebb	-1.47	2.0	5.9	339	-2.94	-8,700		
	Flood	1.57	0.5	8.1	62	0.79	12,800		
	Net	0.10				-2.16	4,000	-2.36	2,900
5 Jun 86	Ebb	-0.67	5.8	6.6	879	-3.90	-4,400		
	Flood	0.88	3.0	7.4	405	2.63	6,500		
	Net	0.21				-1.27	2,100	-2.22	605

* Expressed as billions of litres.
** Total suspended material.
† Sediment dry-weight basis.
†† See text for explanation (paragraphs 53-54).

Table 3

Fluxes of PCB and TSM at the Coggeshall Street Bridge (from USEPA 1983)

Survey Date	Tidal Phase	Tidal Volume*	Total PCB-Aroclor ppb	TSM ppm	PCB/TSM Aroclor ppm**	PCB Flux kg	TSM Flux kg	Tide-Corrected† PCB Flux kg	Tide-Corrected† TSM kg
10 Jan 83	Ebb	-1.51	1.625	22.5	72	-2.45	-33,975		
	Flood	1.44	1.13	32.0	35	1.63	46,080		
	Net	-0.07				-0.83	12,105	-0.82	12,378
11 Jan 83	Ebb	-1.13	1.757	14.7	120	-1.98	-16,611		
	Flood	1.07	0.936	18.0	52	1.00	19,260		
	Net	-0.06				-0.98	2,649	-0.99	2,649
11 Jan 83	Ebb	-1.30	1.311	12.4	106	-1.70	-16,120		
	Flood	1.38	0.674	16.8	40	0.93	23,184		
	Net	0.08				-0.77	7,064	-0.91	5,020

* Expressed as billions of litres.
** Sediment dry-weight basis.
† See text for explanation, assumes 1.42-cu m/sec inflow.

Table 4

PCB Analysis of Composite Suspended Samples at the Coggeshall Street Bridge

Date	Tidal Phase	PCB Aroclor Concentration, ppm 1016	1221	1232	1242	1248	1254	1260	Sum
6 Mar 86	Ebb	ND*	ND	ND	0.0008	ND	0.0005	ND	0.0013
6 Mar 86	Flood	ND	ND	ND	0.0006	ND	0.0007	ND	0.0013
24 Apr 86	Ebb	ND	ND	ND	0.0013	ND	0.0007	ND	0.0020
24 Apr 86	Flood	ND	ND	ND	0.0001	ND	0.0004	ND	0.0005
5 Jun 86	Ebb	ND	ND	ND	0.0039	ND	0.0019	ND	0.0058
5 Jun 86	Flood	ND	ND	ND	0.0017	ND	0.0013	ND	0.0030

* Not detectable, <0.0002 ppm.

Table 5

PCB Analysis of Floatable Samples at the Coggeshall Street Bridge

Time, EST	PCB Aroclor Concentration, µg/0.093 sq m							
	1016	1221	1232	1242	1248	1254	1260	Sum
				6 Mar 86				
0630	ND*	ND	ND	ND	ND	ND	ND	0
0707	ND	ND	ND	ND	ND	ND	ND	0
0806	ND	ND	ND	ND	ND	ND	ND	0
0909	ND	ND	ND	ND	ND	ND	ND	0
1007	ND	ND	ND	ND	ND	ND	ND	0
1107	ND	ND	ND	ND	ND	ND	ND	0
1200	ND	ND	ND	ND	ND	ND	ND	0
1305	ND	ND	ND	ND	ND	ND	ND	0
1406	ND	ND	ND	ND	ND	ND	ND	0
1506	ND	ND	ND	ND	ND	ND	ND	0
1606	ND	ND	ND	ND	ND	ND	ND	0
1701	ND	ND	ND	ND	ND	ND	ND	0
				24 Apr 86				
0602	ND	ND	ND	ND	ND	ND	ND	0
0706	ND	ND	ND	ND	ND	ND	ND	0
0807	ND	ND	ND	ND	ND	ND	ND	0
0907	ND	ND	ND	ND	ND	ND	ND	0
1009	ND	ND	ND	ND	ND	ND	ND	0
1105	ND	ND	ND	ND	ND	ND	ND	0
1206	ND	ND	ND	1.56	ND	0.257	ND	1.817
1306	ND	ND	ND	0.335	ND	0.188	ND	0.523
1414	ND	ND	ND	0.491	ND	0.325	ND	0.816
1515	ND	ND	ND	ND	ND	ND	ND	0
1607	ND	ND	ND	ND	ND	ND	ND	0
1708	ND	ND	ND	ND	ND	0.092	ND	0.092
				5 Jun 86				
0706	ND	ND	ND	1.7	ND	1.7	ND	3.4
0804	ND	ND	ND	1.4	ND	1.3	ND	2.7
0903	ND	ND	ND	1.4	ND	1.1	ND	2.5
1004	ND	ND	ND	1.7	ND	1.3	ND	3.0
1107	ND	ND	ND	1.3	ND	1.0	ND	2.3
1205	ND	ND	ND	0.85	ND	0.90	ND	1.75
1303	ND	ND	ND	0.57	ND	0.78	ND	1.35
1404	ND	ND	ND	ND	ND	ND	ND	0
1503	ND	ND	ND	ND	ND	ND	ND	0
1604	ND	ND	ND	ND	ND	ND	ND	0
1704	ND	ND	ND	ND	ND	ND	ND	0

* Not detectable, <0.01 µ/0.093 sq m.

Table 6

Principal Estuarine Characteristics for the 6 Mar 86 Survey

Station	River Miles	$\bar{U}o$ fps	$\bar{U}s$ fps	$\langle\bar{U}i\rangle$ rms*	$\bar{S}o$ ppt	$\langle\bar{S}i\rangle$ rms	$\bar{U}ov$ rms	$\bar{U}sv$ rms	$\bar{S}ov$ rms
4	2.5	-0.25	0.00	1.44	29.6	1.1	0.07	0.00	0.30
5	2.5	-0.01	0.00	1.26	29.4	0.7	0.03	0.00	0.55
6	2.5	-0.16	0.00	1.27	29.3	0.7	0.04	0.00	0.19

* Root-mean-square.

Table 7

Select Correlations for the 6 Mar 86 Survey

Station	River Miles	Depth ft	$\bar{U}o\bar{C}o$	$\bar{U}s\bar{C}o$	$\bar{U}i\bar{C}i$	$\overline{UovCov}$	$\overline{UsvCov}$	$\overline{UivCiv}$	Total
4	2.5	13	-1.56	0.00	-0.93	0.02	0.00	4.17	1.70
5	2.5	15	-0.04	0.00	0.75	-0.01	0.00	-0.12	0.59
6	2.5	11	-0.78	0.00	0.32	-0.01	0.00	1.41	0.93

Table 8

Principal Estuarine Characteristics for the 24 Apr 86 Survey

Station	River Miles	$\bar{U}o$ fps	$\bar{U}s$ fps	$\langle\bar{U}i\rangle$ rms	$\bar{S}o$ ppt	$\langle\bar{S}i\rangle$ rms	$\bar{U}ov$ rms	$\bar{U}sv$ rms	$\bar{S}ov$ rms
1	0.2	0.26	-0.16	0.62	31.8	0.2	0.07	0.04	0.17
2	1.1	0.08	-0.01	0.28	31.6	0.2	0.19	0.01	0.43
3	2.0	0.13	0.07	0.36	30.6	0.4	0.29	0.03	0.74
4	2.5	-0.09	0.00	1.45	30.1	0.8	0.10	0.00	0.34
5	2.5	0.14	0.00	2.04	29.9	1.1	0.03	0.00	0.52
6	2.5	-0.02	0.00	1.91	30.0	1.0	0.07	0.00	0.26
7	2.8	0.08	-0.14	0.62	29.8	0.7	0.02	0.07	0.46
8	3.3	0.26	0.08	0.49	29.6	0.8	0.04	0.02	0.51

Table 9

Select Correlations for the 24 Apr 86 Survey

Station	River Miles	Depth ft	$\bar{U}o\bar{C}o$	$\bar{U}s\bar{C}o$	$\bar{U}i\bar{C}i$	$\overline{UovCov}$	$\overline{UsvCov}$	$\overline{UivCiv}$	Total
1	0.2	33	0.90	-0.56	0.33	0.02	0.02	1.72	2.43
2	1.1	30	0.39	-0.04	-0.24	0.07	-0.00	1.91	2.09
3	2.0	22	0.59	0.30	-0.05	0.16	0.03	1.13	-0.10
4	2.5	13	-0.65	0.00	0.33	-0.10	0.00	2.57	2.15
5	2.5	15	0.95	0.00	1.28	-0.01	0.00	0.66	2.88
6	2.5	11	-0.16	0.00	0.96	0.04	0.00	0.44	1.28
7	2.8	14	0.86	-1.41	-0.32	0.02	-0.09	-2.47	-3.41
8	3.3	10	1.89	0.59	0.60	0.00	-0.03	0.18	3.24

Table 10

Principal Estuarine Characteristics for the 5 Jun 86 Survey

Station	River Miles	$\bar{U}o$ fps	$\bar{U}s$ fps	$\langle\bar{U}i\rangle$ rms	$\bar{S}o$ ppt	$\langle\bar{S}i\rangle$ rms	$\bar{U}ov$ rms	$\bar{U}sv$ rms	$\bar{S}ov$ rms
1	0.2	-0.05	-0.08	0.58	32.6	0.2	0.06	0.06	0.09
2	1.1	-0.04	-0.00	0.47	32.4	0.2	0.13	0.03	0.15
3	2.0	-0.11	0.08	0.44	31.8	0.2	0.11	0.04	0.22
4	2.5	0.07	0.00	0.81	31.2	0.4	0.07	0.00	0.03
5	2.5	0.12	0.00	0.89	31.2	0.4	0.01	0.00	0.03
6	2.5	0.11	0.00	0.87	31.2	0.4	0.02	0.00	0.02
7	2.8	0.32	-0.14	0.23	30.9	0.5	0.07	0.05	0.15
8	3.3	0.15	0.10	0.34	30.6	1.0	0.09	0.06	0.23

Table 11

Select Correlations for the 5 Jun 86 Survey

Station	River Miles	Depth ft	$\bar{U}o\bar{C}o$	$\bar{U}s\bar{C}o$	$\bar{U}i\bar{C}i$	$\overline{UovCov}$	$\overline{UsvCov}$	$\overline{UivCiv}$	Total
1	0.2	33	-0.19	-0.30	-0.16	-0.05	0.02	1.18	0.49
2	1.1	30	-0.19	-0.02	-0.00	-0.08	0.03	-0.93	-1.21
3	2.0	22	-1.13	0.79	0.41	0.01	0.02	-0.86	-0.76
4	2.5	13	0.51	0.00	-0.10	0.02	0.00	2.03	2.45
5	2.5	15	0.90	0.00	-0.03	0.00	0.00	-0.53	0.35
6	2.5	11	0.76	0.00	0.45	0.00	0.00	-0.69	0.52
7	2.8	14	3.11	-1.39	0.08	0.07	-0.01	-1.87	-0.02
8	3.3	10	2.16	1.51	-0.52	0.06	0.07	-0.23	3.07

Table 12

Settling Velocity Distributions, Grid Cell J-8

Initial Concentration mg/ℓ	Average Settling Velocity mm/sec	Geometric Mean Settling Velocity mm/sec	Standard Deviation	Skewness	Kurtosis	Cumulative Percent Greater than Settling Velocity	Settling Velocity mm/sec
			1045 EST, 4-ft depth				
122	0.650	0.482	4.3	0.18	0.44	10	3.297 E+00
						20	1.596 E+00
						30	9.074 E-01
						40	5.620 E-01
						50	3.679 E-01
						60	2.507 E-01
						70	1.760 E-01
						80	1.266 E-01
						90	9.293 E-02
			1051 EST, 2-ft depth				
180	1.064	1.087	2.3	-0.03	0.33	10	2.816 E+00
						20	2.245 E+00
						30	1.784 E+00
						40	1.412 E+00
						50	1.113 E+00
						60	8.739 E-01
						70	6.831 E-01
						80	5.315 E-01
						90	4.116 E-01

Table 13

Resuspension Rate Estimates

Grid Cell	U m/sec	C_5* mg/ℓ	C_{50}** mg/ℓ	Estimated Resuspension Rate g/sec: Plume† at C_5	Plume†† at C_{50}	Flux Integration‡ at 46 m
J-8	0.015	89	80	2	13	37
G-17	0.09	26	44‡‡	7	42	-

* Observed concentration less background at 5 m from center.
** Observed concentration less background at 46 m from center.
† Resuspension rate estimated by fitting analytical plume results to C_5, using observed currents and W_s = 5 E-04 m/sec.
†† Resuspension rate estimated by fitting analytical plume results to C_5, using observed currents and W_s = 1 E-04 m/sec.
‡ Resuspension rate estimated by calculating flux = area × U × C_{50}, where the area is that of plume at 46 m.
‡‡ Based on a single sample.

Table 14

PCB Analysis of Suspended Samples, 31 March 1986

Time, Est	Grid Cell	PCB Aroclor Concentration, ppm: 1016	1221	1232	1242	1248	1254	1260	Sum
1046	J-8	ND*	ND	ND	0.052	ND	0.028	ND	0.080
1102	J-8	ND	ND	ND	0.102	ND	0.040	ND	0.142
1225	G-17	ND	ND	ND	0.0018	ND	0.0007	ND	0.0025
1230	G-17	ND	ND	ND	0.0023	ND	0.0015	ND	0.0038
1242	G-17	ND	ND	ND	0.0026	ND	0.0012	ND	0.0038

* Not detectable, <0.0002 ppm.

Table 15

PCB Analysis of Floatable Samples, 31 Mar 86

Time, Est	Grid Cell Location	PCB Aroclor Concentration, µg/0.093 sq m							
		1016	1221	1232	1242	1248	1254	1260	Sum
1012	J-8	ND*	ND	ND	0.179	ND	0.040	ND	0.219
1224	G-17	ND	ND	ND	1.21	ND	0.338	ND	1.55
1232	G-17	ND	ND	ND	0.220	ND	0.070	ND	0.29
1241	G-17	ND	ND	ND	0.637	ND	0.470	ND	1.11

* Not detectable, <0.01 µg/0.093 sq m.

Table 16

PCB Analysis of Floatable Sample Produced by Vessel Disturbance Near Grid Cell J-7, 4 Jun 86

Time, EST	PCB Aroclor Concentration, µg/0.093 sq m							
	1016	1221	1232	1242	1248	1254	1260	Sum
0906	ND*	ND	ND	2,400	ND	889	ND	3,289

* Not detectable.

Table 17

PCB Analysis of Suspended Sample Produced by Vessel Disturbance Near Grid Cell J-7, 4 Jun 86

Time, EST	PCB Aroclor Concentration, ppm							
	1016	1221	1232	1242	1248	1254	1260	Sum
0906	ND	ND	ND	1.90	ND	1.67	ND	3.57

* Not detectable.

Table 18

Physical Properties of the Composite Sediment

Parameter	Replicate 1	Replicate 2	Replicate 3
Total solids, percent	35.8	35.6	36.1
Total exchangeable cations, ppm	220	248	212
Oil and grease, ppm	28,000	27,000	30,000

Table 19

Water Tunnel Propeller Speed Calibration

Propeller Speed rpm	Average Current Speed cm/sec	Bed Shear Stress N/sq m
150	6.0	0.015
200	10.2	0.030
240	13.6	0.056
280	17.5	0.077
320	21.3	0.164
440	35.1	0.591

Table 20

Chronology of Bed Shear Stress Application During Tests

Test	Bed Shear Stress, N/sq m: Resuspension Phase (30 min each) 1	Resuspension Phase (30 min each) 2	Mixing Period (30 min)	Depositional Phase (90 min)	Settling Phase (300 min)
I-1	0.164	0.06	0.60	0.164	X
I-2	0.164	0.60	0.60	0.077	X
I-3	0.077	0.164	0.60	0.030	X
II-I	0.030	0.056		0.030	X
II-2	0.056	0.077		0.056	X
II-3	0.077	0.164		0.077	X
III-1	0.60	0.164	0.60	0.164	X
III-2	0.60	0.077	0.60	0.077	X
III-3	0.60	0.030	0.60	0.030	X
IV-1	0.60		0.60	0.077	X*
IV-2	0.60			0.030	
IV-3	0.60			0.015**	

* Settling phase after mixing and before resuspension and depositional test phase.

** Depositional test phase extended to 150 min.

Table 21

Settling Velocity Distributions

Initial Concentration mg/ℓ	Average Settling Velocity mm/sec	Geometric Mean Settling Velocity mm/sec	Standard Deviation	Skewness	Kurtosis	Cumulative Percent Greater than Settling Velocity	Cumulative Settling Velocity mm/sec
			Test I-1				
160	0.327	0.131	4.6	0.18	0.44	10	9.758 E-01
						20	4.596 E-01
						30	2.551 E-01
						40	1.548 E-01
						50	9.946 E-02
						60	6.662 E-02
						70	4.605 E-02
						80	3.264 E-02
						90	2.362 E-02
			Test I-2				
172	0.304	0.145	3.4	0.17	0.41	10	6.926 E-01
						20	3.952 E-01
						30	2.503 E-01
						40	1.686 E-01
						50	1.184 E-01
						60	8.580 E-02
						70	6.366 E-02
						80	4.815 E-02
						90	3.701 E-02
			Test I-3				
184	0.359	0.170	3.7	0.17	0.42	10	9.375 E-01
						20	5.003 E-01
						30	3.033 E-01
						40	1.975 E-01
						50	1.349 E-01
						60	9.538 E-02
						70	6.926 E-02
						80	5.137 E-02
						90	3.877 E-02

(Continued)

Table 21 (Continued)

Initial Concentration mg/ℓ	Average Settling Velocity mm/sec	Geometric Mean Settling Velocity mm/sec	Standard Deviation	Skewness	Kurtosis	Cumulative Percent Greater than Settling Velocity	Settling Velocity mm/sec
				Test II-1			
158	0.169	0.117	2.2	0.19	0.46	10	3.445 E-01
						20	2.271 E-01
						30	1.655 E-01
						40	1.269 E-01
						50	1.005 E-01
						60	8.136 E-02
						70	6.703 E-02
						80	5.598 E-02
						90	4.727 E-02
				Test II-2			
168	0.255	0.118	3.2	0.19	0.47	10	5.607 E-01
						20	3.066 E-01
						30	1.942 E-01
						40	1.324 E-01
						50	9.453 E-02
						60	6.976 E-02
						70	5.278 E-02
						80	4.071 E-02
						90	3.191 E-02
				Test II-3			
176	0.168	0.116	2.5	0.19	0.45	10	3.973 E-01
						20	2.481 E-01
						30	1.728 E-01
						40	1.274 E-01
						50	9.737 E-02
						60	7.637 E-02
						70	6.107 E-02
						80	4.961 E-02
						90	4.080 E-02

(Continued)

Table 21 (Continued)

Initial Concentration mg/ℓ	Average Settling Velocity mm/sec	Geometric Mean Settling Velocity mm/sec	Standard Deviation	Skewness	Kurtosis	Cumulative Percent Greater than Settling Velocity	Cumulative Settling Velocity mm/sec
			Composite II				
167	0.165	0.117	2.6	0.20	0.48	10	4.198 E-01
						20	2.535 E-01
						30	1.741 E-01
						40	1.273 E-01
						50	9.679 E-02
						60	7.561 E-02
						70	6.029 E-02
						80	4.886 E-02
						90	4.011 E-02
			Test III-1				
164	0.307	0.137	3.7	0.17	0.42	10	7.427 E-01
						20	4.014 E-01
						30	2.448 E-01
						40	1.600 E-01
						50,	1.096 E-01
						60	7.761 E-02
						70	5.643 E-02
						80	4.189 E-02
						90	3.165 E-02
			Test III-2				
190	0.364	0.164	4.1	0.18	0.43	10	1.048 E-00
						20	5.258 E-01
						30	3.050 E-01
						40	1.917 E-01
						50	1.270 E-01
						60	8.739 E-02
						70	6.191 E-02
						80	4.489 E-02
						90	3.317 E-02

(Continued)

Table 21 (Concluded)

Initial Concentration mg/ℓ	Average Settling Velocity mm/sec	Geometric Mean Settling Velocity mm/sec	Standard Deviation	Skewness	Kurtosis	Cumulative Percent Greater than Settling Velocity	Cumulative Settling Velocity mm/sec
			Test III-3				
174	0.356	0.153	4.5	0.18	0.44	10	1.092 E-00
						20	5.194 E-01
						30	2.914 E-01
						40	1.785 E-01
						50	1.158 E-01
						60	7.824 E-02
						70	5.453 E-02
						80	3.895 E-02
						90	2.839 E-02
			Composite III				
176	0.337	0.147	4.1	0.18	0.43	10	9.240 E-01
						20	4.662 E-01
						30	2.720 E-01
						40	1.719 E-01
						50	1.144 E-01
						60	7.906 E-02
						70	5.624 E-02
						80	4.093 E-02
						90	3.036 E-02
			Test IV-1				
426	0.509	0.444	6.4	0.15	0.38	10	4.607 E+00
						20	2.089 E+00
						30	1.064 E+00
						40	5.843 E-01
						50	3.391 E-01
						60	2.053 E-01
						70	1.286 E-01
						80	8.276 E-02
						90	5.453 E-02

Table 22

Summary of Erosion and Deposition Test Coefficients

Variables	Sediment Fraction 1	2	3
Deposition			
τ_{cd}, N/sq m	0.42	0.33	0.043
Al	6.4 E-03	3.2 E-03	1.8 E-05
W_s, mm/sec	2.02	1.04	0.006
Erosion			
τ_c, N/sq m	0.6	0.6-0.16	0.060
M, g/sq m/min	--	--	0.25

Table 23

Weight Percentages of Test Material

Test	Percent by Weight - Fraction Number 1	2	3
I-1	18	24	58
I-2	18	24	58
I-3	18	24	58
II-1	0	0	100
II-2	0	0	100
II-3	0	11	89
III-1	18	24	58
III-2	18	24	58
III-3	18	24	58
IV-1	0	28	72
IV-2	0	28	72
IV-3	0	21	79
Sieved composite	30	30	40

Table 24

Suspended Sediment Plume with Depth of 1 m

W_s, mm/sec	τ_{cd}, N/sq m	Frequency	U, Current Speed, m/sec (Frequency of Occurrence) 0.008 (0.17)	0.030 (0.39)	0.053 (0.35)	0.069 (0.09)
		Fraction Escaping 50 m*				
5.000	0.510	0.32	0.00	0.00	0.01	0.03
2.000	0.420	0.20	0.00	0.04	0.16	0.25
1.000	0.330	0.20	0.00	0.19	0.40	0.51
0.006	0.043	0.28	0.96	0.99	1.00	1.00
	Weighted total		0.05	0.13	0.14	0.04
		Fraction Escaping 100 m**				
5.000	0.510	0.32	0.00	0.00	0.00	0.03
2.000	0.420	0.20	0.00	0.00	0.03	0.06
1.000	0.330	0.20	0.00	0.04	0.16	0.25
0.006	0.043	0.28	0.91	0.97	0.98	0.98
	Weighted total		0.04	0.11	0.11	0.03

* Total average escape = 35 percent of released material.
** Total average escape = 29 percent of released material.

Table 25

R/R_o for CAD with Natural Depth (1.0 m), L = 50.0 m,

and Q/A = 8.4 E-06 m/sec

W_s, mm/sec	τ_{cd}, N/sq m	Frequency	U, Current Speed, m/sec (Frequency of Occurrence) 0.008 (0.17)	0.030 (0.39)	0.053 (0.35)	0.069 (0.09)
		H = 2.92 m				
5.000	0.510	0.32	0.00	0.00	0.00	0.00
2.000	0.420	0.20	0.00	0.00	0.00	0.00
1.000	0.330	0.20	0.00	0.00	0.00	0.00
0.006	0.043	0.28	1.00	1.00	1.00	1.00
			Total average R/R_o = 28 percent			
		H = 2.25 m				
5.000	0.510	0.32	0.00	0.00	0.00	0.00
2.000	0.420	0.20	0.00	0.00	0.00	0.00
1.000	0.330	0.20	0.00	0.00	0.00	0.00
0.006	0.043	0.28	1.00	1.00	1.00	1.00
			Total average R/R_o = 28 percent			
		H = 1.59 m				
5.000	0.510	0.32	0.00	0.00	0.00	0.00
2.000	0.420	0.20	0.00	0.00	0.00	0.00
1.000	0.330	0.20	0.00	0.00	0.01	0.04
0.006	0.043	0.28	1.00	1.00	1.00	1.00
			Total average R/R_o = 28 percent			
		H = 0.92 m				
5.000	0.510	0.32	0.00	0.00	0.00	0.00
2.000	0.420	0.20	0.00	0.00	0.00	0.01
1.000	0.330	0.20	0.00	0.00	0.09	0.22
0.006	0.043	0.28	1.00	1.00	1.00	1.00
			Total average R/R_o = 29 percent			

Note: Overall average release = 28 percent based on R/R_o.

Table 26

C/C_o for CAD with Natural Depth (1.0 m), L = 50.0 m, and Q/A = 8.4 E-06 m/sec

W_s, mm/sec	τ_{cd}, N/sq m	Frequency	U, Current Speed, m/sec (Frequency of Occurrence) 0.008 (0.17)	0.030 (0.39)	0.053 (0.35)	0.069 (0.09)
		H = 2.92 m				
5.000	0.510	0.32	0.00	0.00	0.00	0.00
2.000	0.420	0.20	0.00	0.00	0.00	0.00
1.000	0.330	0.20	0.00	0.00	0.03	0.11
0.006	0.043	0.28	1.00	1.00	1.00	1.00
			Total average C/C_o = 28 percent			
		H = 2.25 m				
5.000	0.510	0.32	0.00	0.00	0.00	0.00
2.000	0.420	0.20	0.00	0.00	0.00	0.00
1.000	0.330	0.20	0.00	0.00	0.05	0.15
0.006	0.043	0.28	1.00	1.00	1.00	1.00
			Total average C/C_o = 29 percent			
		H = 1.59 m				
5.000	0.510	0.32	0.00	0.00	0.00	0.00
2.000	0.420	0.20	0.00	0.00	0.00	0.01
1.000	0.330	0.20	0.00	0.00	0.09	0.22
0.006	0.043	0.28	1.00	1.00	1.00	1.00
			Total average C/C_o = 29 percent			
		H = 0.92 m				
5.000	0.510	0.32	0.00	0.00	0.00	0.00
2.000	0.420	0.20	0.00	0.00	0.01	0.04
1.000	0.330	0.20	0.00	0.01	0.18	0.32
0.006	0.043	0.28	1.00	1.00	1.00	1.00
			Total average C/C_o = 30 percent			

Note: Overall average release = 29 percent based on C/C_o.

Table 27

Resuspended Sediment Composition and Depositional Characteristics

Sediment Fraction	Concentration by Weight - Release Source			W_s mm/sec	P*	α day^{-1}
	Dredge	CDF	CAD			
0	0.32	0	0	5	0.95	400
1	0.20	0	0	2	0.95	160
2	0.20	0	0	1	0.95	80
3	0.28	1.00	1.00	0.006	0.65	0.34

* See text for explanation (paragraph 193).

Table 28

Escape Probabilities for Resuspended Sediments

Sediment Fraction	Upper-Harbor Escape Probabilities* - Release Site**		
	Lower	Middle	Upper
0	0	0	0
1	0	0	0
2	0.01	0	0
3	0.76	0.68	0.52

* From Figure 27.
** See Figure 24.

Table 29

Example Midestuary Releases and Escapes for Continuous Releases

Release Source	Sediment Release Rate g/sec	Escape at the Coggeshall Street Bridge g/sec
Dredge	40	7.6
CDF	6*	4.1
CAD	105**	71.4

* Based on 70 mg/ℓ suspended sediment and 0.084 m^3/sec effluent flow rate.
** Based on 1 percent of the sediment inflow rate.

APPENDIX A: CONTAMINANT MIGRATION BY SUSPENSION/BED PARTICLE EXCHANGES

1. An important WES HL study task was to define physical mechanisms that might be responsible for contaminant migration. The mobilization and transport of PCB contaminants from the bed sediments in upper New Bedford Harbor undoubtedly involves many processes, including physiochemical behavior of the sediments and the contaminants, and possibly biological factors. The continual release of PCBs from bed sediments in the presence of general deposition suggests that contaminant material migrates to the surface of the sediment bed by some mechanism(s). From this boundary, contaminants could be mobilized and released into the overlying flow by diffusion of a soluble phase, by biological action, by desorption, by erosion, or by a particle exchange mechanism.

2. The purpose of this appendix is to develop a conceptual and analytical basis for evaluation of a physical process other than erosion possibly involved in the mobilization of sediment-associated contaminants in upper New Bedford Harbor. A new description of a physical particle exchange mechanism is presented in the following paragraphs. In previous laboratory studies on cohesive sediments, exhanges of materials have been observed to operate between the bed and overlying suspension. Those experiments suggest that particle exchange between the bed and suspension could affect mobilization of contaminants in New Bedford Harbor. An analysis of those experiments was made to quantify the order of magnitude with which this mechanism might operate in upper New Bedford Harbor.

3. While particle exchange has been discussed in the literature, an analytic framework for evaluating contaminant mobilization for transport by particle exchange has not been hitherto published.* The particle exchange mechanism described in this appendix is based on aggregation and disaggregation of cohesive particles resulting from collisions at the interface between the suspension and bed.

4. The following sections discuss: (a) baseline conditions,

---

* Before publication of this report, the author learned that K. R. Stolzenbach, Civil Engineering Department, Massachusetts Institute of Technology, Cambridge, MA, had arrived at a similar theory in conjunction with fine tracer particle aggregation at the bed-water interface. Dr. Stolzenbach has submitted journal articles on this subject for publication.

(b) particle exchanges between aggregates, (c) suspended aggregate collision frequency, (d) mass exchange by aggregate collisions at the bed, (e) contaminant migration by particle exchange, and (f) application of the particle exchange mechanism to the migration of contaminants in upper New Bedford Harbor.

Baseline Condition Summary

5. Upper New Bedford Harbor, above the Coggeshall Street Bridge, was found in the three 1986 WES surveys to be a vertically well-mixed, shallow estuary with little vertical circulation and generally low current velocities. Concentrations of suspended material were generally below 10 ppm and increased in the upstream direction. Suspended materials were found to be generally migrating from Buzzards Bay upstream in the estuary, settling in the upper harbor at about 2,500 kg per tidal cycle. However, much of the suspended sediment entering the upper harbor on the flood tide was flushed out on the next ebb tide. Tidal pumping was the dominant transport mechanism for suspended material. Erosion was very slight or undetectable and produced sediment flux in the upstream direction.

6. The escape of PCBs from the upper harbor was documented by the WES field surveys at an average of 1.55 kg per tidal cycle and was linked to contamination of "new" sediments entering the upper harbor or to soluble releases. A source of PCB to the flow in the upper harbor was therefore confirmed. The PCBs associated with suspended sediments or dissolved in the flow dispersed seaward by the action of "to-and-fro" tidal flushing, and horizontal PCB concentration gradients, away from their source in the upper harbor. The PCB fluxes as floatable material were found to be relatively unimportant.

7. A more complete description of baseline conditions is contained in Part III of the main report. One mechanism by which suspended sediment particles could mobilize PCBs from contaminated bed sediments was described in that part as particle exchange.

Particle Exchanges Between Aggregates

8. Clays and fine silts exist in the marine and estuarine environments as particle aggregates. Aggregates can be made up by thousands or millions of

particles. Aggregates, formed by interparticle collisions of cohesive sediment or organic particles, vary in size, strength, and density depending on the cohesive minerals and organic materials present, concentration, and flow conditions. (Aggregate size distributions measured in New Bedford suspended samples had modal sizes ranging from about 15 to 30 μm.) The larger the aggregates grow, the weaker and less dense they tend to become. Suspended aggregates are broken into particles or lower order aggregation by collisions and by turbulent shear greater than they can withstand, especially near the bed. Aggregates are constantly being created and destroyed in estuarine flows, causing individual particles and low-order (strong and small) aggregates to recombine with many different "partners."

9. In a shear flow, steady-state suspended aggregate size distributions reflect a balance between aggregation and disaggregation processes. Aggregate populations undergo simultaneous fluxes of particles toward the larger size (aggregation) and toward the smaller size (disaggregation), while net fluxes are zero if the population distributions are statistically stable.

10. Total exchanges of particles between a flowing suspension and the bed have been found to be greater than net exchanges produced by either erosion or deposition. Krone's (1962)* laboratory studies using radioactive gold-198-labeled cohesive sediments found that a physical particle exchange mechanism operated during both erosion and deposition. Radioactive-labeled sediment particles left suspension at a faster rate than the total sediment was depositing, and in other experiments even moved from suspension onto the bed while the bed was undergoing erosion.

Suspended Aggregate Collision Frequency

11. Particles at the surface of the sediment bed collide with, and can recombine into, aggregates carried by the suspension. Aggregates are diffused and transported in estuarine flows and periodically collide with aggregates that form the bed. Three mechanisms produce collisions of aggregates in a shear flow: Brownian motion, shear imposed by the flow, and differential settling. At the boundary between the sediment bed and the flow, shear is greatest and assumed to be the most important collision mechanism. Shear

---

* See References at the end of the main text.

stress (τ) increases with increased depth in a flow, then becomes constant in the laminar sublayer near the bed. Laminar sublayer shear in the near-bed mean flow (dU/dZ) is related to τ by:

$$\tau = \mu \frac{dU}{dZ} \tag{A1}$$

where μ is the dynamic viscosity.

12. The suspended aggregate collision rate per unit time (J) depends on flow shear and the volume concentration of the particles:

$$J = \frac{4}{3} nR^3 \frac{dU}{dZ} \tag{A2}$$

where n is the number of particles per unit volume and R is the effective radius of aggregates. The collision rate per unit bed area between aggregates in suspension and on the bed is related to J and a factor dependent on aggregate geometry, discussed in the next section.

Mass Exchange by Aggregate Collisions at the Bed

13. As an aggregate in suspension collides with sediment bed aggregate, a cohesive bond immediately forms. Then, if the shear imposed by the flow is greater than the combined-aggregate can withstand, the aggregate is broken. The break point may be different from the point of combination. A particle or low-order aggregate may be torn from the bed or deposited as a result of the collision. Particle exchange is thus considered to be a process of aggregation/disaggregation and not a superposition of erosion and deposition processes. Simultaneous erosion and deposition has been postulated but not demonstrated, and experimental evidence suggests that it does not occur.

14. The mass exchange rate per unit area (K) at the boundary is equal to the collision rate (J) times the average mass (a) exchanged as a result of a collision times the fraction of suspended sediment per unit area (b) involved in collisions with the bed:

$$K = abJ \tag{A3}$$

Combining Equations A1-A3 and converting particle number concentration to specific weight of sediment material (C) yields

$$K = \left| abR^3 \frac{4}{3} \frac{d}{\mu} \right| C\tau_b \tag{A4}$$

$$K = \Theta C \tau_b \tag{A5}$$

where d is the conversion from mass to number of particles per unit volume ($n = dC$), τ_b is the bed shear stress, and Θ is a lumped coefficient describing aggregate geometry and collision characteristics.

Contaminant Migration by Particle Exchanges

15. The flux of particle-associated contaminant at the suspension bottom boundary depends on the mass rate of particle exchange between the bed sediments and suspension, and on the difference in the contaminant concentration between bed and suspended particles.

16. Let S and S_s be the contaminant concentration by dry weight of suspended and bed sediment (micrograms per gram), respectively. For an infinite source or sink of contaminant in the sediment bed, the equation describing mass balance for contaminant associated with the suspended particles is

$$CH \frac{dS}{dt} = K(S_s - S) \tag{A6}$$

where H is the suspension depth, t is time, and C and S_s are assumed to be time invariant. The solution for Equation A6 for the initial condition that $S = S_o$ at $t = 0$ is

$$S = S_s - (S_s - S_o) \exp\left[-\frac{K\,t}{C\,H}\right] \tag{A7}$$

and substituting for K,

$$S = S_s - (S_s - S_o) \exp\left[-\frac{\Theta \tau_b t}{H}\right] \tag{A8}$$

Note that the final solution is independent of C. For the case where $S_s = 0$, the solution to Equation A6 reduces to:

$$S = S_o \exp\left[-\frac{\Theta \tau_b t}{H}\right] \tag{A9}$$

17. To test this theory, data from Krone (1962, Figure 16, pg 45) were fit to estimate Θ and K. The original data are presented in Figure A1, and results are shown in Figure A2. The data were from an experiment with Mare Island Straits sediment in which labeled tracer was added to a suspension during deposition. At $t = 0$ of the experiment, there was no tracer in the bed sediments and Equation A9 applies. Deposition occurred during the experiments, and the removal of tracer from suspension was more rapid than deposition of suspended sediment. The magnitude of S was not measured directly, but the ratio S/S_o equals the observed ratio C_1/C where C_1 is the labeled sediment concentration.

18. Table A1 shows experimental data and derived coefficients K, Θ, and the depositional flux (D) for the first 8 hr of Krone's experiment. Table A1 shows the magnitude of K to be more than half that of D. Such magnitudes of particle exchange might explain how labeled sediment migrated to the sediment bed during Krone's erosion experiments.

19. Figure A2 shows plots of K and Θ versus C. It can be seen that K varies linearly with concentration and extrapolates to zero at zero concentration, as predicted by Equation A5. On the other hand, Θ did not change with C, but probably varies with other sediment properties associated with aggregation (cohesiveness, fluid chemistry, etc.).

Application of Analysis to New Bedford

20. The best method of applying the particle exchange analysis to New Bedford is to develop direct experimental data similar to that of Krone's for native sediments, since the coefficient Θ is expected to be dependent on sediment properties. However, an assessment of the possible importance of the particle exchange mechanism to the migration of contaminants out of the upper New Bedford Harbor was made using the Θ determined for Krone's Mare Island sediments, along with other data specific to New Bedford Harbor.

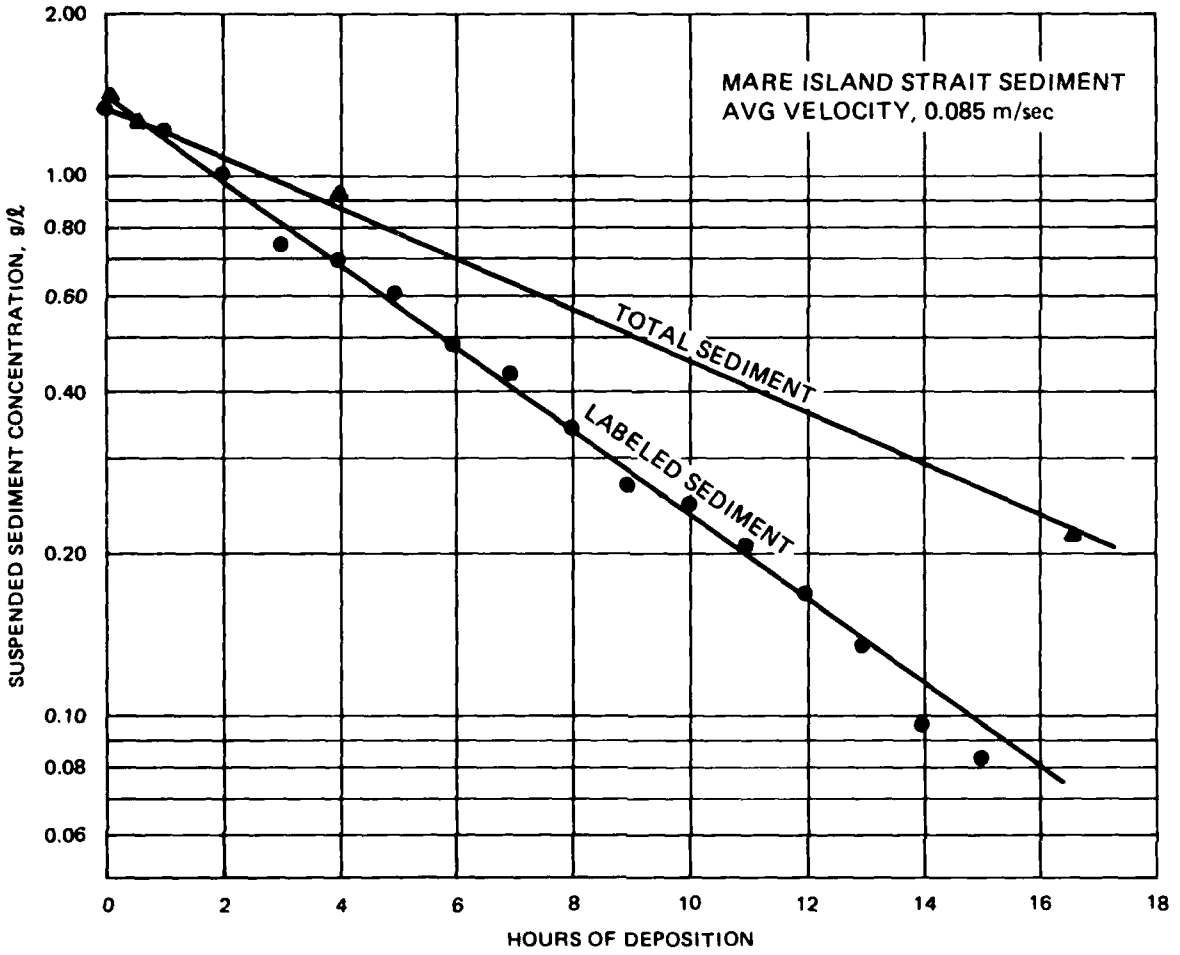

Figure A1. Suspended trace sediment concentration in flume during deposition (after Krone 1962)

21. The increase of contaminant on new suspended sediments entering the upper New Bedford Harbor was calculated using Equation A8. Representative depth, flow, and contaminant concentration conditions were compiled. Contaminant concentrations by sediment dry weight from the WES March and June 1986 surveys were averaged for ebb and flood tides at the Coggeshall Street Bridge. It was assumed that 50 percent of total PCB contaminants was associated with particulates, similar to the findings of EPA's 1983 survey. Tidal current magnitudes (root-mean-square current speeds) from the April and June surveys were converted to shear stresses and averaged for stations 7 and 8 in the upper harbor. The following tabulation summarizes observed and calculated (Equation A8) suspended contaminant concentration of sediments after entering the upper harbor on the flood tide and residing there for 6 hr.

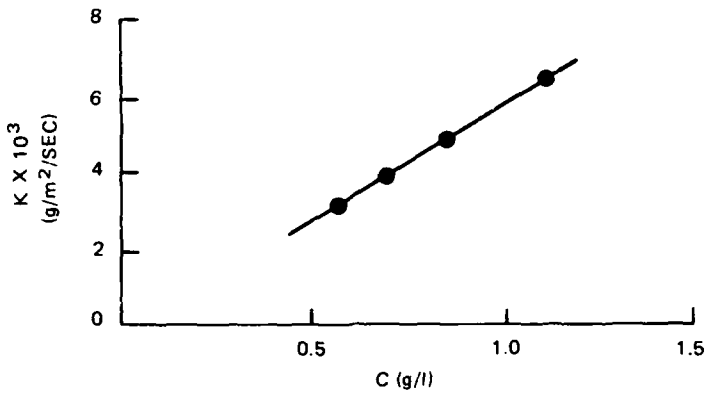

a. Plot of K versus C

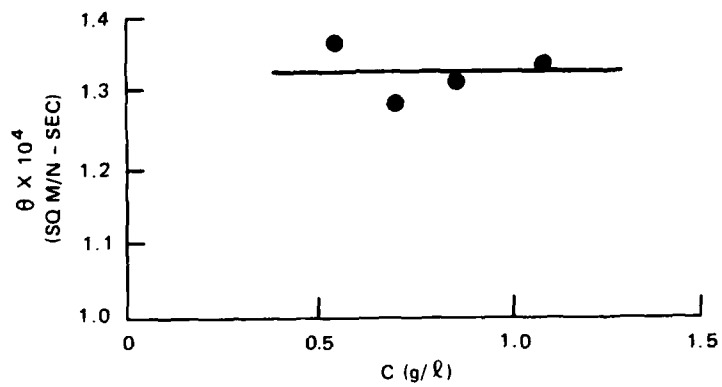

b. Plot of Θ versus C

Figure A2. Particle exchange coefficients by a fit of Equation A9 to Krone's data

Assumed Average Field Conditions	Observed S Average Ebb	Predicted S at t = 6 hr
S_o = 145 µg/g (flood)	S = 295 µg/g	S = 293 µg/g
S_s = 1,000 µg/g		
Θ = 1.33 E-04 sq m/N-sec		
τ_b = 0.066 N/sq m		
H = 1 m		

The assumed conditions are only generally representative of upper New Bedford Harbor. The average bed shear stresses over the entire area of the upper harbor were lower than the assumed value from stations 7 and 8, which would make the predicted final concentration S too large. The assumed S_s may be too low, however, which would make the predicted too small.

22. The close correspondence between predicted and observed values for

Table A1

Suspended Trace Sediment Concentrations in Flume During Deposition (Krone 1962, Figure 16), Mare Island Strait Sediment*

t hr	C g/ℓ	C_1/C	K $g/m^2/sec$	θ sq m/N-sec	D $g/m^2/sec$
0	1.4	1.0	-	-	-
2	1.1	0.87	6.48 E-03	1.37 E-04	11.24 E-03
4	0.87	0.77	4.81 E-03	1.29 E-04	8.76 E-03
6	0.70	0.67	3.95 E-03	1.31 E-04	6.85 E-03
8	0.56	0.58	3.23 E-03	1.34 E-04	5.43 E-03

* $H = 0.305$ m , $\bar{U} = 0.0854$ m/sec , and $\tau_b = 0.043$ N/m^2 .

S maybe largely coincidental but suggests that particle exchange could be an important mechanism for the mobilization and migration of contaminants from upper New Bedford Harbor. Further experimental data are needed to verify this finding.